PAMP-TRIGGERED IMMUNITY COMPONENTS AND LYSM-RECEPTOR-LIKE KINASES

A Dissertation

Presented to the Faculty of the Graduate School

of Cornell University

In Partial Fulfillment of the Requirements for the Degree of

Doctor of Philosophy

by

André Christopher Velásquez

August 2012

PAMP-TRIGGERED IMMUNITY COMPONENTS AND LYSM RECEPTOR-LIKE KINASES

André Christopher Velásquez, Ph. D.

Cornell University 2012

In order to identify components of Pathogen-associated molecular pattern (PAMP)-triggered immunity (PTI) pathways in *Nicotiana benthamiana*, a large-scale forward-genetics screen using virus-induced gene silencing and a cell-death-based assay for assessing PTI was performed. The assay relied on four combinations of PTI-inducing non-pathogens and cell-death-causing challenger pathogens, and was first validated in plants silenced for *FLS2* or *BAK1*. Over 3,200 genes were screened and 14 genes were identified that, when silenced, compromised PTI. A subset of the genes was found to act downstream of FLS2-mediated PTI induction and silencing of three genes compromised production of reactive oxygen species (ROS) in leaves exposed to flg22. The 14 genes encode proteins with potential functions in defense and hormone signaling, protein stability and degradation, energy and secondary metabolism and cell wall biosynthesis and provide a new resource to explore the molecular basis for the involvement of these processes in PTI.

Peptidoglycan (PGN) has been shown to trigger immune responses in *Arabidopsis thaliana*. However, in tomato, PGN did not trigger archetypal immune responses such as mitogen-activated protein kinase activation, ROS

production or protection from subsequent bacterial infections. This lack of responses suggests that PGN is not involved in activating immunity and stopping bacterial colonization in tomato. In *A. thaliana*, immunity against bacteria requires LysM-receptor-like kinases (LysM-RLKs). Two tomato LysM-RLKs, SlBti9 and SlLyk13, were shown to be required for resistance against both pathogenic and non-pathogenic *Pseudomonas syringae* pv. *tomato*. Flagellin-mediated responses were compromised in plants silenced for *SlBti9* and *SlLyk13*, which could explain the increased bacterial susceptibility observed in these plants. RNAi of *SlBti9* and *SlLyk13* also compromised chitin perception, as was reported previously for *A. thaliana* LysM-RLK CERK1. Auto-phosphorylation seems to be required for the activity of these two tomato LysM-RLKs in immunity as cell death mediated by over-expression of these proteins in *N. benthamiana* was abolished in kinase-inactive mutants. SlBti9 and/or SlLyk13 probably function as either pattern recognition receptors for a yet uncharacterized bacterial PAMP or are part of the receptor complex to transduce the signal once the recognition event has occurred.

BIOGRAPHICAL SKETCH

André Christopher Velásquez Landmann did his undergraduate studies at the Universidad Nacional Agraria La Molina in his hometown of Lima, Perú. He started his research in plant microbe-interactions at the International Potato Center (CIP) of Lima, Perú, under the supervision of Elisa Mihovilovich and Dr. Merideth Bonierbale. At CIP, he mapped and characterized the resistance to Potato leafroll virus in a native cultivated landrace of *Solanum tuberosum* ssp. *andigena*, LOP-868, in which he identified a major gene or chromosome region providing high resistance to PLRV infection. André moved to Ithaca to pursue his Ph.D. studies at Cornell University where he worked under the supervision of Dr. Gregory Martin. His research at Cornell involved the identification and characterization of genes involved in PAMP-triggered immunity in *Nicotiana benthamiana* and the role of tomato LysM-receptor-like kinases in immunity against bacterial pathogens.

ACKNOWLEDGMENTS

I would like to thank my advisor Dr. Gregory Martin for giving me the opportunity to work in his laboratory and for being involved as a mentor in developing my academic and research skills.

I am grateful to many people in the Martin laboratory, especially to Dr. Suma Chakravarthy who taught and helped me during the first half of my stay at Cornell University. Diane Dunham also gave me invaluable assistance working in the laboratory during these years in Ithaca. Other members of Cornell University that I would like to thank for their help are Dr. Alan Collmer, Dr. Patrick Boyle, Dr. Hernán Rosli, Dr. Sarah Hind, Dr. Kathy Munkvold, Dr. Richard Pattison and Elise Pasoreck.

My mother has always been an integral part of my life and I would like to thank her for her support all these years. My brother Marcel was the one in charge of making the transition Perú – United States smoother.

An enormous thank you to Anita who corrected my multiple grammatical English mistakes with precision and virtue. She also made me discover that the unexpected might blissfully change your life forever.

My friends in Ithaca were many, and without them life would have been extremely dull. Thank you José and Natalia, for coming to gym torture, talking about all and nothing at the same time and being there. I am grateful to Kike, Luis, Maia, Hinsby, Francisco and Kathleen for unintended happiness that I hope I returned as well.

TABLE OF CONTENTS

LIST OF FIGURES

LIST OF TABLES

CHAPTER I

MOLECULAR MECHANISMS INVOLVED IN THE INTERACTION BETWEEN TOMATO AND *PSEUDOMONAS SYRINGAE* PV. *TOMATO*[1]

The Solanaceae or nightshade family includes many economically important plants such as tomato (*Solanum lycopersicum*), potato (*Solanum tuberosum*), tobacco (*Nicotiana tabacum*), pepper (*Capsicum annuum*) and petunia (*Petunia* spp.). Among these plants, tomato offers many advantages for research. The tomato genome sequence has recently become available (http://solgenomics.net/) and the abundant natural variation present in the 12 wild relatives of tomato can be exploited for enhancing agronomic traits (Peralta *et al.* 2009). Furthermore, tomato is amenable to virus-induced gene silencing (VIGS) and *Agrobacterium*-mediated transformation, and it may be used to study plant pathogenesis as it is susceptible to many devastating pathogens including *Pseudomonas syringae* pv. *tomato*, *Xanthomonas campestris* pv. *vesicatoria*, *Cladosporium fulvum* and *Phytophthora infestans*, among others.

Pseudomonas syringae is classified into more than 40 different pathovars, which are defined either by the hosts that are infected by these bacteria or by the plant from which the bacteria were first isolated. *Pseudomonas syringae* pv.

[1] This chapter has been accepted for publication as part of the book "Molecular Plant Immunity" by John Wiley & Sons, Inc. and was written by André C. Velásquez and Gregory B. Martin.

tomato (*Pst*) is the causal agent of bacterial speck disease in tomato. The disease is characterized by the presence of necrotic spots or specks (henceforth its name) surrounded by chlorotic halos (Figure 1.1). Disease severity is favored by cool moist conditions. The symptoms may occur in leaves or in fruits, reducing not only the yield but also the marketability of tomatoes (Martin 2011).

Pst has proven to be extremely versatile as an experimental system for studying bacterial pathogenesis. Many *Pst* isolates are available and the bacterium is easily manipulated in the laboratory. Furthermore, several *Pst* genomes have been sequenced (Buell *et al.* 2003; Almeida *et al.* 2009; Cai *et al.* 2011; http://www.pseudomonas-syringae.org/) and there is a plethora of mutant strains available, one of which has had all of its effector genes deleted (Cunnac *et al.* 2011).

Plants have an elaborate inducible immune system to defend themselves against most potential pathogens they may encounter. This system involves cell surface proteins known as Pattern Recognition Receptors (PRR), which are involved in recognition of epitopes of molecules essential for microbe survival. When these molecules, known as Pathogen or Microbe-Associated Molecular Patterns (PAMP or MAMP), are perceived, PAMP-triggered immunity (PTI) is elicited preventing the establishment of any non-pathogenic microbe or non-host pathogen (Boller and Felix 2009).

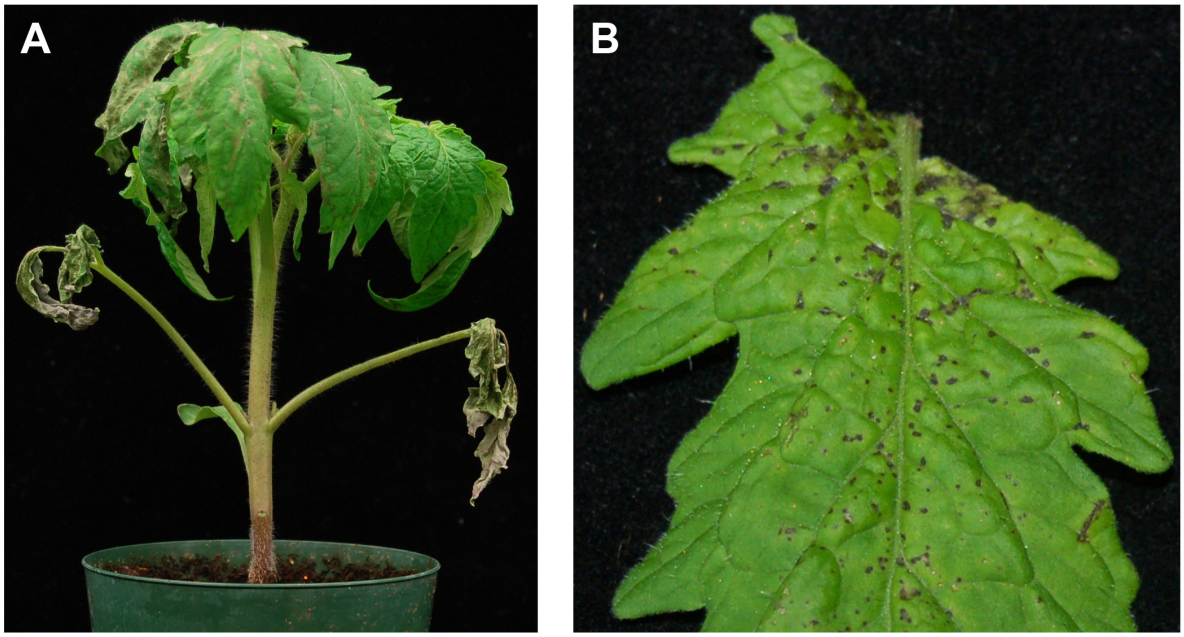

Figure 1.1. Bacterial speck disease symptoms on tomato caused by *Pseudomonas syringae* pv. *tomato*. (A) Tomato Rio Grande-prf3 plants were inoculated with *Pseudomonas syringae* pv. *tomato* DC3000. Lower leaf necrosis and wilting is observed along with necrotic coalescing specks in the upper leaves. Picture was taken 3 days after inoculation. (B) Close-up photograph of a tomato leaf showing the typical necrotic specks surrounded by a chlorotic halo which gives the disease its name.

Through evolution, bacteria have acquired multiple virulence strategies to overcome PTI. The production of toxins to alter plant cell physiology and modulate defenses can create an advantageous environment for a pathogen. *P. syringae* pathovars produce a variety of toxins including coronatine, the toxin produced by *Pst*. Many bacterial pathogens also have a type III secretion system (T3SS), which is used to inject effector proteins into plant cells. In the plant cell, effectors typically suppress PTI and allow colonization, as has been shown for *Pst* effectors AvrPto and AvrPtoB (Martin 2011).

In response to type III effector proteins, plants have in turn evolved resistance (R) proteins to directly or indirectly detect the activity of specific effectors and thereby elicit effector-triggered immunity (ETI). The hypersensitive response (HR), a form of localized programmed cell death (PCD) that occurs where the effector /resistance proteins interact, is a hallmark of ETI that is typically absent during PTI (Bent and Mackey 2007). Over time, evolution will drive the pathogen to either lose or mutate the effector or to acquire a second effector to suppress ETI in order to continue being pathogenic.

PAMP-triggered immunity in the Solanaceae

Bacterial PAMPs recognized by Solanaceous species

Flagellin

The paradigm for PAMP perception by a PRR is the recognition of flagellin by FLS2. The epitope of flagellin that is recognized in plants is flg22, a 22 amino acid peptide from the N-terminus of flagellin (Felix *et al.* 1999). This epitope is

different from that recognized in mammals at the cell surface by TLR5 or intracellularly by the Naip5-Ipaf complex (Smith *et al.* 2003; Lightfield *et al.* 2008), highlighting a fascinating example of convergent evolution in the host towards PAMP recognition.

In tomato, a shortened version of flg22 comprising only 15 amino acids (flg15) is sufficient for robust PTI activation. The flg15 peptide induced a strong extracellular alkalinization of suspension cell cultures and the production of reactive oxygen species (ROS) in leaves. However, flg15 derived from the plant pathogen *Agrobacterium tumefaciens* or the nodule-forming *Sinorhizobium meliloti* were completely inactive in triggering PTI, due to a number of amino acid changes relative to the canonical flg15 (which is derived from the sequence of *Pseudomonas aeruginosa*). This variation/alteration may have evolved by these bacteria as a mechanism to evade plant recognition (Felix *et al.* 1999). A similar mechanism of avoidance of flagellin detection appears to be present in *Ralstonia solanacearum* and *Xanthomonas campestris* pv. *campestris* (*Xcc*) in their interaction with *Arabidopsis thaliana* (Pfund *et al.* 2004; Sun *et al.* 2006).

Flagellin recognition seems to be a particularly important PAMP in *Nicotiana benthamiana* and tomato interactions with *P. syringae*, as deletion of *fliC*, the gene encoding for flagellin, renders attenuated *P. syringae* strains (which were lacking AvrPto and AvrPtoB effectors) as virulent as the wild-type strain in their hosts (Kvitko *et al.* 2009; Velásquez and Martin unpublished).

Other PAMPs

There are several other bacterial PAMPs that are recognized in plants. However, little is known about the majority of them (Figure 1.2).

Cold-shock proteins (CSP), a group of RNA-binding proteins from bacteria, are recognized by tomato. A small RNA-binding motif (RNP-1) required for CSP activity, csp15, is the epitope recognized in plants. The csp15 peptide induces ethylene biosynthesis and ROS production in tomato plants (Felix and Boller 2003). How CSPs, which are cytoplasmic proteins, are able to be perceived by plant cell surface PRRs is still currently unknown, but CSPs might be released during bacterial growth or lysis at a sufficient concentration to allow detection by the plant immune system.

Lipopolysaccharides (LPS), components of the outer membranes of Gram negative bacteria, have been shown to be recognized by pepper. Prior exposure to LPS from *Xcc* prevents HR and disease development in pepper leaves and induces defense gene expression (Newman *et al.* 2002). LPS also causes stomatal closure in tomato possibly as a mechanism to avoid bacterial invasion (Melotto *et al.* 2006).

Harpins are proteins secreted by the T3SS in *P. syringae* that trigger a hypersensitive response from outside the plant cells. In some *P. s.* pv. *tabaci* strains, the gene encoding for hairpin (*hrpZ*) is disrupted allowing this bacterium to avoid eliciting plant defense responses and therefore being able to infect tobacco plants (Tsunemi *et al.* 2011).

Figure 1.2. PAMP-triggered immunity in the Solanaceae. A *Pseudomonas syringae* pv. *tomato* (*Pst*) bacterium is depicted coming into contact with a plant cell. Bacterial pathogen-associated molecular patterns (PAMPs) are recognized by cell surface pattern recognition receptors (PRRs) to trigger PAMP-triggered immunity (PTI) in order to stop colonization by potential pathogens. PAMPs recognized by plants in the Solanaceae family include lipopolysaccharide (LPS), cold-shock protein (CSP) and the type III secretion system (T3SS). The corresponding PRRs for these PAMPs have not yet been identified. Flagellin is the only known PAMP in the Solanaceae for which the corresponding PRR, FLS2, has been characterized. Flagellin perception occurs through the PRR FLS2, a leucine-rich repeat-containing (LRR) receptor-like kinase (RLK), which after ligand binding, associates immediately with the adaptors BAK1 and/or BKK1, both of which are involved in flagellin sensing and in additional PTI signaling pathways. The extracellular portion of Bti9 has LysM domains and this protein likely plays a role in PAMP perception; the identity of the PAMP is unknown but may be a carbohydrate-containing molecule.

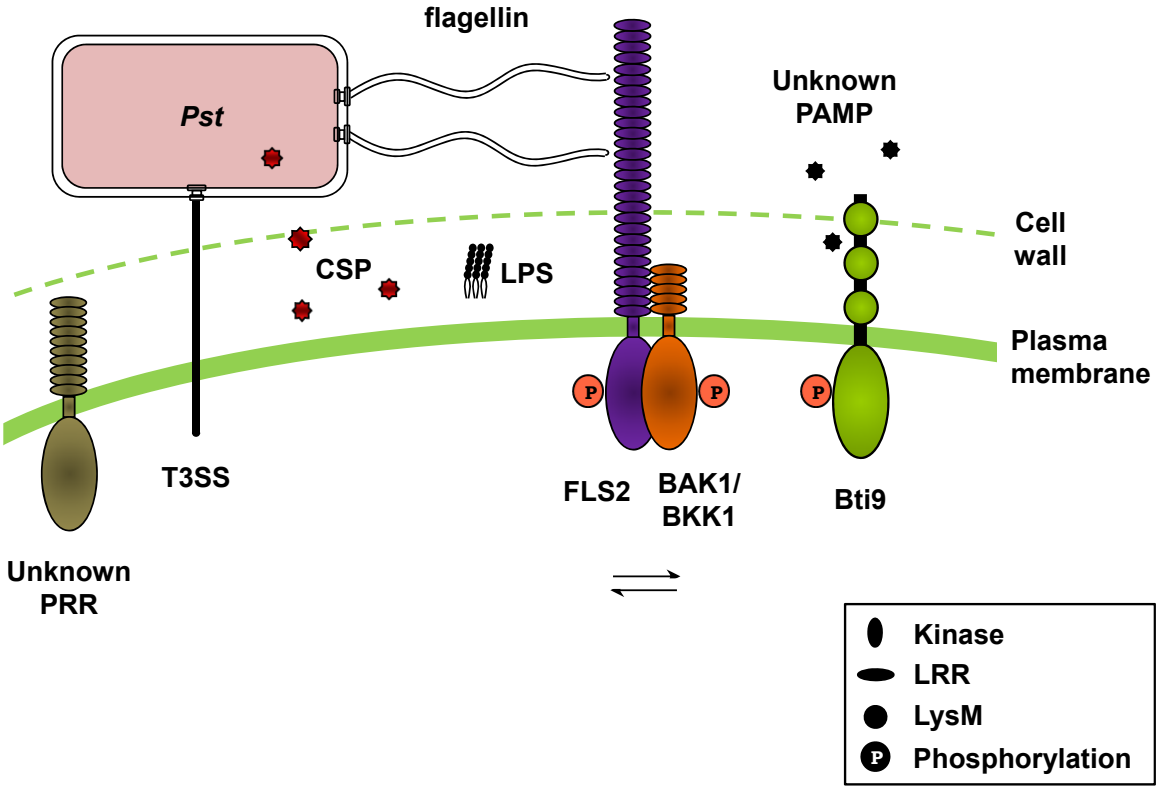
flagellin
Pst
Unknown
PAMP
Cell
wall
CSP
LPS
Plasma
membrane
T3SS
FLS2
BAK1/
BKK1
Bti9
Unknown
PRR
P
Kinase
LRR
LysM
Phosphorylation

The T3SS itself may be a target of the plant surveillance system. A *Pst* effectorless mutant (but still carrying an intact T3SS) grew less in *N. benthamiana* plants than a T3SS deficient mutant, suggesting that the T3SS elicits plant defenses (Cunnac *et al.* 2011). ROS production was also higher in a *P. fluorescens* strain carrying a cosmid with a functional T3SS from *P. s.* pv. *syringae* than in the wild-type *P. fluorescens* (Oh *et al.* 2010). Interestingly, animal immune systems are also able to respond to bacterial TTSS by sensing the basal body inner rod protein PrgJ (Miao *et al.* 2010).

Genes in the Solanaceae involved in PTI

FLS2

FLS2 is the PRR responsible for flagellin recognition (Figure 1.2). FLS2 is a single-pass transmembrane receptor-like kinase (RLK) that has 28 extracellular leucine-rich repeats (LRR). Its kinase activity is required for PTI signaling (Gómez-Gómez *et al.* 2001). Tomato FLS2 (SlFLS2) differs slightly in the flagellin epitope it recognizes when compared with that of *A. thaliana*. SlFLS2 is able to recognize *E. coli* flg15 while AtFLS2 is unable to do so (Robatzek *et al.* 2007).

Upon flagellin recognition, typical PTI responses ensue including ROS production, a calcium burst, mitogen-activated protein kinase (MAPK) phosphorylation, gene induction and callose deposition. Silencing of *NbFLS2* in *N. benthamiana* plants not only abrogates all these responses but also makes

plants more susceptible to *P. syringae* (Hann and Rathjen 2007; Heese *et al.* 2007).

Transcriptional control of *FLS2* requires ethylene-dependent transcription factors AtEIN3 and AtEIL1, which depend on AtEIN2 for their accumulation. FLS2 mRNA accumulation is impaired in plants mutated for any of the above mentioned transcription factors, highlighting their importance and that of the plant hormone ethylene in FLS2-mediated pathways (Boutrot *et al.* 2010).

MAPK cascades are known to be involved in flg22 responses (Pitzschke *et al.* 2009). Flg22-induced signaling requires at least two MAPKs, NbSIPK and NbWIPK, as evidenced by the de-regulation of ROS production after elicitor treatment when both of these genes are silenced in *N. benthamiana* and the lack of induction of flg22-responsive genes after RNAi of *NbSIPK* (Segonzac *et al.* 2011).

After perception of flg22, endocytosis of FLS2 is required for proper FLS2 signaling (Robatzek *et al.* 2006). The need for *de novo* FLS2 synthesis to replace the PRR after its endocytosis may explain why there is a refractory period until flagellin stimulation can proceed again. Once stimulated, quenching of the signal is facilitated by proteasomal degradation of FLS2 by AtPUB12 and AtPUB13, two U-box E3 ubiquitin ligases (Lu *et al.* 2011).

EFR

In members of the Brassicaceae, the translation elongation factor Tu (EF-Tu) is recognized by the PRR EF-Tu receptor (EFR), which is also transmembrane

LRR-RLK (Zipfel *et al.* 2006). Stable expression of AtEFR in transformants of *N. benthamiana* or tomato plants made these plants responsive to elf18, the epitope of EF-Tu recognized by EFR, and importantly, more resistant to different bacterial pathogens including *P. syringae* (Lacombe *et al.* 2010).

BTI9/CERK1

In *A. thaliana*, chitin perception is mediated by AtCERK1, a transmembrane RLK with 3 extracellular LysM domains (Miya *et al.* 2007; Wan *et al.* 2008). AtCERK1 has been shown to bind chitin *in vitro* and as such it is believed to be part of the chitin PRR complex (Petutschnig *et al.* 2010). Surprisingly, AtCERK1 also seems to be involved in bacterial perception, as not only ROS production to *Pst* extracts is reduced in plants lacking *AtCerk1* but also these plants are more susceptible to *Pst* infection (Gimenez-Ibanez *et al.* 2009a, 2009b). It is unknown whether or not AtCERK1 plays a direct or indirect role in binding of a *Pst* PAMPs.

In tomato, the LysM-RLK family has expanded and consists of at least 13 proteins instead of only the 5 identified in *A. thaliana*. Tomato RNAi lines with reduced expression of *SlBti9*, *SlLyk11*, *SlLyk12* and *SlLyk13* (the four proteins which, based on amino acid similarity, reside in the same clade as AtCERK1) were more susceptible to *Pst* infection (Zeng *et al.* 2011). Similarly, silencing of *NbCERK1* in *N. benthamiana* rendered plants more susceptible to *P. syringae* (Segonzac *et al.* 2011).

The identity of the bacterial PAMP whose recognition is mediated by Bti9/CERK1 is still unknown (Figure 1.2). It is possibly a carbohydrate-containing elicitor, since LysM domains have been shown to bind only to N-acetylglucosamine-comprising molecules (Buist *et al.* 2008). Peptidoglycan (PGN), which is an essential component of the bacterial cell wall, is known to activate PTI in *A. thaliana* (Gust *et al.* 2007). However, PGN may not be the PAMP whose perception is mediated by Bti9/CERK1, as an *A. thaliana cerk1* mutant still gave a ROS response when PGN was used as an elicitor (Gimenez-Ibanez *et al.* 2009b), although functional redundancy in PGN detection cannot be excluded.

BAK1/SERK3

BAK1/SERK3 is a transmembrane RLK with 5 extracellular LRR involved in brassinosteroid signaling through its association with the brassinosteroid receptor, BRI1 (Li *et al.* 2002; Nam and Li 2002). Unexpectedly, it was found that BAK1 is also required as an adaptor for different PTI signaling cascades. BAK1 associates with FLS2 or EFR after flg22 or elf18 elicitor treatment, respectively (Chinchilla *et al.* 2007; Roux *et al.* 2011). BKK1/SERK4, which belongs to the same LRR RLK subfamily as BAK1, seems to have a partially redundant role with BAK1 in PTI signaling (Roux *et al.* 2011; Figure 1.2).

Silencing of *NbBAK1* in *N. benthamiana* reduces ROS production after flg22 and csp22 (a larger peptide encompassing csp15) treatment, which correlates with increased growth of *P. syringae* in those plants (Heese *et al.* 2007). In *A.*

thaliana, signaling pathways for other bacterial PAMPs, including elf18, PGN, LPS and hairpin are also compromised in *bak1* knockout mutants, highlighting the importance of BAK1/BKK1 in multiple PTI signaling pathways (Shan *et al.* 2008).

Other genes involved in PAMP-triggered immunity

A large-scale VIGS screen and a cell-death-based assay were used in *N. benthamiana* to identify genes involved in PTI (Chakravarthy *et al.* 2010). *HCBT*, a gene that catalyzes the first step in phytoalexin biosynthesis, was found in this screen. Phytoalexin biosynthesis is directly targeted by *P. syringae* effectors (Zhou *et al.* 2011) and camalexin (the major phytoalexin in *A. thaliana*) biosynthesis and exudation by roots is induced by flg22 (Millet *et al.* 2010). Phytoalexins are believed to have antimicrobial properties and as such could potentially halt the growth of an invading pathogen during the PTI response in *N. benthamiana*.

There is an antagonistic effect between auxin and salicylic acid (SA) during plant defense, with auxin promoting susceptibility and SA inducing defense (Wang *et al.* 2007). *Drm3* was another gene found to be involved in PTI, which shows similarity to a pea gene repressed by auxin (Chakravarthy *et al.* 2010). Drm3 might therefore act as positive regulator of PTI, which becomes derepressed when the auxin response is inhibited during PTI.

A putative proteasome 26S subunit homolog and an ubiquitin-activating enzyme were also discovered in the screen for genes involved in PTI

(Chakravarthy *et al.* 2010). Five *A. thaliana* U-box E3 ubiquitin ligases (PUB12, PUB13, PUB22, PUB23 and PUB24) have been shown to have a role in PTI by quenching the response to different PAMPs after elicitor stimulation (Trujillo *et al.* 2008; Lu *et al.* 2011), highlighting the importance of ubiquitination in PTI.

PTI suppression of effector delivery into host cells

It was recently shown that PTI blocks translocation of effectors into plant cells (Crabill *et al.* 2010; Oh *et al.* 2010). Effector-Cya fusion translocation was suppressed in tissue that had been previously induced for PTI with *P. fluorescens*, T3SS-defficient *Pst* or flg21 (Crabill *et al.* 2010). The basis for this effector delivery failure is still unknown and will require future work. However, this phenomenon has already been exploited for the discovery of genes involved in PTI, as in the cell-death-based assay used in the VIGS screen described above (Chakravarthy *et al.* 2010). This assay required PTI induction for inhibition of effector translocation in order to suppress disease and ETI-associated cell death, none of which can occur in the absence of effector delivery. Only when a gene involved in PTI was silenced, was inhibition of cell death compromised.

Pseudomonas syringae pv. tomato virulence mechanisms

When considering virulence, it is important first to differentiate between the quality of being pathogenic and virulent in a plant. Pathogenicity refers to the ability of a particular organism to cause disease in a plant. Virulence alludes to

the degree of disease a pathogenic organism produces in a host. Therefore, *Pst* is a pathogenic organism in tomato that may be more virulent in certain tomato varieties than in others; the outcome of this interaction depends on the particular host-pathogen combination.

The disease cycle of bacterial speck starts with *Pst* inoculum originating from contaminated seeds, soil or leaves, or being spread by aerosols and rain splashes until the bacteria arrive at a susceptible tomato host. *Pst* is able to survive epiphytically on tomato leaf surfaces and when the conditions are appropriate, *Pst* infects plants through stomata or wounds. Once in the apoplast, *Pst* multiplies intercellularly and after a few days causes the typical necrotic lesions surrounded by chlorotic halos of bacterial speck (Hirano and Upper 2000).

One of the best studied *Pst* strains is DC3000, a rifampicin-resistant mutant of strain DC52, which has been extensively used due to its ability to infect the model species *A. thaliana*. *Pst* DC3000 is not pathogenic in *N. benthamiana*. However, if the gene for *hopQ1-1*, the major effector being recognized by this plant, is deleted, *Pst* DC3000 becomes pathogenic which allows this model plant species to be used for research with *Pst* (Wei *et al.* 2007). This finding has been used to demonstrate that distant movement of *Pst* Δ*hopQ1-1* from inoculation sites in *N. benthamiana* leaves occurs mainly through xylem vessels. Distant colonization does not require flagellum-mediated motility and could involve type IV pili (Misas-Villamil *et al.* 2011). *Pst* might shed off the

unnecessary flagellum once it is inside the apoplast to help it avoid host recognition.

Once *Pst* reaches the apoplast, it is adapted to assimilate and catabolize nutrients that are abundant in tomato apoplast (Rico and Preston 2008). *Pst* T3SS expression is also upregulated when bacteria are in the apoplast (Rico and Preston 2008), which ultimately leads to effector delivery into the host cell cytoplasm.

Siderophores are important virulence determinants in many pathosystems in which the pathogen needs to sequester iron from iron-limited environments, such as the plant apoplast. *Pst* DC3000 has three siderophores - yersiniabactin, pyoverdin and citrate - none of which seem to have any effect on *Pst* virulence in tomato plants (Jones and Wildermuth 2011).

Coronatine

Coronatine is a *Pst* phytotoxin that is composed of two molecules, the polyketide coronofacic acid (CFA) coupled through an amide bond to coronamic acid (CMA), an amino acid derivative synthesized from isoleucine. Coronatine biosynthesis genes are either chromosomally encoded (e.g., in *Pst* DC3000) or, as in some strains like *Pst* PT23.2, located in a plasmid (Bender *et al.* 1989).

In tomato, *Pst* mutants without CFA (*Pst* Δcfa6) do not cause the typical chlorotic halos around specks while *Pst* mutants without CMA (*Pst* Δc*maA*) exhibit less necrotic lesions on leaves (Uppalapati *et al.* 2007). Thus, CFA and CMA appear to have different effects on symptom formation in tomato. In

Streptomyces scabies, there is a CFA-like biosynthetic cluster but not one for CMA. A knockout strain for this cluster reduces the virulence of *S. scabies* on tobacco plants (Bignell *et al.* 2010). The importance of CFA in other pathosystems and the fact that CFA has been found linked to other amino acids besides CMA (Bender *et al.* 1999) suggests that each molecule may have evolved independently to exert its own contribution to virulence.

Coronatine structure closely resembles that of a jasmonic acid (JA)-isoleucine conjugate and as such it is believed to act as an agonist of JA signaling. Antagonistic crosstalk between JA and SA pathways may contribute to increased susceptibility against *Pst* and partially to coronatine effect on virulence (Uppalapati *et al.* 2005; Uppalapati *et al.* 2007). It was shown *in vitro* that coronatine is 1000-fold more potent agonist than JA-Ile for COI1, the F-box protein that targets the JA transcriptional repressors (jasmonate ZIM domain proteins, JAZ) for degradation to activate JA signaling (Katsir *et al.* 2008). Therefore, coronatine might exert its effect by manipulating JA hormonal regulation (Figure 1.3).

Bacterial inoculation causes stomata to close as a mechanism to prevent bacteria from accessing the apoplastic space. However, successful pathogens like *Pst* are able to cause tomato stomata to reopen. In *A. thaliana*, purified coronatine reopens stomata and a *Pst* coronatine-deficient mutant is unable to do so (Melotto *et al.* 2006), implicating coronatine in the early stages of bacterial invasion.

Figure 1.3. *Pseudomonas syringae* pv. *tomato* virulence strategies that are used to overcome PAMP-triggered immunity. After *Pseudomonas syringae* pv. *tomato* (*Pst*) comes into contact with plant cells, it deploys its virulence factors in order to suppress PAMP-triggered immunity (PTI) and become established in the plant apoplast. The main virulence factors used by *Pst* are a phytotoxin, coronatine, and effectors, proteins injected into the plant cell by the type III secretion system (T3SS). The PTI processes being attacked by *Pst* virulence factors are diverse and include hormone signaling, vesicle trafficking and pattern recognition receptor (PRR) complex formation. The phytotoxin coronatine is an agonist of SCF^{COI1}, an F-box protein that targets the jasmonic acid (JA) repressors for proteasomal degradation to activate JA signaling. In turn, hormonal JA signaling upregulation by coronatine contributes to enhanced bacterial virulence. The T3SS delivers, in the case of *Pst* strain DC3000, up to 28 effectors to manipulate host immunity, including HopM1, AvrPto and AvrPtoB. HopM1 targets AtMIN7 for polyubiquitination and proteasomal degradation; the latter being involved in vesicle trafficking and as such, it may be involved in plant cell wall defenses and antimicrobial deployment. AvrPto is myristoylated *in planta* to target this effector to the plasma membrane where, along with AvrPtoB, interferes with PRR complex formation (e.g., BAK1 and FLS2 association) to disrupt PTI. Both AvrPto and AvrPtoB are phosphorylated *in planta* and this post-translational modification contributes to their virulence-enhancing activities.

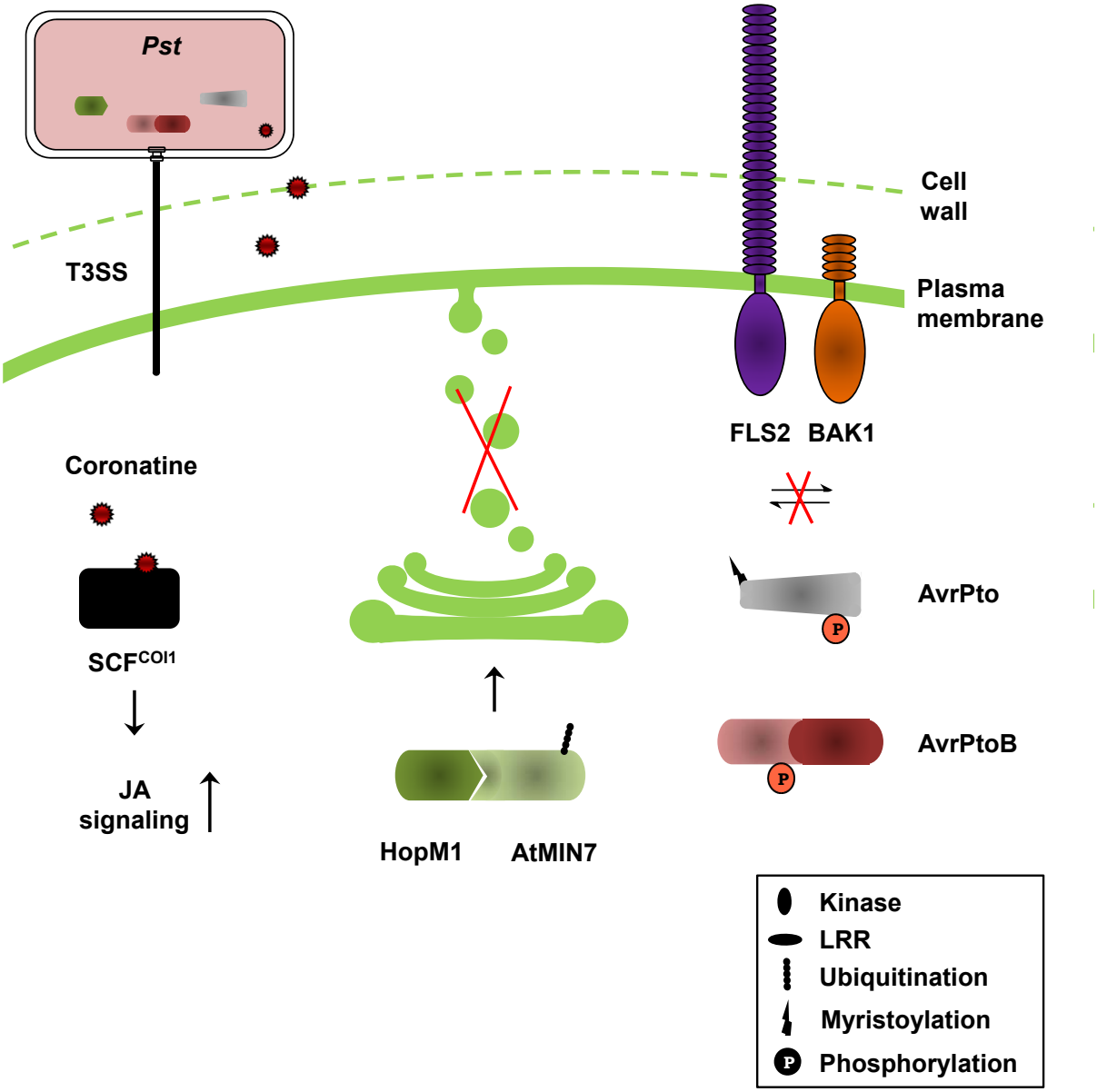
Pst
T3SS
Cell wall
Plasma membrane
FLS2
BAK1
Coronatine
SCF^COI1
JA signaling
HopM1
AtMIN7
AvrPto
AvrPtoB
P
Kinase
LRR
Ubiquitination
Myristoylation
Phosphorylation

Type III effector proteins

Translocation of effectors is accomplished by the T3SS, and thus the T3SS is a pathogenicity determinant

of *Pst*. The T3SS is a complex structure that is composed of two pairs of rings that span the inner and outer bacterial plasma membranes, joined by a rod that traverses the peptidoglycan cell wall. An extracellular pilus (composed of HrpA subunits) delivers the effectors into host cells (Roine *et al.* 1997; Cornelis 2006).

Effectors evolved to promote virulence but in some cases they can be recognized by host R proteins to activate ETI. They typically have no amino acid sequence similarity to proteins of known function. Many effectors require chaperones for their translocation into host cells, which are quite often located in a locus contiguous to that of the effector (Badel *et al.* 2003; López-Solanilla *et al.* 2004). The number of effectors varies within *Pst* strains with *Pst* DC3000 having 28 and *Pst* T1 having 25 (Cai *et al.* 2011; Cunnac *et al.* 2011).

Effectors can be classified according to their mode of action in redundant effector groups (REG; Kvitko *et al.* 2009). Deletions of some individual effectors may have no apparent virulence effect because another effector in the same REG compensates for its loss. It is thought that members of a REG may target the same protein in the host or distinct proteins that contribute to the same process thus their observed redundant phenotypes on virulence (Schneider and Collmer 2010).

AvrPto

AvrPto is a small 18 kDa protein with a modular structure that is recognized in tomato by the R protein Pto. AvrPto is subject to post-translational modifications within the host including N-myristoylation which has been shown to target the effector to the plasma membrane in tobacco cells (Shan *et al.* 2000). Mutation of glycine 2, the amino acid to which the myristoyl group attaches to in AvrPto, abolishes not only virulence activity but also the ability of the plant to recognize the effector (Thara *et al.* 2004), thus implicating this post-translational modification in all known activities of AvrPto *in planta*.

AvrPto has two virulence determinants with additive effects in tomato, the **Ω** loop in the structured core of the protein and the C-terminal domain. AvrPto homologs in most *P. syringae* pathovars have the key amino acid residues of the **Ω** loop and/or the C-terminal domain conserved, highlighting the importance of these two domains in virulence (Nguyen *et al.* 2011).

The **Ω** loop has been shown to be required for suppression of MAPK activity in tomato and also for recognition by Pto (Yeam *et al.* 2009). It is unclear whether AvrPto suppresses MAPKs by interacting with the PTI adaptor BAK1 or the PRRs FLS2 and EFR. There are conflicting reports of AvrPto co-immunoprecipitating with BAK1, FLS2 and EFR in *A. thaliana* and consequently blocking PTI signaling (Shan *et al.* 2008; Xiang *et al.* 2008; Xiang *et al.* 2011). Despite these differences, it seems clear that the virulence effect of the **Ω** loop is due to AvrPto interference with PRR complexes (Figure 1.3).

The C-terminus of AvrPto is subject to phosphorylation at serines 147 and 149. This post-translational modification is required for the virulence-enhancing effect of this domain and contributes to disease-promoting ethylene biosynthesis (Anderson *et al.* 2006; Yeam *et al.* 2009). Furthermore, this phosphorylation at the C-terminus is required for the recognition of AvrPto by a yet uncharacterized R protein in tobacco, Rpa (Yeam *et al.* 2009).

AvrPtoB

AvrPtoB (also known as HopAB2) is a 59 kDa effector which also has a modular structure and is recognized by tomato Pto. Post-translational modification also occurs in AvrPtoB as it is phosphorylated on serine 258 *in planta*. This phosphorylation is required for AvrPtoB virulence enhancing activity in tomato (Xiao *et al.* 2007a).

AvrPto and AvrPtoB belong to the same REG. Both AvrPto and AvrPtoB upregulate genes involved in ethylene biosynthesis to promote disease development in tomato (Cohn and Martin 2005). Both effectors are also involved in suppressing PAMP-responsive miRNA production in *A. thaliana* (Navarro *et al.* 2008).

In tomato, the N-terminal region of AvrPtoB (from amino acids 1-387) is all that is needed to confer full virulence to the effector (Xiao *et al.* 2007b, Zeng *et al.* 2011). This region carries two virulence determinants. $AvrPtoB_{1-387}$ suppresses MAPK activation in *A. thaliana* while $AvrPtoB_{1-307}$ is sufficient to

induce ethylene biosynthesis and promote virulence in tomato plants (Xiao *et al.* 2007b).

AvrPtoB$_{1-307}$ virulence and its recognition by Pto in tomato require amino acid phenylalanine 173 (Xiao *et al.* 2007b). Substitution of phenylalanine 173 to alanine abolishes interaction of AvrPtoB with two LysM-RLKs involved in tomato immunity, SlBti9 and SlLyk13. Furthermore, AvrPtoB$_{1-307}$ interferes *in vitro* with SlBti9 kinase activity suggesting this is the mechanism of action of this AvrPtoB domain (Zeng *et al.* 2011). However, in *A. thaliana* it was shown that the homolog of the two tomato LysM-RLKs, AtCERK1, is targeted for vacuolar degradation by AvrPtoB to promote virulence and that this required the C-terminus of AvrPtoB (Gimenez-Ibanez *et al.* 2009a). Discrepancies aside, it is clear from these reports that AvrPtoB targets LysM-RLKs to enhance *Pst* virulence.

The AvrPtoB$_{1-387}$ N-terminal region of AvrPtoB has been shown to interact with AtBAK1 and the crystal structure of this complex has recently been solved (Cheng *et al.* 2011). AvrPtoB$_{1-387}$ interferes with AtBAK1 kinase activity *in vitro*, which has been demonstrated to be required for efficient PTI signal transduction (Schwessinger *et al.* 2011), and this is therefore likely to be the basis for AvrPtoB suppression of MAPK activation (Figure 1.3).

The conserved effector locus, CEL

The conserved effector locus (*CEL*) is a genomic region conserved in many different *P. syringae* pathovars. In *Pst* DC3000 the CEL has twelve open reading

frames (ORF). The *CEL* encodes two well characterized effectors belonging to the same REG, *avrE1* and *hopM1*; the effectors *hopAA1-1* and *hopN1*; three chaperones, *shcE*, *shcM* and *shcN*; the hairpin *hrpW1* and four still uncharacterized ORFs (Figure 1.4).

Deletion of the *CEL* drastically reduces *Pst* bacterial growth and symptoms in tomato (Badel *et al.* 2003). Knockout strains for either *avrE1* or *hopM1* reduce symptom development but have no effect on bacterial growth. However, deletion of both effectors fully reproduces the CEL deletion as both bacterial growth and symptom formation are compromised (Badel *et al.* 2006). In *A. thaliana*, callose deposition is suppressed by both AvrE1 and HopM1 (DebRoy *et al.* 2004). The same effect has been shown for AvrE1 in *N. benthamiana* (Kvitko *et al.* 2009). HopM1 targets AtMIN7, a protein involved in vesicle trafficking, for proteasomal degradation to suppress cell wall-associated host defenses which explains how this effector might be able to suppress callose deposition (Nomura *et al.* 2006; Figure 1.3).

Two other effectors encoded in the *CEL* with known effect on *Pst* disease development are *hopN1* and *hopAA1-1*. HopN1 seems to have a negative effect on the spread of disease symptoms as a knockout *hopN1 Pst* strain produces more necrotic speck lesions than the wild-type strain without any commensurate effect on bacterial growth. HopN1 has been shown to have cysteine protease activity *in vitro*, but how this contributes to *Pst* virulence is unknown (López-Solanilla *et al.* 2004). HopAA1-1, on the other hand, appears to have a positive effect on disease development, as it causes cell death when

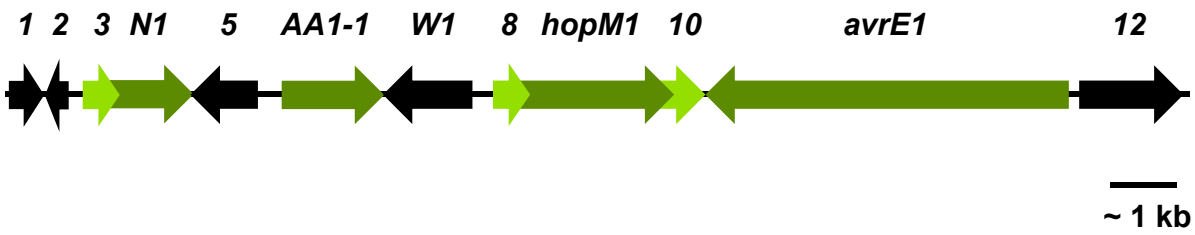

Figure 1.4. *Pseudomonas syringae* pv. *tomato* strain DC3000 *conserved effector locus* genome organization. The *conserved effector locus* (*CEL*) is a conserved genomic region in *Pseudomonas syringae* strains that carries several virulence determinants. There are 12 ORFs in the *CEL* of *P. syringae* pv. *tomato* (*Pst*) strain DC3000 which correspond to the following genes: 1 = *PSPTO_1367*, 2 = *PSPTO_1368*, 3 = *shcN*, N1 = *hopN1*, 5 = *PSPTO_1371*, AA1-1 = *hopAA1-1*, W1 = *hrpW1*, 8 = *shcM*, *hopM1*, 10 = *shcE*, *avrE1*, 12 = *PSPTO_1378*. Chaperones are shown in light green while bacterial effectors are shown in dark green. Arrows indicate the direction of transcription. Overlapping arrows show the presence of two operons in the *CEL*. *Pst* DC3000 NCBI reference sequence number is NC_004578. The bar at the bottom of the image represents a 1 kb distance. Image is drawn to scale.

over expressed in tomato (Munkvold *et al.* 2008) and functions redundantly with *PSPTO4723* (a non effector gene which is not encoded in the CEL) in promoting disease-associated chlorosis (Munkvold *et al.* 2009).

Other effectors

HopAO1 is an effector with tyrosine phosphatase activity *in vitro*. This activity is required for HopAO1 function since mutation of cysteine 378 not only abolished tyrosine phosphatase activity but the respective mutant allele, when over-expressed in *Pst* Δ*hopAO1*, also failed to restore to wild-type levels the reduced bacterial growth of *Pst* Δ*hopAO1* in tomato (Espinosa *et al.* 2003).

There appears to be a hierarchical mode of action of *Pst* effectors *in planta*. In *N. benthamiana*, AvrPto or AvrPtoB alone increase the growth of a *Pst* effectorless mutant (*Pst* Δ28E) while hopM1 or AvrE1 have no effect, unless AvrPto or AvrPtoB are also present (Cunnac *et al.* 2011). This suggest that the REG comprised of AvrPto and AvrPtoB needs to be deployed first to interfere with PRR complexes before the AvrE1/HopM1 REG can have its effect on virulence. Remarkably, a minimum set of only eight effectors, out of 28, is all that is needed to restore near full bacterial growth to *Pst* Δ28E in *N. benthamiana* highlighting possible extensive effector functional redundancy *in planta* (Cunnac *et al.* 2011).

Effector-triggered immunity in the Solanaceae

The gene-for-gene model was first proposed by H. H. Flor. It asserts that for every effector gene (also known as avirulence - *Avr* - gene) in the pathogen there may exist a corresponding resistance (*R*) gene in the host. When both the avirulence and resistance proteins are present in a host-pathogen interaction, resistance (usually accompanied by a HR) ensues (Flor 1971).

Pto

Pto is a gene that was introgressed into *S. lycopersicum* from the wild tomato species *S. pimpinellifollium*. So far, *Pto* is the only *R* gene against *Pst* found in tomato and thus it has been extensively introgressed into many processing tomato varieties around the world. Pto interacts and confers resistance against the sequence unrelated *Pst* effectors AvrPto and AvrPtoB (Kim *et al.* 2002; Figure 1.5).

In addition to *Pto*, the Pto region encodes 5 paralogs of *Pto* (*PtoA*, *Fen*, *PtoC*, *PtoD*, and the pseudogene *PtoF*) and *Prf* (Figure 1.6). It is not uncommon for *R* genes to be in clusters with multiple paralogs which could potentially recombine with each other to give rise to new recognition specificities. Except for *PtoA* and *PtoF*, all the other genes in the *Pto* locus are transcribed in tomato leaves. Pto and its paralogs encode for protein kinases of which only Pto and Fen have been shown to have kinase activity *in vitro* (Loh and Martin 1995; Chang *et al.* 2002).

Figure 1.5. Pto and Fen recognition of bacterial effectors AvrPto and AvrPtoB in tomato. *Pseudomonas syringae* pv. *tomato* (*Pst*) effectors AvrPto and AvrPtoB are delivered via the type III secretion system (T3SS) into the plant cell where they are detected by the host immune surveillance system. The resistance protein Pto, a kinase, physically interacts with both effectors and in concert with the NBS LRR protein Prf elicits effector-triggered immunity (ETI) that ultimately results in a defense response including the hypersensitive response (HR). Fen is a Pto-related protein kinase that recognizes the N-terminus of AvrPtoB ($AvrPtoB_{1-387}$) and requires Prf to trigger ETI. However, if Pto is absent, full length AvrPtoB targets Fen for polyubiquitination and proteasomal degradation to abolish ETI. Pto, Fen and AvrPto have all been shown to be myristoylated *in planta* and this post-translational modification contributes to their activities.

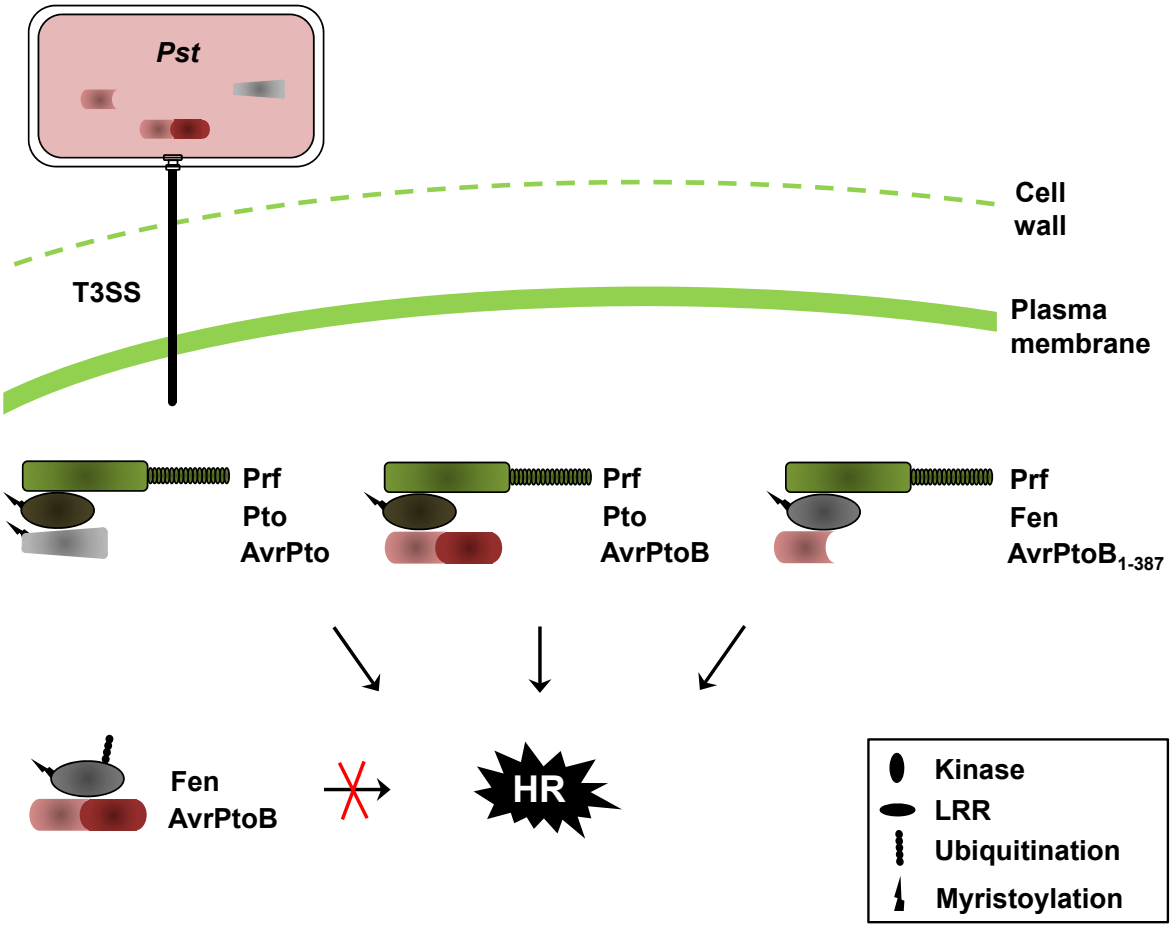
Pst
Cell wall
T3SS
Plasma membrane
Prf
Pto
AvrPto
Prf
Pto
AvrPtoB
Prf
Fen
AvrPtoB1-387
Fen
AvrPtoB
HR
Kinase
LRR
Ubiquitination
Myristoylation

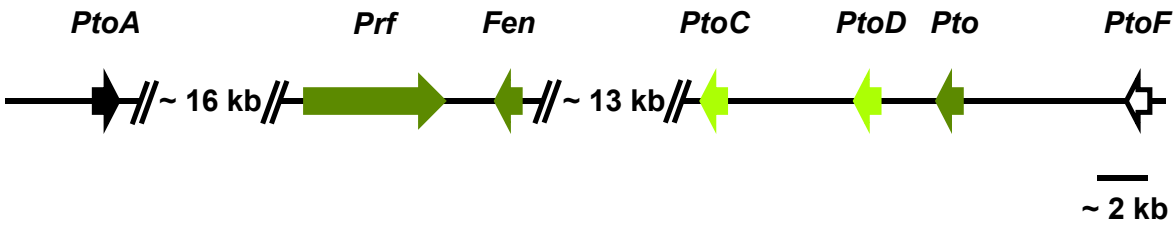

Figure 1.6. Tomato cultivar Rio Grande *Pto* haplotype genomic organization. The *Pto* locus has been introgressed into tomato cultivar Rio Grande from *Solanum pimpinellifollium* to confer resistance against *Pseudomonas syringae* pv. *tomato* (*Pst*). There are 5 paralogs of *Pto* also present in the *Pto* haplotype, one of which is a pseudogene (*PtoF*, shown in white). Genes transcribed in tomato are indicated in green, with arrows pointing in the direction of transcription. Genes known to be involved in resistance against *Pst* expressing AvrPto or AvrPtoB effectors are shown in dark green (Pto, Fen and Prf). The Genbank number for the Pto haplotype is AF220602. The bar at the bottom of the image represents a 2 kb distance. Image is drawn to scale.

Pto is potentially myristoylated, as it carries the expected motif for this modification at its N terminus (Martin *et al.* 1993). Myristoylation is typically associated with localization of the modified protein to the plasma membrane. However, when Pto is expressed under its native promoter in *N. benthamiana* its localization appears to be cytoplasmic, even though it was shown that Pto can be myristoylated *in planta* (de Vries *et al.* 2006). This post-translational modification may therefore be important for Pto signaling rather than for its localization (de Vries *et al.* 2006). In transgenic tomatoes (cultivar Moneymaker, which lacks *Pto*) expressing Pto under its own promoter, mutation of the amino acid to which the myristoyl group attaches in Pto diminished its recognition of AvrPto but not of AvrPtoB. Expressing a kinase-inactive variant of Pto abolished all recognition of AvrPto and AvrPtoB, indicating that amino acids required for kinase activity are essential for signaling, while those for myristoylation are not (Balmuth and Rathjen 2007).

The crystal structures of the complexes between Pto and AvrPto and between Pto and AvrPtoB have been solved (Xing *et al.* 2007; Dong *et al.* 2009) revealing two interaction surfaces in each complex. One of the contact interfaces of Pto with either effector is shared between the complexes, which is surprising considering that AvrPto and AvrPtoB have such distinct structural folds (Dong *et al.* 2009). This shared interface surface involves the Pto P + 1 loop, a region adjacent of the kinase activation loop of Pto. AvrPto interacts with this P + 1 loop through its **Ω** loop, a domain also necessary for AvrPto virulence activity *in planta* (Yeam *et al.* 2009), and causes the kinase activity of Pto to be inhibited

in vitro (Xing *et al.* 2007). Mutations at the P + 1 loop of Pto result in an effector-independent constitutive HR phenotype that requires Prf. It is believed that Pto both 'primes' Prf for activation and then holds Prf in an inactive state for signaling. Interaction of Pto with either effector relieves this inhibitory effect, therefore triggering the ETI signaling cascade. Kinase activity is not essential for this effect *per se*, but the structural conformation of amino acids in this region are, since several kinase inactive mutants still cause constitutive cell death (Xing *et al.* 2007).

Fen

Fen is a kinase encoded by a member of the *Pto* family that confers sensitivity to the insecticide Fenthion. Fen is also an R protein which recognizes the N-terminus of AvrPtoB (AvrPtoB$_{1-387}$; Abramovitch *et al.* 2003). The structure of the C-terminal domain of AvrPtoB was solved and unexpectedly, it had a similar fold to that of eukaryotic E3-ubiquitin ligases, enzymes involved in attachment of ubiquitin molecules to proteins to signal them for proteasomal degradation (Janjusevic *et al.* 2006). After the N-terminus of AvrPtoB has bound Fen, the C-terminus of AvrPtoB can ubiquitinate and target Fen for proteasomal degradation while Pto is recalcitrant to this activity (Rosebrock *et al.* 2007; Ntoukakis *et al.* 2009). Therefore, in tomato plants carrying Fen but lacking Pto, full length AvrPtoB is a *Pst* pathogenicity determinant (Figure 1.5).

In wild tomato species, Fen recognition of the N-terminus of AvrPtoB is more common than Pto resistance to full length AvrPto and AvrPtoB. It is tempting to

speculate that the *Fen* gene arose first and that after AvrPtoB acquired the C-terminal E3-ligase domain, *Pto* evolved. This is further supported by the fact that AvrPtoB truncations which do not carry a C-terminal domain exist in certain *P.* syringae strains in nature (Lin *et al.* 2006).

Fen causes cell death when overexpressed in *N. benthamiana*, a phenotype that resembles the one observed when Pto carrying mutations at the P + 1 loop is overexpressed. Cell death requires Fen kinase activity and an intact putative myristoylation site, similar to the requirements shown for Pto signaling in *N. benthamiana* (Mucyn *et al.* 2009).

Prf

Prf is a nucleotide binding site (NBS)-LRR protein, the largest class of R proteins. *Prf* is located in the *Pto* locus, immediately downstream of *Fen*. It is absolutely required for both Pto and Fen-mediated resistance.

When expressed under their own native promoters in *N. benthamiana*, the Prf and Pto proteins physically interact with each other and form higher molecular weight complexes (Mucyn *et al.* 2006). Prf interaction with Pto requires the N-terminus domain of Prf (which lies outside of the NBS or LRR regions) and induces Pto auto-phosphorylation (Mucyn *et al.* 2006). Prf interaction with Fen is similar to that with Pto, showing the same requirements for Prf N-terminus and causing the same post-translational modifications (auto-phosphorylation) in Fen (Mucyn *et al.* 2009). The higher molecular weight complexes observed for Prf in *N. benthamiana* are also observed in tomato and comprise not only Prf

and Pto, but also Fen, PtoC and possibly PtoD, all of which could contribute to effector recognition diversification (Gutierrez *et al.* 2010).

Races of Pseudomonas syringae pv. tomato

Pst can be classified into two races, depending on the recognition of a particular strain by a plant carrying the *Pto* gene. Race 0 encompasses those strains that are recognized by Pto due to the presence of a functional AvrPto or AvrPtoB while race 1 consists of those strains that are not recognized by *Pto* carrying tomatoes.

The presence of the gene coding for *avrPto* or *avrPtoB* is not sufficient to determine if a strain is race 0. For instance, *Pst* T1 is a race 1 strain that lacks *avrPto* and although it expresses *avrPtoB* in a hrp-dependent manner, AvrPtoB protein does not accumulate allowing *Pst* T1 to be virulent in *Pto*-expressing tomato lines (Lin *et al.* 2006). Isolation and evaluation of the presence of *avrPto* and *avrPtoB* in nineteen *Pst* race 1 strains from California, U.S.A. revealed that even though all strains encoded *avrPtoB*, as with *Pst* T1, AvrPtoB protein could not be detected in any of these strains. Nonetheless, there seemed to be a mild recognition by Pto of these strains, as they grew better on tomatoes lacking *Pto* or when their corresponding *avrPtoB* gene was deleted. All the California race 1 strains that expressed AvrPto (which were only about 25 % of the strains) had key amino acids in the effector necessary for interaction with Pto mutated and therefore, were unable of being recognized by Pto (Kunkeaw *et al.* 2010). It could potentially become problematic for tomato growers if these mutations in

AvrPto become prevalent in *Pst* strains since this could render Pto-mediated resistance ineffective.

ETI is involved in non-host resistance to Pseudomonas syringae pathovars

P. syringae has many pathovars of which only a few are able to infect tomato in the field. It is possible, however, to artificially inoculate tomato plants with several pathovars and reproduce their pathovar-specific symptoms on tomato, although the growth and symptoms produced by these bacteria are reduced relative to those observed by a true pathovar *tomato* strain (Lin and Martin 2007).

Ten *P. syringae* pathovars were evaluated for the presence of *avrPto* or *avrPtoB* genes. Most pathovars carried *avrPto* or *avrPtoB* and as such, were able to grow better on tomato plants lacking a functional Pto pathway. Therefore, Pto-mediated recognition may restrict the ability of *P. syringae* pathovars to cause disease in tomato (Lin and Martin 2007).

Effector-triggered immunity signaling pathways in the Solanaceae

MAPK cascades

MAPK cascades contribute to transduce extracellular signals to transcription factors for the proper activation of defense responses (Pitzschke *et al.* 2009). In its simplest form, a MAPK cascade consists of a MAPK kinase kinase (MAPKKK) phosphorylating a MAPK kinase (MAPKK) which in turn phosphorylates a

MAPK which ultimately will alter the regulation or localization of transcription factors and other defense-associated proteins (Figure 1.7).

MAPKKKα is a protein kinase that contributes to signal transduction in both ETI and disease development in the Solanaceae. RNAi of *NbMAPKKK*α in *N. benthamiana* compromises the HR caused by recognition of AvrPto by Pto and also that of *C. fulvum* Avr9 by Cf-9. Furthermore, silencing of *SlMAPKKK*α in tomato decreases *Pst* disease symptoms and growth (del Pozo *et al.* 2004). In addition to MAPKKKα, the HR signaling pathway activated by recognition of AvrPto by Pto requires the MAPKKs SlMKK2 and SlMKK3 and the MAPKs SlMPK3 and SlNTF6 (Ekengren *et al.* 2003).

SlMAPKKKα interacts with and requires for proper function the regulatory 14-3-3 protein, SlTFT7. RNAi of *NbTFT7* in *N. benthamiana* compromises the HR induced by a variety of effector/R protein combinations, including that of AvrPto/Pto (Oh *et al.* 2010). Since SlTFT7 can also interact with SlMKK2, it is possible that SlTFT7 acts as a scaffold to promote efficient signal transfer during MAPK cascades (Oh and Martin 2011).

Another MAPKKK involved in ETI is SlMAPKKK**ε**. RNAi of *SlMAPKKK***ε** compromised the Pto resistance pathway to *Pst* and resistance to *X. campestris* pv. *vesicatoria* expressing the effectors AvrXv3 and AvrRxv. Epistasis experiments determined that MAPKK NbMEK2 (the SlMKK2 ortholog) and MAPKs NbSIPK and NbWIPK (the SlMPK3 orthologs) are involved in the NbMAPKKK**ε** signaling pathway (Melech-Bonfil and Sessa 2010). As noted

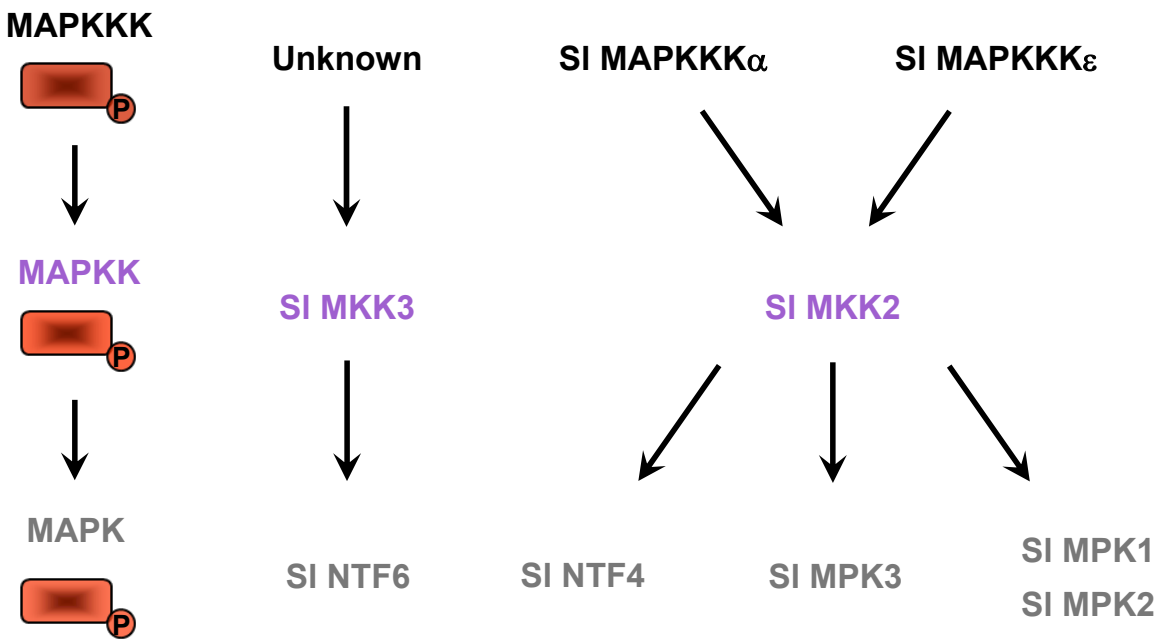

Figure 1.7. Tomato mitogen-activated protein kinase cascades. Mitogen-activated protein kinase (MAPK) cascades are used to transduce extracellular signals for the activation of defense responses. A MAPK phosphorelay module consists of a MAPK kinase kinase (MAPKKK), a MAPK kinase (MAPKK) and a MAPK. Different tomato MAPK cascades are shown, the relationships of which have been determined either biochemically or by epistasis experiments. MAPKKK are depicted in black, MAPKK in purple and MAPK in grey.

earlier, NbSIPK and NbWIPK are also involved in PTI signaling responses after flagellin detection (Segonzac *et al.* 2011).

The signaling cascade after NbMEK2 activation involves the MAPKs NbSIPK, NbWIPK and NbNTF4. These three MAPKs interacted with and phosphorylated *in planta* the transcription factor NbWRKY8, revealing a link between MAPK cascades and defense gene regulation. Simultaneous knock down by RNAi of these three MAPKs in *N. benthamiana* suppressed phosphorylation of NbWRY8 by constitutively active NtMEK2^{DD} and increased susceptibility to oomycete and fungal pathogens. This increased susceptibility was also observed when *NbWRKY8* was silenced, although the effect was smaller (Ishihama *et al.* 2011). Expression of constitutively active NtMEK2^{DD} causes a HR in plants. This PCD response requires light and ROS production by the chloroplasts and is characterized by loss of membrane potential, electrolyte leakage and tissue dehydration (Liu *et al.* 2007).

Chaperones

NBS-LRR proteins, many of which are involved in immunity require for their proper regulation and maintenance of a recognition-competent state, the chaperone HSP90 and its co-chaperones SGT1 and RAR1 (Kadota *et al.* 2009). In transgenic *N. benthamiana* plants overexpressing Pto, RNAi of *NbHSP90* and of *NbSGT1* compromises ETI to *P. syringae* pv. *tabaci* expressing AvrPto, probably through their effect on Prf (Peart *et al.* 2002; Lu *et al.* 2003). *NbSGT1* silencing compromises not only the HR caused by AvrPto recognition of Pto,

but also by a variety of HR inducers including INF1 from *Phytophthora infestans* and Avr9 and Tobacco Mosaic Virus (TMV) recognition by Cf-9 and N, respectively (Peart *et al.* 2002).

Chaperones could be directly implicated in stability and accumulation of proteins involved in ETI. There was a reduction on Rx (a NBS-LRR protein) protein accumulation after silencing of *NbHSP90* in *N. benthamiana* plants expressing Rx which correlated with a decrease in resistance to PVX, highlighting the importance of chaperones in ETI (Lu *et al.* 2003).

Other signaling components

ROS production is required for the ETI response. NADPH oxidases (designated as RBOH in plants) are enzymes required for this ROS production (Torres *et al.* 2002). Two calcium-dependent protein kinases (CDPK) from potato, StCDPK4 and StCDPK5, have been shown to phosphorylate StRBOHB *in vitro*. Overexpression of StCDPK5 in *N. benthamiana* triggers ROS production possibly by phosphorylating and activating RBOHB since VIGS of *NbRBOHB* abrogates this response (Kobayashi *et al.* 2007).

The hormone salicylic acid regulates multiple defense signaling networks. NPR1 interacts with TGA transcription factors when SA levels increase to activate immunity SA-responsive promoters (Pieterse and van Loon 2004). The Pto resistance pathway is dependent on NPR1 and TGA transcription factors as RNAi of *SlNPR1*, *SlTGA1a* and *SlTGA2.2* caused loss of resistance to *Pst* expressing AvrPto in tomato (Ekengren *et al.* 2003).

Autophagic pathways have been reported to be involved in controlling the spread of the HR. In *N. benthamiana* plants silenced for the homologs of certain autophagic genes from yeast (*NbBeclin1* (*NbAtg6*), *NbPI3K* (*NbVPS34*, a phosphoinositide 3-kinase), *NbATG3* and *NbATG7*) unrestricted cell death occurs when N-mediated resistance against TMV is activated. *Beclin*-silenced plants also show spreading necrosis when Pto is recognized by AvrPto or Cf9 by Avr9. Furthermore, no autolysosomal structures, indicative of cells undergoing autophagic processes, are observed in these silenced plants but are observed in empty vector control plants after the onset of the HR (Liu *et al.* 2005).

Conclusions and Future prospects

We have much yet to learn from the interaction of *Pst* and its host, tomato. We are probably not even close to identifying the full spectrum of PAMPs present in *Pst* or in any bacterium and less than a handful of PRRs have been identified to date. Also, even though the first genome of *Pst* came out more than 8 years ago (Buell *et al.* 2003), we still do not fully understand the function of most effectors - for some, there is not even a report to date of a virulence-promoting phenotype.

PTI and ETI, the two forms of immunity present in plants, are usually differentiated by the amplitude of the response observed, with the latter also causing an HR while the former does not. However, for flagellin, the best characterized PAMP recognized by plants; it has been shown that infiltration into *N. benthamiana* leaves causes cell death (Hann and Rathjen 2007). Since

flagellin causes cell death, can it still be considered a PAMP? The conservation of the PTI eliciting region of flagellin may not be used as the determinant to define it as a PAMP, as many bacteria (e.g., *Agrobacterium tumefaciens*, *Xcc*) have this region altered so that their flagellin is unable to be detected by the plant immune system (Felix *et al.* 1999; Sun *et al.* 2006). Also, if an effector is conserved in a whole class of microbes (e.g., AvrE1, which is conserved in most strains of *P. syringae*; Baltrus *et al.* 2011) and is recognized by the plant immune system, should this effector be considered a PAMP? Does a PAMP need not to have any role in virulence and if so, then, would the TTSS still be considered a PAMP? What then, defines a PAMP? Even though natural processes are a continuum, it is important to discern if PTI and ETI are indeed two mechanistically distinct processes. This will help in the identification of approaches for enhancing these two forms of plant immunity to decrease pathogen infection and enhance agricultural productivity.

PTI is known to halt the invasion of potential pathogens. PTI probably relies on a multi-layered defense mechanism, including the recently reported suppression of effector delivery (Crabill *et al.* 2010; Oh *et al.* 2010) and phytoalexin production up-regulation after PTI induction, phytoalexins being known to have *in vitro* anti-microbial activity (Millet *et al.* 2010). Understanding the executors of PTI and how pathogen colonization is suppressed is still one of the tasks at hand of which almost nothing is known.

Why does *Pst* have so many effectors? We and others have speculated that the redundancy in effector function allows effectors to become deleted from

bacteria without any loss in virulence, due to targeting of the same immunity processes by different effectors at the same time. The answer to the above question will not be fulfilled until the function of most effectors is characterized, a task that will require many more years of research.

Pto has been widely used to control the occurrence of tomato bacterial speck in processing tomatoes. Epidemics of bacterial speck are quite rare and so major yield losses due to this disease are not common. Why *Pto* has remained so effective in the field in controlling bacterial speck for the last 30 years while many resistance genes are rendered useless after a few years of being deployed is unknown. Is this because there are no other effectors in *Pst* besides AvrPto and AvrPtoB that belong to the same REG targeting early PTI responses; so that these two effectors are conserved despite the presence of *Pto* in a large acreage of cultivated tomato? Alterations of key amino acids for Pto recognition or suppression of AvrPtoB protein expression coupled with appropriate environmental conditions, might allow new strains to evade Pto recognition and favor a major outbreak of this disease (Lin *et al.* 2006; Kunkeaw *et al.* 2010). Therefore, there is the need to look for new resistance genes to *Pst* in the wide pool of wild relatives of tomato; although so far, *Pto* has been the only gene identified.

Taking advantage of new technologies being developed is also fundamental for the understanding of *Pst*-tomato interactions. Next generation sequencing can provide valuable insight into exploring hypothesis for future research. RNA-seq with its decreasing cost, its deep coverage of the transcriptome and

the lack of reliance on known genomic sequence (although a reference genome is desirable) might help understand some of the processes that occur during PTI and ETI. Sequencing the genome of wild tomato plants, using as a reference genome that of cultivated tomato, might help uncover regions with new resistance specificities against *Pst* and other pathogens. These new *R* genes might be introduced into existing commercial varieties in order to have better control on diseases and decrease the reliance on chemicals for pathogen control.

Acknowledgments

We thank Anne Rea for her helpful suggestions during the preparation of this manuscript. A. Velásquez's research is supported by National Science Foundation grant IOB-0841807.

REFERENCES

Abramovitch R.B., Kim Y.J., Chen S., Dickman M.B., and Martin G.B. 2003. *Pseudomonas* type III effector AvrPtoB induces plant disease susceptibility by inhibition of host programmed cell death. EMBO J 22:60-69.

Almeida N.F., Yan S., Lindeberg M., Studholme D.J., Schneider D.J., Condon B., Liu H., Viana C.J., Warren A., Evans C., Kemen E., Maclean D., Angot A., Martin G.B., Jones J.D., Collmer A., Setubal J.C., and Vinatzer B.A. 2009. A draft genome sequence of *Pseudomonas syringae* pv. *tomato* T1 reveals a type III effector repertoire significantly divergent from that of *Pseudomonas syringae* pv. *tomato* DC3000. Mol Plant Microbe Interact 22:52-62.

Anderson J.C., Pascuzzi P.E., Xiao F., Sessa G., and Martin G.B. 2006. Host-mediated phosphorylation of type III effector AvrPto promotes *Pseudomonas* virulence and avirulence in tomato. Plant Cell 18:502-514.

Badel J.L., Nomura K., Bandyopadhyay S., Shimizu R., Collmer A., and He S.Y. 2003. *Pseudomonas syringae* pv. *tomato* DC3000 HopPtoM (CEL ORF3) is important for lesion formation but not growth in tomato and is secreted and translocated by the Hrp type III secretion system in a chaperone-dependent manner. Mol Microbiol 49:1239-1251.

Badel J.L., Shimizu R., Oh H.S., and Collmer A. 2006. A *Pseudomonas syringae* pv. *tomato avrE1/hopM1* mutant is severely reduced in growth and lesion formation in tomato. Mol Plant Microbe Interact 19:99-111.

Balmuth A., and Rathjen J.P. 2007. Genetic and molecular requirements for function of the Pto/Prf effector recognition complex in tomato and *Nicotiana benthamiana*. Plant J 51:978-990.

Baltrus D.A., Nishimura M.T., Romanchuk A., Chang J.H., Mukhtar M.S., Cherkis K., Roach J., Grant S.R., Jones C.D., and Dangl J.L. 2011 Dynamic evolution of pathogenicity revealed by sequencing and comparative genomics of 19 *Pseudomonas syringae* isolates. PLoS Pathog 7:e1002132.

Bender C.L., Alarcon-Chaidez F., and Gross D.C. 1999. *Pseudomonas syringae* phytotoxins: Mode of action, regulation, and biosynthesis by peptide and polyketide synthetases. Microbiol Mol Biol Rev 63:266-292.

Bender C.L., Malvick D.K., and Mitchell R.E. 1989. Plasmid-mediated production of the phytotoxin coronatine in *Pseudomonas syringae* pv. *tomato*. J Bacteriol 171:807-812.

Bent A.F., and Mackey D. 2007. Elicitors, effectors, and R genes: the new paradigm and a lifetime supply of questions. Annu Rev Phytopathol 45:399-436.

Bignell D.R., Seipke R.F., Huguet-Tapia J.C., Chambers A.H., Parry R.J., and Loria R. 2010. *Streptomyces scabies* 87-22 contains a coronafacic acid-like biosynthetic cluster that contributes to plant-microbe interactions. Mol Plant Microbe Interact 23:161-175.

Boller T., and Felix G. 2009. A renaissance of elicitors: perception of microbe-associated molecular patterns and danger signals by pattern-recognition receptors. Annu Rev Plant Biol 60:379-406.

Boutrot F., Segonzac C., Chang K.N., Qiao H., Ecker J.R., Zipfel C., and Rathjen J.P. 2010. Direct transcriptional control of the *Arabidopsis* immune receptor FLS2 by the ethylene-dependent transcription factors EIN3 and EIL1. Proc Natl Acad Sci U.S.A. 107:14502-14507.

Buell C.R., Joardar V., Lindeberg M., Selengut J., Paulsen I.T., Gwinn M.L., Dodson R.J., Deboy R.T., Durkin A.S., Kolonay J.F., Madupu R., Daugherty S., Brinkac L., Beanan M.J., Haft D.H., Nelson W.C., Davidsen T., Zafar N., Zhou L., Liu J., Yuan Q., Khouri H., Fedorova N., Tran B., Russell D., Berry K., Utterback T., Van Aken S.E., Feldblyum T.V., D'Ascenzo M., Deng W.L., Ramos A.R., Alfano J.R., Cartinhour S., Chatterjee A.K., Delaney T.P., Lazarowitz S.G., Martin G.B., Schneider D.J., Tang X., Bender C.L., White O., Fraser C.M., and Collmer A. 2003. The complete genome sequence of the *Arabidopsis* and tomato pathogen *Pseudomonas syringae* pv. *tomato* DC3000. Proc Natl Acad Sci U.S.A. 100:10181-10186.

Buist G., Steen A., Kok J., and Kuipers O. P. 2008. LysM, a widely distributed protein motif for binding to (peptido)glycans. Mol Microbiol 68:838-847.

Cai R., Lewis J., Yan S., Liu H., Clarke C.R., Campanile F., Almeida N.F., Studholme D.J., Lindeberg M., Schneider D., Zaccardelli M., Setubal J.C., Morales-Lizcano N.P., Bernal A., Coaker G., Baker C., Bender C.L., Leman S., and Vinatzer B.A. 2011. The Plant Pathogen *Pseudomonas syringae* pv. *tomato* Is Genetically Monomorphic and under Strong Selection to Evade Tomato Immunity. PLoS Pathog 7:e1002130.

Chakravarthy S., Velásquez A.C., Ekengren S.K., Collmer A., and Martin G.B. 2010. Identification of *Nicotiana benthamiana* genes involved in pathogen-associated molecular pattern-triggered immunity. Mol Plant Microbe Interact 23:715-726.

Chang J.H., Tai Y.S., Bernal A.J., Lavelle D.T., Staskawicz B.J., and Michelmore R.W. 2002. Functional analyses of the *Pto* resistance gene family in tomato and the identification of a minor resistance determinant in a susceptible haplotype. Mol Plant Microbe Interact 15:281-291.

Cheng W., Munkvold K.R., Gao H., Mathieu J., Schwizer S., Wang S., Yan Y., Wang J., Martin G.B., and Chai J. 2011. The AvrPtoB-BAK1 complex reveals two structurally similar kinase-interacting domains in a single type III effector. Cell Host Microbe. *In press*.

Chinchilla D., Zipfel C., Robatzek S., Kemmerling B., Nurnberger T., Jones J.D., Felix G., and Boller T. 2007. A flagellin-induced complex of the receptor FLS2 and BAK1 initiates plant defence. Nature 448:497-500.

Cohn J.R., and Martin G.B. 2005. *Pseudomonas syringae* pv. *tomato* type III effectors AvrPto and AvrPtoB promote ethylene-dependent cell death in tomato. Plant J 44:139-154.

Cornelis G.R. 2006. The type III secretion injectisome. Nat Rev Microbiol 4:811-825.

Crabill E., Joe A., Block A., van Rooyen J.M., and Alfano J.R. 2010. Plant immunity directly or indirectly restricts the injection of type III effectors by the *Pseudomonas syringae* type III secretion system. Plant Physiol 154:233-244.

Cunnac S., Chakravarthy S., Kvitko B.H., Russell A.B., Martin G.B., and Collmer A. 2011. Genetic disassembly and combinatorial reassembly identify a minimal functional repertoire of type III effectors in *Pseudomonas syringae*. Proc Natl Acad Sci U.S.A. 108:2975-2980.

de Vries J.S., Andriotis V.M.E., Wu A.J., and Rathjen J.P. 2006. Tomato *Pto* encodes a functional N-myristoylation motif that is required for signal transduction in *Nicotiana benthamiana*. Plant J 45:31-45.

DebRoy S., Thilmony R., Kwack Y.B., Nomura K., and He S.Y. 2004. A family of conserved bacterial effectors inhibits salicylic acid-mediated basal immunity and promotes disease necrosis in plants. Proc Natl Acad Sci U.S.A. 101:9927-9932.

del Pozo O., Pedley K.F., and Martin G.B. 2004. MAPKKKalpha is a positive regulator of cell death associated with both plant immunity and disease. EMBO J 23:3072-3082.

Dong J., Xiao F., Fan F., Gu L., Cang H., Martin G.B., and Chai J. 2009. Crystal structure of the complex between *Pseudomonas* effector AvrPtoB and the tomato Pto kinase reveals both a shared and a unique interface compared with AvrPto-Pto. Plant Cell 21:1846-1859.

Ekengren S.K., Liu Y., Schiff M., Dinesh Kumar S.P., and Martin G.B. 2003. Two MAPK cascades, NPR1, and TGA transcription factors play a role in Pto-mediated disease resistance in tomato. Plant J 36:905-917.

Espinosa A., Guo M., Tam V.C., Fu Z.Q., and Alfano J.R. 2003. The *Pseudomonas syringae* type III-secreted protein HopPtoD2 possesses protein tyrosine phosphatase activity and suppresses programmed cell death in plants. Mol Microbiol 49:377-387.

Felix G., and Boller T. 2003. Molecular sensing of bacteria in plants. The highly conserved RNA-binding motif RNP-1 of bacterial cold shock proteins is recognized as an elicitor signal in tobacco. J Biol Chem 278:6201-6208.

Felix G., Duran J.D., Volko S., and Boller T. 1999. Plants have a sensitive perception system for the most conserved domain of bacterial flagellin. Plant J 18:265-276.

Flor H.H. 1971. Current status of the gene-for-gene concept. Annu Rev Phytopathol 9:275-296.

Gimenez-Ibanez S., Hann D.R., Ntoukakis V., Petutschnig E., Lipka V., and Rathjen J.P. 2009a. AvrPtoB targets the LysM receptor kinase CERK1 to promote bacterial virulence on plants. Curr Biol 19:423-429.

Gimenez-Ibanez S., Ntoukakis V., and Rathjen J.P. 2009b. The LysM receptor kinase CERK1 mediates bacterial perception in *Arabidopsis*. Plant Signal Behav 4:539-541.

Gómez-Gómez L., Bauer Z., and Boller T. 2001. Both the extracellular leucine-rich repeat domain and the kinase activity of FLS2 are required for flagellin binding and signaling in *Arabidopsis*. Plant Cell 13:1155-1163.

Gust A.A., Biswas R., Lenz H.D., Rauhut T., Ranf S., Kemmerling B., Gotz F., Glawischnig E., Lee J., Felix G., and Nurnberger T. 2007. Bacteria-derived peptidoglycans constitute pathogen-associated molecular patterns triggering innate immunity in *Arabidopsis*. J Biol Chem 282:32338-32348.

Gutierrez J.R., Balmuth A.L., Ntoukakis V., Mucyn T.S., Gimenez-Ibanez S., Jones A.M., and Rathjen J.P. 2010. Prf immune complexes of tomato are oligomeric and contain multiple Pto-like kinases that diversify effector recognition. Plant J 61:507-518.

Hann D.R., and Rathjen J.P. 2007. Early events in the pathogenicity of *Pseudomonas syringae* on *Nicotiana benthamiana*. Plant J 49:607-618.

Heese A., Hann D.R., Gimenez-Ibanez S., Jones A.M., He K., Li J., Schroeder J.I., Peck S.C., and Rathjen J.P. 2007. The receptor-like kinase SERK3/BAK1 is a central regulator of innate immunity in plants. Proc Natl Acad Sci U.S.A. 104:12217-12222.

Hirano S.S., and Upper C.D. 2000. Bacteria in the leaf ecosystem with emphasis on *Pseudomonas syringae* – a pathogen, ice nucleus, and epiphyte. Microbiol Mol Biol Rev 64:624-653.

Ishihama N., Yamada R., Yoshioka M., Katou S., and Yoshioka H. 2011. Phosphorylation of the *Nicotiana benthamiana* WRKY8 transcription factor by MAPK functions in the defense response. Plant Cell 23:1153-1170.

Janjusevic R., Abramovitch R.B., Martin G.B., and Stebbins C.E. 2006. A bacterial inhibitor of host programmed cell death defenses is an E3 ubiquitin ligase. Science 311:222-226.

Jones A.M., and Wildermuth M.C. 2011. The phytopathogen *Pseudomonas syringae* pv. *tomato* DC3000 has three high-affinity iron-scavenging systems functional under iron limitation conditions but dispensable for pathogenesis. J Bacteriol 193:2767-2775.

Kadota Y., Shirasu K., and Guerois R. 2010. NLR sensors meet at the SGT1-HSP90 crossroad. Trends Biochem Sci 35:199-207.

Katsir L., Schilmiller A.L., Staswick P.E., He S.Y., and Howe G.A. 2008. COI1 is a critical component of a receptor for jasmonate and the bacterial virulence factor coronatine. Proc Natl Acad Sci U.S.A. 105:7100-7105.

Kim Y.J., Lin N.C., and Martin G.B. 2002. Two distinct *Pseudomonas* effector proteins interact with the Pto kinase and activate plant immunity. Cell 109:589-598.

Kobayashi M., Ohura I., Kawakita K., Yokota N., Fujiwara M., Shimamoto K., Doke N., and Yoshioka H. 2007. Calcium-dependent protein kinases regulate the production of reactive oxygen species by potato NADPH oxidase. Plant Cell 19:1065-1080.

Kunkeaw S., Tan S., and Coaker G. 2010. Molecular and evolutionary analyses of *Pseudomonas syringae* pv. *tomato* race 1. Mol Plant Microbe Interact 23:415-424.

Kvitko B.H., Park D.H., Velásquez A.C., Wei C.F., Russell A.B., Martin G.B., Schneider D.J., and Collmer A. 2009. Deletions in the repertoire of *Pseudomonas syringae* pv. *tomato* DC3000 type III secretion effector genes reveal functional overlap among effectors. PLoS Pathog 5:e1000388.

Lacombe S., Rougon-Cardoso A., Sherwood E., Peeters N., Dahlbeck D., van Esse H.P., Smoker M., Rallapalli G., Thomma B.P., Staskawicz B., Jones J.D., and Zipfel C. 2010. Interfamily transfer of a plant pattern-recognition receptor confers broad-spectrum bacterial resistance. Nat Biotechnol 28:365-369.

Li J., Wen J., Lease K.A., Doke J.T., Tax F.E., and Walker J.C. 2002. BAK1, an *Arabidopsis* LRR receptor-like protein kinase, interacts with BRI1 and modulates brassinosteroid signaling. Cell 110:213-222.

Lightfield K.L., Persson J., Brubaker S.W., Witte C.E., von Moltke J., Dunipace E.A., Henry T., Sun Y.H., Cado D., Dietrich W.F., Monack D.M., Tsolis R.M., and Vance R.E. 2008. Critical function for Naip5 in inflammasome activation by a conserved carboxy-terminal domain of flagellin. Nat Immunol 9:1171-1178.

Lin N.C., and Martin G.B. 2007. Pto- and Prf-mediated recognition of AvrPto and AvrPtoB restricts the ability of diverse *Pseudomonas syringae* pathovars to infect tomato. Mol Plant Microbe Interact 20:806-815.

Lin N.C., Abramovitch R.B., Kim Y.J., and Martin G.B. 2006. Diverse AvrPtoB homologs from several *Pseudomonas syringae* pathovars elicit Pto-dependent resistance and have similar virulence activities. Appl Environ Microbiol 72:702-712.

Liu Y., Ren D., Pike S., Pallardy S., Gassmann W., and Zhang S. 2007. Chloroplast-generated reactive oxygen species are involved in hypersensitive response-like cell death mediated by a mitogen-activated protein kinase cascade. Plant J 51:941-954.

Liu Y., Schiff M., Czymmek K., Talloczy Z., Levine B., and Dinesh-Kumar S.P. 2005. Autophagy regulates programmed cell death during the plant innate immune response. Cell 121:567-577.

Loh Y-T., and Martin G.B. 1995. The *Pto* bacterial resistance gene and the *Fen* insecticide sensitivity gene encode functional protein kinases with serine/threonine specificity. Plant Physiol 108:1735-1739.

Lopez-Solanilla E., Bronstein P.A., Schneider A.R., and Collmer A. 2004. HopPtoN is a *Pseudomonas syringae* Hrp (type III secretion system) cysteine protease effector that suppresses pathogen-induced necrosis associated with both compatible and incompatible plant interactions. Mol Microbiol 54:353-365.

Lu D., Lin W., Gao X., Wu S., Cheng C., Avila J., Heese A., Devarenne T.P., He P., and Shan L. 2011. Direct ubiquitination of pattern recognition receptor FLS2 attenuates plant innate immunity. Science 332:1439-1442.

Lu R., Malcuit I., Moffett P., Ruiz M.T., Peart J., Wu A.J., Rathjen J.P., Bendahmane A., Day L., and Baulcombe D.C. 2003. High throughput virus-induced gene silencing implicates heat shock protein 90 in plant disease resistance. EMBO J 22:5690-5699.

Martin G.B. 2011. Suppression and activation of the plant immune system by *Pseudomonas syringae* effectors AvrPto and AvrPtoB. In: Effectors in Plant-Microbe Interactions. Wiley-Blackwell pp. 1-22.

Martin G.B., Brommonschenkel S.H., Chunwongse J., Frary A., Ganal M.W., Spivey R., Wu T., Earle E.D., and Tanksley S.D. 1993. Map-based cloning of a protein kinase gene conferring disease resistance in tomato. Science 262:1432-1436.

Melech-Bonfil S., and Sessa G. 2010. Tomato MAPKKKepsilon is a positive regulator of cell-death signaling networks associated with plant immunity. Plant J 64:379-391.

Melotto M., Underwood W., Koczan J., Nomura K., and He S.Y. 2006. Plant stomata function in innate immunity against bacterial invasion. Cell 126:969-980.

Miao E.A., Mao D.P., Yudkovsky N., Bonneau R., Lorang C.G., Warren S.E., Leaf I.A., and Aderem A. 2010. Innate immune detection of the type III secretion apparatus through the NLRC4 inflammasome. Proc Natl Acad Sci U.S.A. 107:3076-3080.

Millet Y.A., Danna C.H., Clay N.K., Songnuan W., Simon M.D., Werck-Reichhart D., and Ausubel F.M. 2010. Innate immune responses activated in *Arabidopsis* roots by microbe-associated molecular patterns. Plant Cell 22:973-990.

Misas-Villamil J.C., Kolodziejek I., and van der Hoorn R.A. 2011. *Pseudomonas syringae* colonizes distant tissues in *Nicotiana benthamiana* through xylem vessels. Plant J 67:774-782.

Miya A., Albert P., Shinya T., Desaki Y., Ichimura K., Shirasu K., Narusaka Y., Kawakami N., Kaku H., and Shibuya N. 2007. CERK1, a LysM receptor kinase, is essential for chitin elicitor signaling in *Arabidopsis*. Proc Natl Acad Sci U.S.A. 104:19613-19618.

Mucyn T.S., Wu A.J., Balmuth A.L., Arasteh J.M., and Rathjen J.P. 2009. Regulation of tomato Prf by Pto-like protein kinases. Mol Plant Microbe Interact 22:391-401.

Mucyn T.S., Clemente A., Andriotis V.M.E., Balmuth A.L., Oldroyd G.E.D., Staskawicz B.J., and Rathjen J.P. 2006. The tomato NBARC-LRR protein Prf interacts with Pto kinase in vivo to regulate specific plant immunity. Plant Cell 18:2792-2806.

Munkvold K.R., Martin M.E., Bronstein P.A., and Collmer A. 2008. A survey of the *Pseudomonas syringae* pv. *tomato* DC3000 type III secretion system effector repertoire reveals several effectors that are deleterious when expressed in *Saccharomyces cerevisiae*. Mol Plant Microbe Interact 21:490-502.

Munkvold K.R., Russell A.B., Kvitko B.H., and Collmer A. 2009. *Pseudomonas syringae* pv. *tomato* DC3000 type III effector HopAA1-1 functions redundantly with chlorosis-promoting factor PSPTO4723 to produce bacterial speck lesions in host tomato. Mol Plant Microbe Interact 22:1341-1355.

Nam K.H., and Li J. 2002. BRI1/BAK1, a receptor kinase pair mediating brassinosteroid signaling. Cell 110:203-212.

Navarro L., Jay F., Nomura K., He S.Y., and Voinnet O. 2008. Suppression of the microRNA pathway by bacterial effector proteins. Science 321:964-967.

Newman M.A., von Roepenack-Lahaye E., Parr A., Daniels M.J., and Dow J.M. 2002. Prior exposure to lipopolysaccharide potentiates expression of plant defenses in response to bacteria. Plant J 29:487-495.

Nguyen H.P., Yeam I., Angot A., and Martin G.B. 2010. Two virulence determinants of type III effector AvrPto are functionally conserved in diverse *Pseudomonas syringae* pathovars. New Phytol 187:969-982.

Nomura K., DebRoy S., Lee Y.H., Pumplin N., Jones J., and He S.Y. 2006. A bacterial virulence protein suppresses host innate immunity to cause plant disease. Science 313:220-223.

Ntoukakis V., Mucyn T.S., Gimenez-Ibanez S., Chapman H.C., Gutierrez J.R., Balmuth A.L., Jones A.M., and Rathjen J.P. 2009. Host inhibition of a bacterial virulence effector triggers immunity to infection. Science 324:784-787.

Oh C.S., and Martin G.B. 2011. Tomato 14-3-3 protein TFT7 interacts with a MAP kinase kinase to regulate immunity-associated programmed cell death mediated by diverse disease resistance proteins. J Biol Chem 286:14129-14136.

Oh C.S., Pedley K.F., and Martin G.B. 2010. Tomato 14-3-3 protein 7 positively regulates immunity-associated programmed cell death by enhancing protein abundance and signaling ability of MAPKKKalpha. Plant Cell 22:260-272.

Oh H.S., Park D.H., and Collmer A. 2010. Components of the *Pseudomonas syringae* type III secretion system can suppress and may elicit plant innate immunity. Mol Plant Microbe Interact 23:727-739.

Peart J.R., Lu R., Sadanandom A., Malcuit I., Moffett P., Brice D.C., Schauser L., Jaggard D.A.W., Xiao S., Coleman M.J., Dow M., Jones J.D.G., Shirasu K., and Baulcombe D.C. 2002. Ubiquitin ligase-associated protein SGT1 is required for host and nonhost disease resistance in plants. Proc Natl Acad Sci U.S.A. 99:10865-10869.

Peralta I.E., Spooner D.M., and Knapp S. 2009. Taxonomy of wild tomatoes and their relatives (Solanum section Lycopersicoides, sect. Juglandifolia, sect. Lycopersicon; Solanaceae). Syst Bot Monogr 84:1-186.

Petutschnig E.K., Jones A.M.E., Serazetdinova L., Lipka U., Lipka V. 2010. The LysM-RLK CERK1 is a major chitin binding protein in *Arabidopsis thaliana* and subject to chitin-induced phosphorylation. J Biol Chem 285:28902-28911.

Pieterse C.M., and Van Loon L.C. 2004. NPR1: the spider in the web of induced resistance signaling pathways. Curr Opin Plant Biol 7:456-464.

Pitzschke A., Schikora A., and Hirt H. 2009. MAPK cascade signalling networks in plant defence. Curr Opin Plant Biol 12:421-426.

Rico A., and Preston G.M. 2008. *Pseudomonas syringae* pv. *tomato* DC3000 uses constitutive and apoplast-induced nutrient assimilation pathways to catabolize nutrients that are abundant in the tomato apoplast. Mol Plant Microbe Interact 21:269-282.

Robatzek S., Bittel P., Chinchilla D., Kochner P., Felix G., Shiu S.H., and Boller T. 2007. Molecular identification and characterization of the tomato flagellin receptor LeFLS2, an orthologue of *Arabidopsis* FLS2 exhibiting characteristically different perception specificities. Plant Mol Biol 64:539-547.

Robatzek S., Chinchilla D., and Boller T. 2006. Ligand-induced endocytosis of the pattern recognition receptor FLS2 in *Arabidopsis*. Genes Dev 20:537-542.

Roine E., Wei W., Yuan J., Nurmiaho-Lassila E.L., Kalkkinen N., Romantschuk M., and He S.Y. 1997. Hrp pilus: An hrp-dependent bacterial surface appendage produced by *Pseudomonas syringae* pv. *tomato* DC3000. Proc Natl Acad Sci U.S.A. 94:3459-3464.

Rosebrock T.R., Zeng L., Brady J.J., Abramovitch R.B., Xiao F., and Martin G.B. 2007. A bacterial E3 ubiquitin ligase targets a host protein kinase to disrupt plant immunity. Nature 448:370-374.

Roux M., Schwessinger B., Albrecht C., Chinchilla D., Jones A., Holton N., Malinovsky F.G., Tor M., de Vries S., and Zipfel C. 2011. The *Arabidopsis* leucine-rich repeat receptor-like kinases BAK1/SERK3 and BKK1/SERK4 are required for innate immunity to hemibiotrophic and biotrophic pathogens. Plant Cell 23:2440-2455.

Schneider D.J., and Collmer A. 2010. Studying plant-pathogen interactions in the genomics era: beyond molecular Koch's postulates to systems biology. Annu Rev Phytopathol 48:457-479.

Schwessinger B., Roux M., Kadota Y., Ntoukakis V., Sklenar J., Jones A., and Zipfel C. 2011. Phosphorylation-dependent differential regulation of plant growth, cell death, and innate immunity by the regulatory receptor-like kinase BAK1. PLoS Genet 7:e1002046.

Segonzac C., Feike D., Gimenez-Ibanez S., Hann D.R., Zipfel C., and Rathjen J.P. 2011. Hierarchy and roles of pathogen-associated molecular pattern-induced responses in *Nicotiana benthamiana*. Plant Physiol 156:687-699.

Shan L., He P., Li J., Heese A., Peck S.C., Nurnberger T., Martin G.B., and Sheen J. 2008. Bacterial effectors target the common signaling partner BAK1 to disrupt multiple MAMP receptor-signaling complexes and impede plant immunity. Cell Host Microbe 4:17-27.

Shan L., Thara V.K., Martin G.B., Zhou J.M., and Tang X. 2000. The *Pseudomonas* AvrPto protein is differentially recognized by tomato and tobacco and is localized to the plant plasma membrane. Plant Cell 12:2323-2338.

Smith K.D., Andersen-Nissen E., Hayashi F., Strobe K., Bergman M.A., Barrett S.L., Cookson B.T., and Aderem A. 2003. Toll-like receptor 5 recognizes a conserved site on flagellin required for protofilament formation and bacterial motility. Nat Immunol 4:1247-1253.

Sun W., Dunning F.M., Pfund C., Weingarten R., and Bent A.F. 2006. Within-species flagellin polymorphism in *Xanthomonas campestris* pv. *campestris* and its impact on elicitation of *Arabidopsis* FLAGELLIN SENSING2-dependent defenses. Plant Cell 18:764-779.

Thara V.K., Seilaniantz A.R., Deng Y., Dong Y., Yang Y., Tang X., and Zhou J.M. 2004. Tobacco genes induced by the bacterial effector protein AvrPto. Mol Plant Microbe Interact 17:1139-1145.

Torres M.A., Dangl J.L., and Jones J.D. 2002. *Arabidopsis* gp91phox homologues AtrbohD and AtrbohF are required for accumulation of reactive oxygen intermediates in the plant defense response. Proc Natl Acad Sci U.S.A. 99:517-522.

Trujillo M., Ichimura K., Casais C., and Shirasu K. 2008. Negative regulation of PAMP-triggered immunity by an E3 ubiquitin ligase triplet in *Arabidopsis*. Curr Biol 18:1396-1401.

Tsunemi K., Taguchi F., Marutani M., Watanabe-Sugimoto M., Inagaki Y., Toyoda K., Shiraishi T., and Ichinose Y. 2011. Degeneration of hrpZ gene in *Pseudomonas syringae* pv. *tabaci* to evade tobacco defence: an arms race between tobacco and its bacterial pathogen. Mol Plant Pathol 12:709-714.

Uppalapati S.R., Ayoubi P., Weng H., Palmer D.A., Mitchell R.E., Jones W., and Bender C.L. 2005. The phytotoxin coronatine and methyl jasmonate impact multiple phytohormone pathways in tomato. Plant J 42:201-217.

Uppalapati S.R., Ishiga Y., Wangdi T., Kunkel B.N., Anand A., Mysore K.S., and Bender C.L. 2007. The phytotoxin coronatine contributes to pathogen fitness and is required for suppression of salicylic acid accumulation in tomato inoculated with *Pseudomonas syringae* pv. *tomato* DC3000. Mol Plant Microbe Interact 20:955-965.

Wan J., Zhang X.C., Neece D., Ramonell K.M., Clough S., Kim S.Y., Stacey M.G., and Stacey G. 2008. A LysM receptor-like kinase plays a critical role in chitin signaling and fungal resistance in *Arabidopsis*. Plant Cell 20:471-481.

Wang D., Pajerowska-Mukhtar K., Culler A.H., and Dong X. 2007. Salicylic acid inhibits pathogen growth in plants through repression of the auxin signaling pathway. Curr Biol 17:1784-1790.

Wei C.F., Kvitko B.H., Shimizu R., Crabill E., Alfano J.R., Lin N.C., Martin G.B., Huang H.C., and Collmer A. 2007. A *Pseudomonas syringae* pv. *tomato* DC3000 mutant lacking the type III effector HopQ1-1 is able to cause disease in the model plant *Nicotiana benthamiana*. Plant J 51:32-46.

Xiang T., Zong N., Zhang J., Chen J., Chen M., and Zhou J.M. 2011. BAK1 is not a target of the *Pseudomonas syringae* effector AvrPto. Mol Plant Microbe Interact 24:100-107.

Xiang T., Zong N., Zou Y., Wu Y., Zhang J., Xing W., Li Y., Tang X., Zhu L., Chai J., and Zhou J. M. 2008. *Pseudomonas syringae* effector AvrPto blocks innate immunity by targeting receptor kinases. Curr Biol 18:74-80.

Xiao F., Giavalisco P., and Martin G.B. 2007a. *Pseudomonas syringae* type III effector AvrPtoB is phosphorylated in plant cells on serine 258, promoting its virulence activity. J Biol Chem 282:30737-30744.

Xiao F., He P., Abramovitch R.B., Dawson J.E., Nicholson L.K., Sheen J., and Martin G.B. 2007b. The N-terminal region of *Pseudomonas* type III effector AvrPtoB elicits Pto-dependent immunity and has two distinct virulence determinants. Plant J 52:595-614.

Xing W., Zou Y., Liu Q., Liu J., Luo X., Huang Q., Chen S., Zhu L., Bi R., Hao Q., Wu J.W., Zhou J.M., and Chai J. 2007. The structural basis for activation of plant immunity by bacterial effector protein AvrPto. Nature 449:243-247.

Yeam I., Nguyen H.P., and Martin G.B. 2010. Phosphorylation of the *Pseudomonas syringae* effector AvrPto is required for FLS2/BAK1-independent virulence activity and recognition by tobacco. Plant J 61:16-24.

Zeng L., Velásquez A.C., Munkvold K.R., Zhang J., and Martin G.B. 2011. A tomato LysM receptor-like kinase promotes immunity and its kinase activity is inhibited by AvrPtoB. Plant J. DOI: 10.1111/j.1365-313X.2011.04773.x.

Zhou H., Lin J., Johnson A., Morgan R.L., Zhong W., and Ma W. 2011. *Pseudomonas syringae* type III effector HopZ1 targets a host enzyme to suppress isoflavone biosynthesis and promote infection in soybean. Cell Host Microbe 9:177-186.

Zipfel C., Kunze G., Chinchilla D., Caniard A., Jones J.D.G., Boller T., and Felix G. 2006. Perception of the bacterial PAMP EF-Tu by the receptor EFR restricts *Agrobacterium*-mediated transformation. Cell 125:749-760.

CHAPTER II

IDENTIFICATION OF *NICOTIANA BENTHAMIANA* GENES INVOLVED IN PATHOGEN-ASSOCIATED MOLECULAR PATTERN-TRIGGERED IMMUNITY[2]

Summary

In order to identify components of PAMP-triggered immunity (PTI) pathways in *Nicotiana benthamiana*, we conducted a large-scale forward-genetics screen using virus-induced gene silencing and a cell-death-based assay for assessing PTI. The assay relied on four combinations of PTI-inducing non-pathogens and cell death-causing challenger pathogens and was first validated in plants silenced for *FLS2* or *BAK1*. Over 3,200 genes were screened and 14 genes were identified that, when silenced, compromised PTI as judged by the cell-death-based assay. Further analysis indicated that the 14 genes were not involved in a general cell death response. A subset of the genes was found to act downstream of FLS2-mediated PTI induction and silencing of three genes compromised production of reactive oxygen species in leaves exposed to flg22. The 14 genes encode proteins with potential functions in defense and hormone signaling, protein stability and degradation, energy and secondary metabolism

[2] This chapter has been published in the journal Molecular Plant-Microbe Interactions (Volume 23, Nº 6, 2010, pp. 715 - 726) by Suma Chakravarthy, André C. Velásquez, Sophia K. Ekengren, Alan Collmer and Gregory B. Martin. S. C. and A. V. contributed equally to this work and are considered co-first authors. S. C. performed the experiments shown in Figure 2.6 and in Table 2.3.

and cell wall biosynthesis and provide a new resource to explore the molecular basis for the involvement of these processes in PTI.

Introduction

Plants are constantly threatened by disease-causing organisms in their environment. To protect themselves, plants have evolved elaborate inducible mechanisms to prevent or slow down pathogen infection. The first line of inducible plant defense involves the detection of slowly evolving epitopes present in molecules that are of key importance to a pathogen's lifestyle. These epitopes are referred to as pathogen or microbial associated molecular patterns (PAMPs or MAMPs) and are present not only in pathogens but also in diverse microbes. PAMPs are recognized by pattern recognition receptors (PRRs) and this perception triggers PAMP-triggered immunity (PTI), which effectively prevents colonization of plant tissues by potential pathogens (Bent and Mackey 2007). Successful bacterial pathogens deploy effectors that suppress PTI and cause disease, and some plants have in turn evolved resistance (*R*) genes that recognize the activity of effectors, which leads to effector-triggered immunity (ETI; Bent and Mackey 2007).

Bacterial PAMPs include flagellin, cold-shock protein (CSP), elongation factor Tu (EF-Tu) and peptidoglycan (PGN; Boller and Felix 2009). The two best characterized plant PRRs are from *Arabidopsis* and both recognize bacterial PAMPs: FLS2 detects a 22-amino acid epitope (flg22) in flagellin and EFR detects an 18-amino acid epitope (elf18) in EF-Tu (Chinchilla *et al.* 2006; Zipfel

et al. 2006). Both of these proteins are LRR receptor-like kinases (LRR-RLKs) and FLS2, in particular, has been studied intensively. FLS2 directly binds the flg22 peptide after which it associates with the BRI1-associated kinase (BAK1; Chinchilla *et al.* 2007; Heese *et al.* 2007). Plants with disrupted expression of the *FLS2* or *BAK1* genes are compromised for PTI and more susceptible to certain bacterial pathogens (Zipfel *et al.* 2004; Heese *et al.* 2007). In addition to FLS2 and EFR, there are several less well-characterized PRRs in plants (Ron and Avni 2004; Miya *et al.* 2007; Gimenez-Ibanez *et al.* 2009)

Activation of a PRR by its cognate PAMP leads to a variety of rapid responses including an oxidative burst, an intracellular increase in calcium concentration, cell wall callose deposition, MAPK activation, phytoalexin production and a complex transcriptional response (Schwessinger and Zipfel 2008). PTI-induced transcriptional responses include up-regulation of a large number of genes including many that encode receptor-like kinases, some of which may be involved in PAMP perception, and of transcription factors which could be involved in amplifying the PTI response (Navarro *et al.* 2004; Thilmony *et al.* 2006). Interestingly, many of the genes induced by EF-Tu or PGN are similar to flg22-induced genes (Zipfel *et al.* 2006; Gust *et al.* 2007) suggesting that there is significant overlap among the responses to different PAMPs.

Different genetic and molecular approaches have been used to dissect signaling pathways in PTI, yet relatively little is known about PRRs or the processes that these host receptors activate in plants during the PTI response (Zipfel 2009). Two recent reports used large-scale genetic screens to identify

components of the elf 18-induced signaling pathway in *Arabidopsis* (Saijo *et al.* 2009; Li *et al.* 2009). The studies involved screening of 137,500 or >60,000 EMS-mutagenized lines and identified genes involved in ER quality control (ER-QC) that were responsible for the proper biogenesis of EFR.

Loss-of-function studies using virus-induced gene silencing (VIGS) is a powerful method that has been used to identify genes involved in plant defense responses. A gene that acts as a regulator of immunity-associated cell death, and genes involved in R gene signaling or stabilization were identified during large-scale VIGS screens (Lu *et al.* 2003; del Pozo *et al.* 2004; Peart *et al.* 2005). Genome-wide RNA interference (RNAi) screens also have been used to discover components of the animal innate immune response (Foley and O'Farrell 2004; Alper *et al.* 2008; Cronin *et al.* 2009).

In order to identify genes involved in PTI, we conducted a VIGS-based screen in *N. benthamiana*, a species being increasingly used as a model to study plant-microbe interactions (Goodin *et al.* 2008). Knowledge gained from this species is also potentially transferable to closely related Solanaceous species such as tomato, potato and pepper. To efficiently assay for PTI in leaves of *N. benthamiana*, we relied on a previously developed cell-death-based assay (Oh and Collmer 2005). In this assay, a non-pathogen is first infiltrated into leaves in order to induce PTI. Several hours later, a 'challenger' inoculation is performed in a partially overlapping area with a cell-death-causing bacterium. Cell death caused by the challenger may be the result either of the hypersensitive response (HR) or disease caused by pathogenic bacteria. In the

leaf area where PTI has been induced by inoculation of the non-pathogen, challenger cell death is delayed or does not occur (Klement *et al.* 2003; Oh and Collmer 2005). Conversely, appearance of cell death in the overlapping area of inoculation indicates a breakdown of PTI. The lack of cell death in the overlapping area is likely the result of impaired delivery of effectors, as indicated by the reduced delivery by *Pseudomonas syringae* pv. *tomato* DC3000 challenger inoculum of the AvrPto-Cya translocation reporter into PTI-induced tissue (Oh *et al.* 2010). This method has the advantage that it measures overall plant response to live bacteria instead of that to individual PAMPs.

In this study we report the screening of over 3,200 genes by a combined approach of VIGS and the PTI cell-death-based assay. Fourteen genes were identified that appear to act in pathways involved in defense and hormone signaling, protein stability and degradation, energy and secondary metabolism or cell wall biosynthesis. This collection of genes provides a resource to further investigate the molecular basis for the involvement of each of these processes in PTI.

Materials and Methods

Bacterial strains

Bacterial strains used in this study are listed in Table 2.1. *Pseudomonas* strains were grown in King's B (KB) medium at 30 ˚C. *A. tumefaciens* and *E. coli* strains were grown in Luria Bertani (LB) medium at 30 and 37 ˚C, respectively.

Table 2.1. Strains used in this study.

Strain	Features	Reference
Agrobacterium tumefaciens GV2260	Disarmed Ti plasmid; Rif^R	McBride and Summerfelt (1990)
Agrobacterium tumefaciens GV3101	Disarmed Ti plasmid; Rif^R, Gen^R	Holsters *et al.* (1980)
Escherichia coli DH5α	*F - φ 80 lacZ ΔM15 Δ(lacZYA-argF)U169 recA1 endA1 hsdR17(rk-,mk+) gal- phoA supE44 thi-1 gyrA96 relA1 λ-*	Invitrogen
Pseudomonas fluorescens 55	Wild type; Amp^R, Chl^R, Nx^R, Spc^R	Huang *et al.* (1988)
Pseudomonas putida KT2440	Plasmid free derivative from strain mt-2 ; Amp^R	Nelson *et al.* (2002)
Pseudomonas syringae pv. *tabaci* 11528	Wild type; Rif^R	American Type Culture Collection
Pseudomonas syringae pv. *tomato* DC3000	Wild type; Amp^R, Rif^R	Cuppels (1986)
Pst DC3000 Δ*hrcQ-U*	Δ$hrcQ_B$-*hrcU*::ΩSp^R; $TTSS^-$; Rif^R, Spc^R	Badel *et al.* (2006)
Pst DC3000 Δ*hopQ1-1*	Δ*hop1-1*; Rif^R	Wei *et al.* (2007)

Antibiotics were used at the following concentrations: ampicillin (100 μg/mL), kanamycin (50 μg/mL), rifampicin (10 μg/mL) and spectinomycin (50 μg/mL).

Virus-induced gene silencing (VIGS)

VIGS was performed as described earlier (Velasquez *et al.* 2009). All *N. benthamiana* plants were kept in a growth chamber with 16 hour day length, a temperature of 20 - 22 °C, and 50% relative humidity (RH) for at least 3½ weeks before they were used for the assays.

PAMP-triggered immunity assay

The PTI cell-death-assay was performed as described (Chakravarthy *et al.* 2009). The inducers were *P. fluorescens* 55 (Pf) at 10^9 CFU/mL, *P. putida* KT2240 (Pp) at 10^8 CFU/mL and *A. tumefaciens* GV2260 (Agro) at 5 x 10^8 CFU/mL. The challengers were *Pst* DC3000 (DC) at 2 x 10^7 CFU/mL, *Pst* DC3000 Δ*hopQ1-1* (Q1-1) at 1 x 10^6 CFU/mL and *P. syringae* pv. *tabaci* 11528 (Ptab) at 1 x 10^6 CFU/mL. The time between induction and challenge was 7 hours.

Appearance of cell death in the overlapping area where the inducer and challenger were infiltrated indicated that PTI was compromised. Cell death due to ETI started 2 days after infiltration while that caused by disease appeared by day 4. Evaluation of plants was terminated when the TRV2 control plants started to show cell death in the overlapping area. A Fisher's exact test (α = 0.05) was used to establish if the number of times in which PTI was

compromised was significantly different for a particular gene as compared to the TRV2 control. This test is used to determine if there are nonrandom associations between two categorical variables, i.e. if silencing had any effect on the observed breakdown of PTI.

PTI assay using flg22 as an inducer

The same procedure as that described for the cell-death-based assay was employed, except that 50 µM flg22 (GenScript, Piscataway NJ, USA) and *Pst* DC3000 at 1 x 10^7 CFU/mL were used as the inducer and challenger, respectively.

Evaluation of cell death progression due to challenger inoculation

To prepare the inoculum, *Pst* DC3000 and *Pst* DC3000 Δ*hopQ1-1* were streaked on KB plates with the appropriate antibiotics and grown overnight at 30˚C. The next day, bacteria were spread with 150 µl of sterile liquid KB and grown for an additional day. Cells were then re-suspended in 10 mM $MgCl_2$ to the desired OD_{600}. The inocula used were 3 x 10^6, 6 x 10^6 and 2 x 10^7 CFU/mL for DC3000 and 1 x 10^5, 3 x 10^5 and 1 x 10^6 CFU/mL for ΔhopQ1-1. Data obtained for one titer each of DC3000 and DC3000 Δ*hopQ1-1* are presented, while the other data obtained are not shown.

Seven week-old *N. benthamiana* plants silenced for the candidate genes were inoculated with DC3000 and Δ*hopQ1-1* using a blunt syringe. Plants were kept in a room with continuous light, 22 - 24˚C temperature and 30% RH. The

extent of cell death was scored as full (>75% of the infiltrated area showed necrosis), partial (10-75%), or none (<10% cell death). Plants were evaluated until there was 100% cell death in all the spots for a particular inoculum level.

Measurement of ROS production

About 20 days after VIGS was initiated, silenced plants were assayed for ROS production. Discs from young leaves were punched out with a cork borer size 1 (4 mm diameter). Leaf discs were floated adaxial side up in a 96-well black plate (Nunc, Roskilde, Denmark) containing 200 μl water per well, and left at room temperature for overnight to 24 hours. The next day, the water was removed, and 100 μl of a solution containing the following was added: 100 nM flg22 (GenScript, Piscataway NJ, USA), 34 μg/mL luminol (Sigma, St. Louis MO, USA) and 20 μg/mL horseradish peroxidase (type VI-A, Sigma) in water. Luminescence was measured using the GENios Pro plate reader (Tecan S/N 508000007) and analyzed using Magellan software (Tecan). Three leaf discs per plant were taken, and at least 3 plants silenced for each gene were considered in each experiment. Controls lacking flg22 were included for each plant.

RNA extraction and cDNA synthesis

RNA was isolated from leaf tissue following the Concert™ Plant RNA Reagent method from Invitrogen (Carlsbad CA, USA). Genomic DNA contamination was removed with RQ1 RNase-free DNase from Promega (Madison WI, USA) and the RNA purified using the RNeasy Mini Kit from Qiagen (Valencia CA, USA). One

μg of DNase-treated RNA was used for first-strand cDNA synthesis with 0.5 μg oligo $(dT)_{12-18}$ primer and 200 U Superscript III reverse transcriptase (RT) from Invitrogen in a 20 μl reaction. A negative control without the RT enzyme was included for each RNA sample to verify the absence of contaminating genomic DNA.

Reverse transcription-PCR (RT-PCR) to analyze gene expression

Tissue was harvested from wild-type *N. benthamiana* plants inoculated either with a suspension of 1 x 10^9 CFU/mL *P. fluorescens* or with 10 mM $MgCl_2$. The *P. fluorescens* inoculum was prepared as described for the cell-death-based assay. Samples were taken at 6, 12, and 24 hours after infiltration.

RT-PCR was performed in a 25 μL reaction volume with 1 mL cDNA, 0.2 μM of each primer, 0.2 mM of each dNTP and 0.625 U of Fisher Scientific Taq polymerase (Fair Lawn NJ, USA). PCR amplicons were run on a 1.5 % agarose gel, stained with ethidium bromide and visualized using the Gel Doc™ XR from Bio-Rad Laboratories (Hercules CA, USA). RT-PCR of Elongation factor 1α was used as a loading control.

FLS2 primers used to evaluate gene induction were the same as reported by Hann and Rathjen (2007); the *plastocyanin* primers were designed using the VIGS construct sequence (see Table 2.2).

Table 2.2 Primers used in this study. Abbreviation: Ta = Primer annealing temperature.

Primer	Sequence	Ta	Reference
Nb ADH F	5'-GGGTCCTCAGATTGATTCAA-3'	50 ˚C	This study
Nb ADH R	5'-TTCCGTGTCCACTCATCTTA-3'		
Nb BAK1 F	5'-CTTATTCGGGTAGCTCTTCTCT-3'	52 ˚C	This study
Nb BAK1 R	5'-GTCTAACAAACACCCACTATCTGA-3'		
Nb Cath F	5'-AGCGCCTTCTTGGAGTTA-3'	52 ˚C	This study
Nb Cath R	5'-TGGGATATGCAGGTTCACA-3'		
Nb Cyc F	5'-CCTTACTATCGGCGGCACACCAG-3'	55 ˚C	This study
Nb Cyc R	5'-GATCCAACAGCCTCAGCCTTCTTA-3'		
Nb CycTC9299 F	5'-GCAAGCCGTTACACTACAAAGGAT-3'	55 ˚C	This study
Nb CycTC9299 R	5'-CCCGAAAACCGACCCACAATAAG-3'		
Nb CytC F	5'-AATATGGCTGTGATGTGGGA-3'	50 ˚C	This study
Nb CytC R	5'-CAATGGTTTATCTTCCTGCG-3'		
Nb Drm F	5'-TGACAAGCTCTGGGATGATA-3'	50 ˚C	This study
Nb Drm R	5'-CAAGATCTAGAAGCACTAGCAC-3'		
Nb EF1α F	5'-AAGGTCCAGTATGCCTGGGTGCTTGAC-3'	52 ˚C	Hann and Rathjen (2007)
Nb EF1α R	5'-AAGAATTCACAGGGACAGTTCCAATACCA-3'		

Table 2.2 (Continued)

Primer	Sequence	Ta	Reference
Nb FLS2 F	5'-CTGTGTACAAGGGTAGACTGGAAGATGG-3'	52 ˚C	Hann and Rathjen (2007)
Nb FLS2 R	5'-GGAGAGGTGCAAGGACAAAGCCAATTT-3'		
Nb HCBT F	5'-TGCCATAGATGAGCCAAAAC-3'	52 ˚C	This study
Nb HCBT R	5'-TCAATCGCCTTAAACCTCACTCTC-3'		
Nb Plasto F	5'-ATCCCATACAAGACGCTAAAACAA-3'	48 ˚C	This study
Nb Plasto R	5'-GCTAACCCGCCTACACG-3'		
Nb Serk2 F	5'-AATCTAGGTTTTAGGTGGTGGCGG-3'	52 ˚C	Hann and Rathjen (2007)
Nb Serk2 R	5'-CTGAAGCTTGCCCAATGTGTCAG-3'		

Reverse transcription-PCR (RT-PCR) and SYBR Green I gel staining to evaluate the degree of gene silencing

To investigate whether the VIGS constructs were efficient in inducing gene silencing, we tested plants silenced for a subset of 5 genes by RT-PCR, and used BAK1 as a control. Primers for RT-PCR were designed using the Vector NTI Advance 10 Software from Invitrogen (Carlsbad CA, USA). Their sequences and annealing temperatures are listed in Table 2.2. For each gene, one of the primers used to confirm silencing annealed to a sequence outside the region targeted by VIGS. Tissue used to evaluate silencing efficiency
was collected from *N. benthamiana* plants 3½ weeks after initiating VIGS. The procedure for RNA isolation and cDNA preparation was the same as described above. RT-PCR followed by SYBR Green I gel staining was performed as described below.

The cDNA was diluted 5-fold with water, and 5 μl each was used in a PCR reaction with EF1α control primers or gene-specific primers. PCR was performed with Promega GoTaq (Madison WI, USA) in 25 μl volumes. The number of cycles for amplification depended on the individual primer pairs. A low cycle number was chosen, that would detect products well before the saturation phase of the reaction was reached. Typically this was about 4 cycles less than the cycle number used for regular RT-PCR for that primer pair. Cycle numbers were *EF1α*: 20, *Cathepsin B*: 24, *HCBT:* 27, *BAK1:* 27, *Cytochrome C*: 28, *Drm-3*: 29, *Cyclophilin:* 20 and *Cyclophilin homolog*: 23. PCR products were run on a 1% agarose gel, and subsequently stained with a 1:10,000 dilution of

SYBR Green I gel stain (Invitrogen, Carlsbad CA, USA). Band intensities were measured using the Quantity One 4.6.3 software from Bio-Rad Laboratories and used to plot the graphs shown in Figure 2.3.

Results

A cell-death-based assay for PTI is validated in plants silenced for FLS2 or BAK1

We initially optimized the cell-death-based assay for PTI by evaluating 18 different combinations of inducers and challengers (Table 2.3; Figure 2.1.A). The combinations tested varied in their effectiveness of inducing PTI, as seen by the occurrence or lack of cell death in the overlapping area of inoculation (Table 2.3). This suggested that there exist differences in the nature of PTI induced by different bacteria, as well as in the ability of the challengers to overcome the PTI response. Four combinations of inducers and challengers were ultimately chosen based on their ability to consistently show inhibition of cell death in the overlapping area of inoculation in wild-type *N. benthamiana* plants (Table 2.4).

These four inducer-challenger combinations were tested on plants silenced for *FLS2* or *BAK1*, genes which have been shown to act as important components of PTI in *N. benthamiana* (Hann and Rathjen 2007; Heese *et al.* 2007). Cell death was observed in the overlapping area of inoculation with 3 of the 4 inducer/challenger combinations tested on *FLS2*- or *BAK1*-silenced plants (Figure 2.1.B). This indicated a compromised PTI response in the plants silenced for *FLS2* or *BAK1* and validated the cell-death-based assay. These

Table 2.3. Evaluation of different combinations of inducers/challengers in the cell-death-based assay.

Inducer	Challenger		
	***P.s.* pv. *tomato* DC3000 (DC)**	**DCΔ*hopQ1-1***	***P.s.* pv. *tabaci***
A. tumefaciens GV2260	93%	53%	**0%**
A. tumefaciens GV3101	93%	20%	13%
E. coli DH5α	100%	80%	53%
P. fluorescens 55	**0%**	**7%**	48%
P. putida KT2440	**0%**	7%	47%
DC3000 Δ*hrcQ-U*	33%	33%	59%

A minimum of 15 wild-type *N. benthamiana* plants was evaluated for each assay. The percentage of times cell death was seen in the overlapping area of inoculation, indicating compromised PTI is shown. The four combinations shown in bold were selected for performing the cell death assay for the screen. These combinations showed strong induction of PTI, as was seen by little or no appearance of cell death in the overlapping area of inoculation.

Figure 2.1. Assay for PTI. A, Diagram depicting the cell-death-based assay to determine the involvement of a particular gene in PAMP-triggered immunity. **(i)** Virus-induced gene silencing (VIGS) of the candidate gene. **(ii)** Four weeks after initiating VIGS, PTI is induced in silenced plants by infiltration of a non-pathogen onto leaves. **(iii)** A partially overlapping area is challenged with a HR- or disease-causing strain 7 hours after PTI induction. Cell death typically appears 2 - 5 days later in the challenged area. This assay has two possible outcomes: **(iv)** Lack of cell death in the overlapping area due to induction of PTI, or **(v)** Cell death in the overlapping area due to compromised PTI. **B,** PTI assay using the four different combinations of PTI inducers and cell-death-causing challengers (see Table 1) on non-silenced TRV2 control plants and *FLS2*- or *BAK1*-silenced plants. Photographs were taken 2 days after inoculation of the HR-causing strain (*P.s.* pv. *tomato* DC3000 or DC) and 4 to 5 days after inoculation of the disease-causing strains (DCΔ*hopQ1-1* and *P.s.* pv. *tabaci*). The red box indicates those combinations of inducers and challengers where PTI was compromised, as observed by the occurrence of cell death in the overlapping area of inoculation.

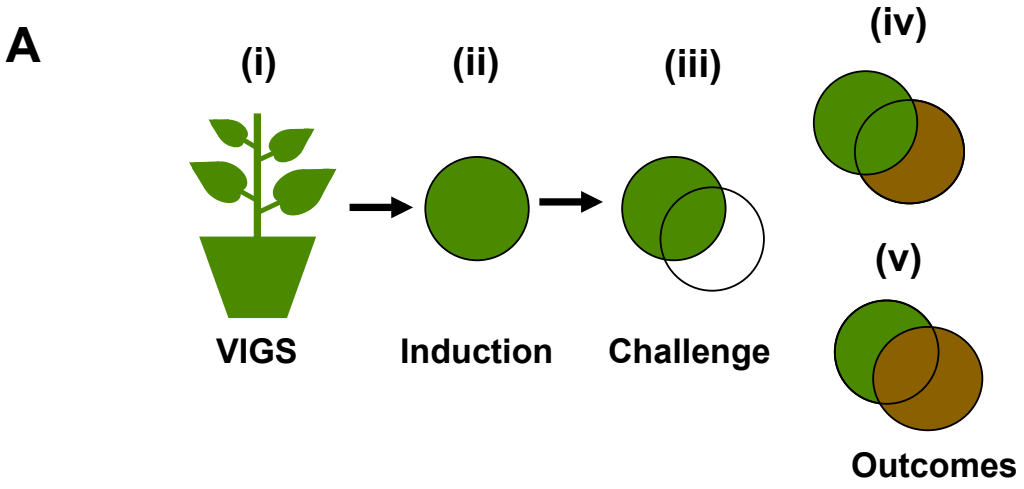
A
(i)
(ii)
(iii)
(iv)
(v)
VIGS
Induction
Challenge
Outcomes

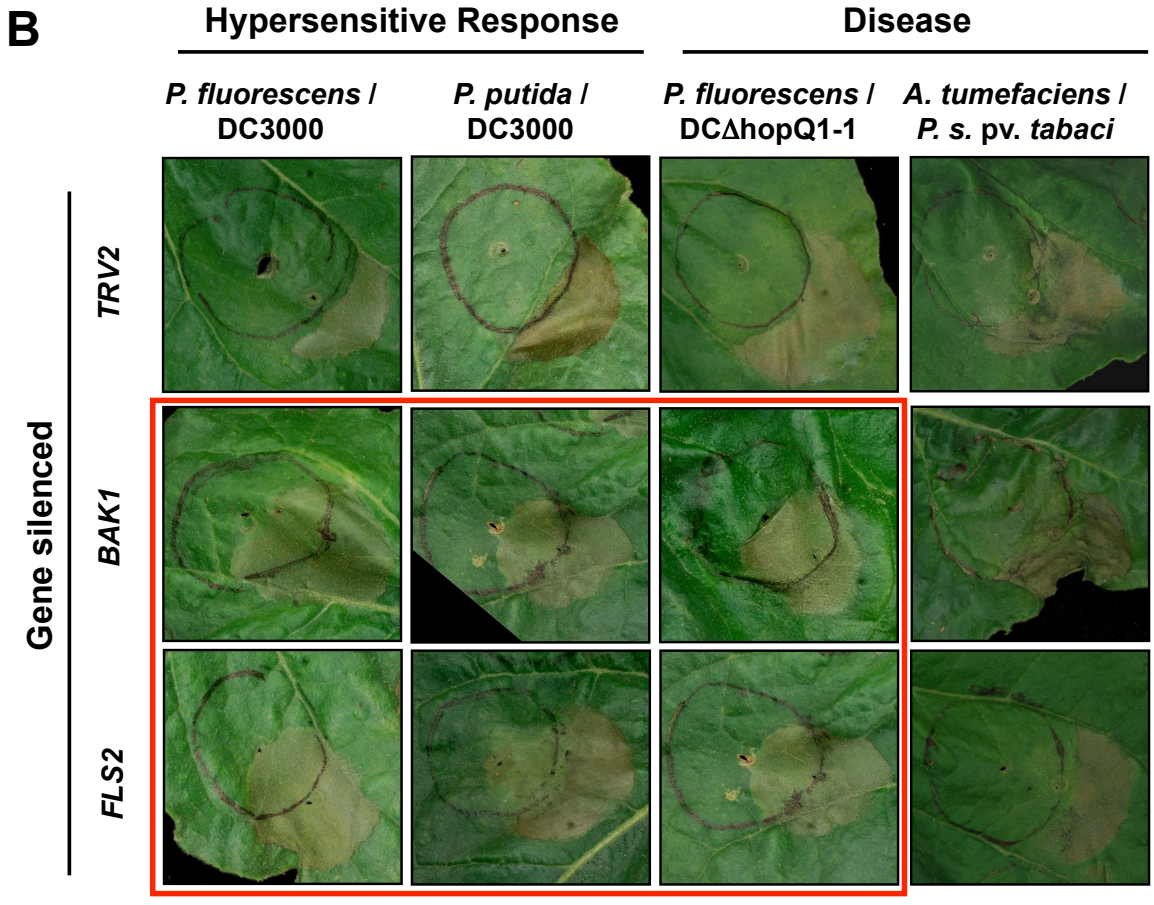
B
Hypersensitive Response
Disease
P. fluorescens / DC3000
P. putida / DC3000
P. fluorescens / DCΔhopQ1-1
A. tumefaciens / P. s. pv. tabaci
Gene silenced
TRV2
BAK1
FLS2

Table 2.4. The combinations of PTI-inducing and hypersensitive response (HR)- or disease-causing challenge microbes used in the assays.

Inducer	Challenger	Combination	Outcome*
P. fluorescens 55	*P. s.* pv. *tomato* DC3000	Pf/DC	HR
P. putida KT2440	*P. s.* pv. *tomato* DC3000	Pp/DC	HR
P. fluorescens 55	*P. s.* pv. *tomato* DC3000 Δ*hopQ1-1*	Pf/Q1-1	Disease
A. tumefaciens GV2260	*P. s.* pv. *tabaci* 11528	Agro/Ptab	Disease

*Expected outcome in the overlapping infiltration area if PTI resulting from the inducer is compromised by silencing of a particular gene.

results also suggest that flagellin is one of the most important PAMPs of *P. fluorescens* and *P. putida* recognized by *N. benthamiana* as silencing of *FLS2* was able to attenuate the PTI response despite the presumed presence of other PAMPs in these bacteria.

Screening of a VIGS library identifies seven genes as playing a role in PTI

We silenced 3,072 genes from a previously constructed VIGS library derived from leaf tissues exposed to various biotic and abiotic elicitors (cNbME; *N. benthamiana* mixed-elicitor cDNA, del Pozo *et al.* 2004). The elicitors used were *Agrobacterium tumefaciens*, *P. syringae* pv. *tabaci*, *P. syringae* pv. *tomato*, salicylic acid, jasmonic acid, and ethylene. The cell death assay was performed on gene-silenced plants using the four different inducer-challenger combinations. *FLS2*-silenced and *BAK1*-silenced plants were included as controls in every experiment, and cell death in the overlapping inducer-challenger leaf area was observed between 22 - 75% of the time for these two genes depending on the inducer-challenger combination (Table 2.5). Seven genes, representing just 0.23% of the 3,072 genes screened, were ultimately identified as compromising PTI when silenced (Table 2.5, Figure 2.2 and Figure 2.3). Each of these 7 genes was silenced a minimum of 15 additional times and tested with each of the 4 inducer-challenger combinations (Table 2.5). These follow-up experiments were evaluated for each of the 7 genes with a Fisher's exact test ($\alpha = 0.05$), which revealed that PTI was compromised for at least one of the inducer-challenger combinations (Table 2.5). The genes that were

Table 2.5. Percentage of plants in which PTI was compromised when candidate genes from the cNbME VIGS library were silenced and evaluated using the cell-death-based assay.

Gene silenced	Category	Pf/DC	Pp/DC	Pf/Q1-1	Agro/Ptab
TRV2		0%	0%	0%	0%
BAK1	Signaling	**53%**	**22%**	**44%**	3%
FLS2	PRR	**75%**	**48%**	**66%**	5%
ALDH	Secondary metabolism	8%	4%	**21%**	8%
Cathepsin B	Protease	17%	17%	**33%**	8%
Cyclophilin	Protein folding	**33%**	**26%**	**44%**	4%
Cytochrome C	Secondary metabolism	**32%**	8%	**32%**	4%
Drm-3	Hormone signaling	**45%**	11%	17%	6%
HCBT	Secondary metabolism	**20%**	**24%**	16%	8%
Plastocyanin	Secondary metabolism	**29%**	13%	**38%**	13%

A minimum of 16 plants was evaluated for each assay. Percentages in bold represent those combinations where PTI was compromised as determined by pairwise comparisons of the TRV2 control with each of the candidate genes with a Fisher's exact test ($\alpha = 0.05$). Abbreviations: *HCBT* = Anthranilate N-hydroxycinnamoyl/benzoyltransferase, *ALDH* = Aldehyde dehydrogenase, Agro = *A. tumefaciens*, DC = *Pst* DC3000, Pf = *P. fluorescens*, Pp = *P. putida*, Ptab = *P. s.* pv. *tabaci*, Q1-1 = *Pst* DC3000 Δ*hopQ1-1*.

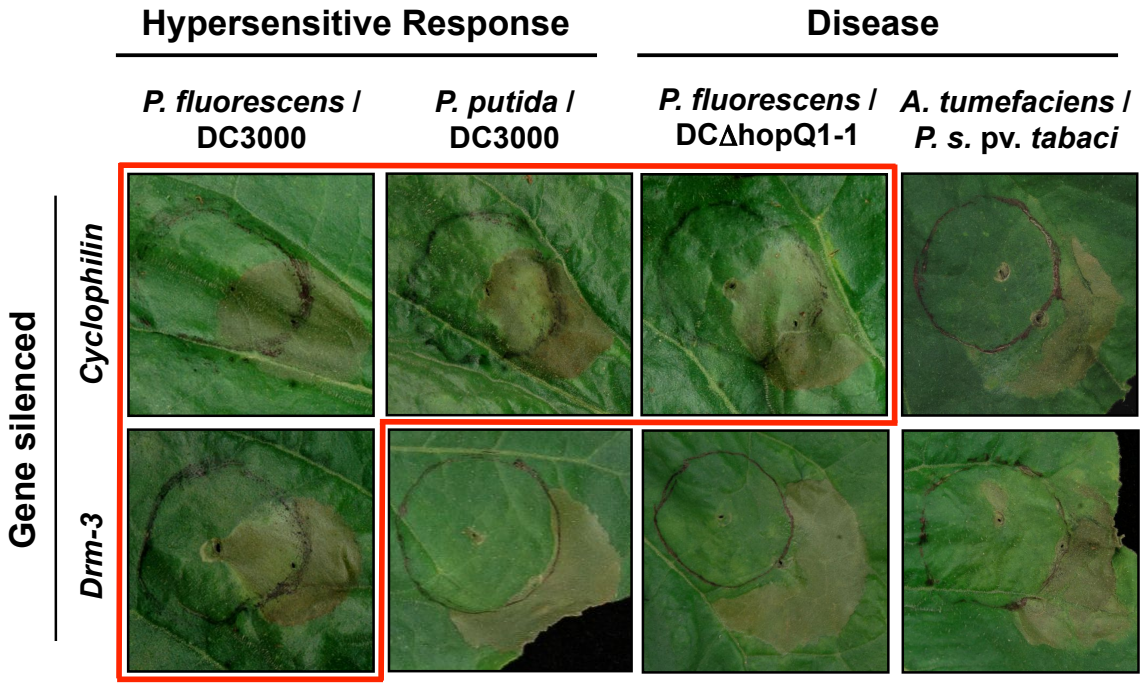

Figure 2.2. Cell-death-based assay for two candidate genes identified from the VIGS library screen. *Cyclophilin-* and *Drm3*-silenced plants were photographed 2 days after inoculation of the HR-causing strain (*P.s.* pv. *tomato* DC3000) and 4 to 5 days after inoculation of the disease-causing strains (Δ*hopQ1-1* and *P.s.* pv. *tabaci*). The red box indicates those combinations of inducers and challengers where PTI was compromised, as observed by the occurrence of cell death in the overlapping area of inoculation.

Figure 2.3. Reverse transcription PCR (RT-PCR) followed by SYBR Green I gel staining to show the degree of silencing in a subset of genes obtained from the screen. RNA was isolated from silenced plants and TRV-only non-silenced plants, and used to prepare cDNA. PCR was performed with *EF1α* control primers or gene-specific primers. Products were run on a gel, stained with SYBR Green I, and band intensities quantified. The band intensities of gene-specific products were normalized using the *EF1α* band intensities. Average values from 3 plants with standard deviation is shown in the graphs, and the gene silenced is indicated. *BAK-1* silenced plants were also analyzed as a control. An asterisk (*) indicates those genes that were significantly different from the control with p value < 0.05, as judged by a T-test.

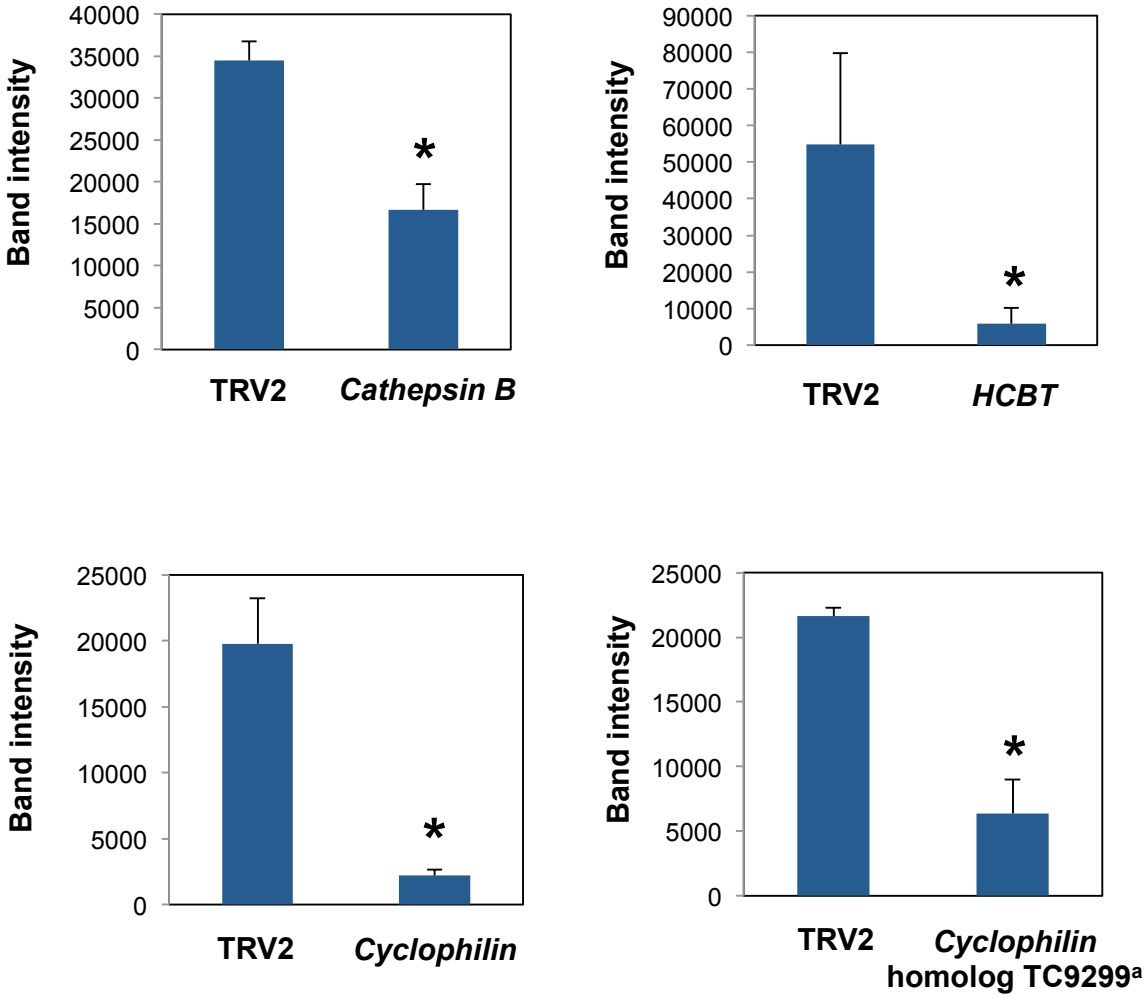

[a]The *cyclophilin homolog* was predicted to be co-silenced based on nucleotide sequence identity with *cylophilin.* The TIGR TC ID of the homolog is given.

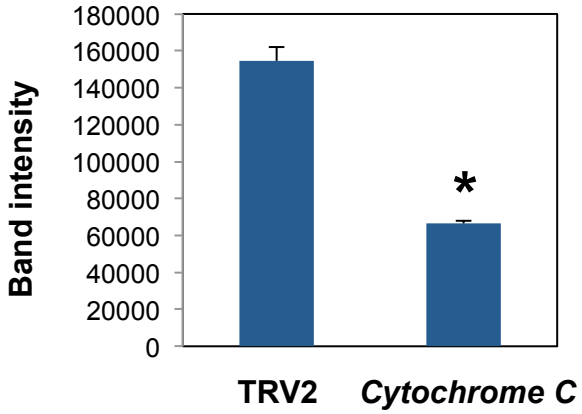
Band intensity
180000
160000
140000
120000
100000
80000
60000
40000
20000
0
*
TRV2
Cytochrome C

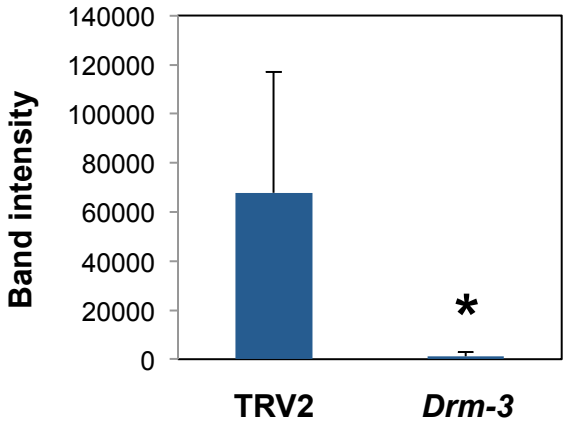
Band intensity
140000
120000
100000
80000
60000
40000
20000
0
*
TRV2
Drm-3

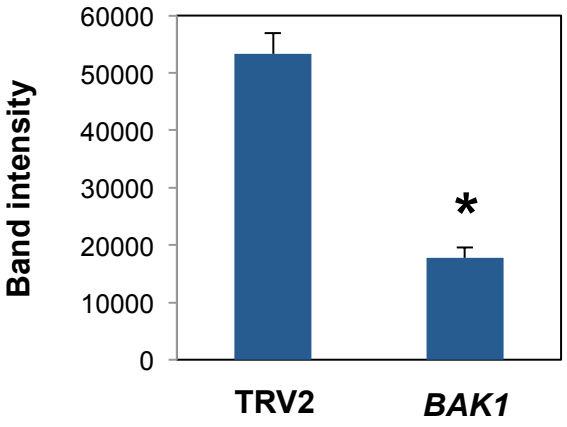
Band intensity
60000
50000
40000
30000
20000
10000
0
*
TRV2
BAK1

identified from this screen encode proteins with putative functions in protein stability and degradation, hormone signaling and secondary metabolism (Table 2.6).

We next performed bacterial growth assays with plants silenced for each of the 7 genes. Gene-silenced plants were syringe-inoculated with the non-pathogen *P. fluorescens* or an attenuated pathogenic strain of *Pst* DC3000 lacking the effectors *avrPto, avrPtoB* and *hopQ1-1* (Kvitko *et al.* 2009). Growth assays with the DC3000 triple mutant were performed with or without pre-induction of PTI with *P. fluorescens*. We also dip-inoculated silenced plants with *P.s.* pv. *tabaci* or *P.s.* pv. *syringae* B728a. No changes in bacterial growth were detected in any of the gene-silenced plants as compared to TRV-only infected plants. These results may suggest that the cell-death-based assay is more sensitive than bacterial population assays in detecting subtle defects in PTI responses. Specifically, the higher inoculum level of the challenger in the cell death assay as compared to that used in a standard bacterial growth assay may allow better detection of a breakdown in PTI.

The plastocyanin gene is induced during the PTI response

The expression of a large number of genes is induced during the PTI response in plants (Navarro *et al.* 2004; Zipfel *et al.* 2004). Some of these genes, for example, those encoding the PRRs FLS2 and EFR1, have established roles in PTI (Chinchilla *et al.* 2006; Zipfel *et al.* 2006). To examine whether PTI causes increased expression of any of the seven genes identified from our library

Table 2.6. BLAST analysis of genes from the cNbME VIGS library and immunity-induced gene library that were found to be involved in PTI.

Gene	Source	Closest hit
Aldehyde dehydrogenase	*N. benthamiana*	*N. tabacum* aldehyde dehydrogenase, mitochondrial (ALDH3).
Alternative oxidase	Tomato	*S. lycopersicum* alternative oxidase 1b. Transfers electrons from the ubiquinone pool to oxygen without energy
Anionic peroxidase	Tomato	*S. lycopersicum* lignin forming anionic peroxidase precursor.
Cathepsin B	*N. benthamiana*	*N. benthamiana* cathepsin B-like cysteine protease.
Cinnamic acid 4-hydroxylase	Tomato	*S. lycopersicum* cinnamic acid 4-hydroxylase. Phenylpropanoid biosynthesis.
Cyclophilin	*N. benthamiana*	*N. benthamiana* cyclophylin with peptidyl-prolyl cis-trans isomerase (PPI rotamase) activity which helps in protein folding.
Cytochrome C	*N. benthamiana*	*N. tabacum* cytochrome c, putative.
Drm-3	*N. benthamiana*	*Nicotiana tabacum* dormancy/auxin associated family protein, similar to Auxin-repressed 12.5 kDa protein.
EDS1	*N. tabacum*	*N. tabacum* lipase class 3 family protein / disease resistance protein-related, similar to EDS1 (enhanced disease susceptibility 1).
HCBT	*N. benthamiana*	*Nicotiana tabacum* transferase family protein, similar to anthranilate N-hydroxycinnamoyl / benzoyltransferase from *Dianthus caryophyllus*. Phytoalexin biosynthesis.
Plastocyanin	*N. benthamiana*	*Nicotiana tabacum*. Weakly similar to NtEIG-A1, a plastocyanin-like domain-containing protein.
Proteasome 26S subunit	Tomato	S. lycopersicum weakly similar to a putative protein in *A. thaliana* and to *S. tuberosum* proteasome 26S ATPase subunit 1 variant.
Transducin	Tomato	*S. lycopersicum* weakly similar to transducin family protein (G protein). WD-40 repeat family protein.
Ubiquitin activating enzyme	Tomato	*S. lycopersicum* ubiquitin activating enzyme. Also nearly identical to SUMO activating enzyme 1b (SAE1b) from *A. thaliana*.

Table 2.6. (Continued).

Gene	Category	SOL	Genbank accession	E value
Aldehyde dehydrogenase	Secondary metabolism	SGN-U446111	Y09876.1	0.00
Alternative oxidase	Energy metabolism	SGN-U589545	AI780606	0.00
Anionic peroxidase	Cell wall protein	SGN-U579084	AI778712	0.00
Cathepsin B	Protease	SGN-U511999	DQ492287.1	0.00
Cinnamic acid 4-hydroxylase	Secondary metabolism	SGN-U581122	AI484136	0.00
Cyclophilin	Protein folding	SGN-U515692		0.00
Cytochrome C	Secondary metabolism	SGN-U431551 SGN-U431552		1.00E-137 1.00e-130
Drm-3	Hormone signaling	SGN-U441469 SGN-U441472		0.00 0.00
EDS1	Defense signaling	SGN-U423107	AF480489.1	0.00
HCBT	Secondary metabolism	SGN-U437020		1.00E-137
Plastocyanin	Secondary metabolism	SGN-U500422		1.00E-139
Proteasome 26S subunit	Protein stability	SGN-U573521	AI484715	0.00
Transducin	Signaling	SGN-U572067	BE353168	0.00
Ubiquitin activating enzyme	Protein stability	SGN-U586274	AI483239	0.00

screen, we performed RT-PCR on RNA isolated from *N. benthamiana* leaves that had been infiltrated with either the non-pathogen *P. fluorescens (Pf)* or 10 mM $MgCl_2$ (Figure 2.4). Transcript abundance of *FLS2* was increased at 6 and 12 hours after *Pf* infiltration as compared to the $MgCl_2$ treatment (Figure 2.4) and returned to control levels 24 hours after treatment (not shown). Of the seven genes tested, only the *plastocyanin* gene showed increased transcript abundance – visible at 12 and 24 hours after *Pf* infiltration as compared to the $MgCl_2$ control.

Screening of a collection of immunity-induced genes identifies seven as playing a role in PTI

The result with the *plastocyanin* gene indicated that at least some genes whose silencing compromises PTI are upregulated by PAMPs. As a second approach to identify genes involved in PTI, we therefore took advantage of a previous transcriptional profiling study that had identified >400 genes from tomato whose expression was increased during both PTI and ETI responses to *P. syringae* pv. *tomato* (Mysore *et al.* 2002). We focused on a subset of these genes that was implicated as being induced by PAMPs and, in addition, a few genes with known roles in defense signaling, such as *EDS1, SGT1, RAR1* and *NPR1* (Table 2.7). A fragment from each of these 133 genes was cloned into the TRV2 vector and gene silencing and subsequent cell death assays were performed as described above for the cNbME VIGS library. From this screen, seven genes representing 5.2% of the set were ultimately found to compromise PTI as

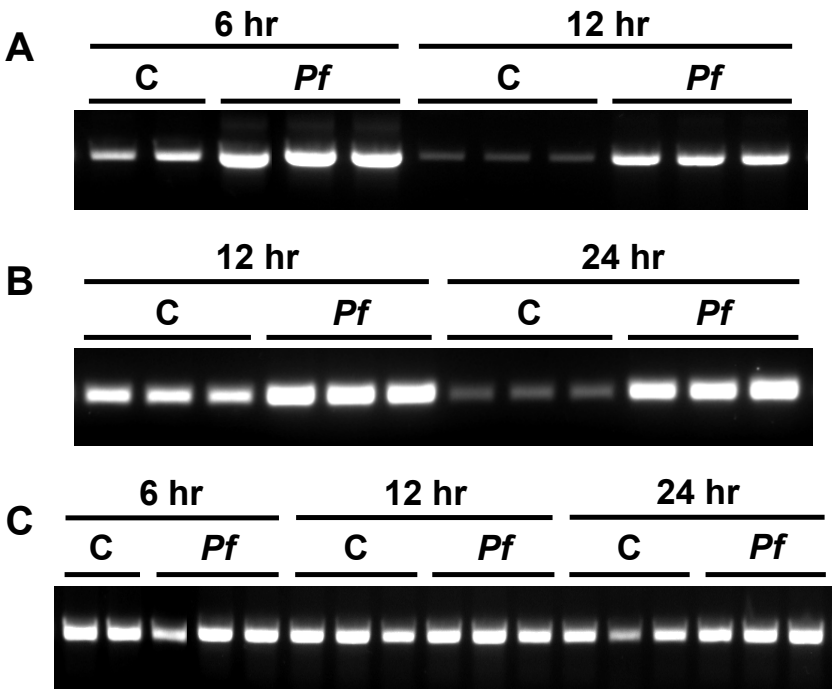

Figure 2.4. A gene predicted to encode a plastocyanin is induced by PAMPs. *N. benthamiana* leaves were infiltrated with either the non-pathogen *P. fluorescens* (*Pf*, 1 x 10^9 CFU/mL) as a source of PAMPs or with 10 mM $MgCl_2$ as a control (C). RNA was isolated from tissues at 6, 12 and 24 hours after inoculation and transcript abundance was examined by RT-PCR. Only the time points at which transcript abundances were increased relative to the control are shown. Each of the three lanes within each treatment/time point corresponds to a different plant. **A,** *FLS2*; **B,** the *plastocyanin* gene; **C,** e*longation factor 1a* (control for similar abundance of RNA in each lane).

Table 2.7. List of genes that comprised the immunity-induced gene collection.

APR N°[1]	BLAST Annotation from SOL Genome Network (SGN) / Gene name	SGN Unigene ID	GenBank Accession N°[2]	Source of VIGS clone
3	UDP-glucose:glucosyltransferase.	SGN-U582049	AW928895	This study
4	UDP-glucose:glucosyltransferase.	SGN-U569846	AI778508	This study
9	Homologous to *Arabidopsis* CBL-interacting protein kinase 14 (CIPK14).	SGN-U574324	AW398724	This study
12	Glutathione peroxidase.	SGN-U578117	AI486950	This study
13	Annexin, homologous to *Arabidopsis* calcium-binding protein Annexin 4 (ANN4).	SGN-U578779	AI488621	This study
14	Glutathione S-transferase.	SGN-U581941	AW625637	This study
29	No significant match.	SGN-U604819	AY125864	This study
30	Homologous to *Arabidopsis* glycoside hydrolase family 28 protein / polygalacturonase (pectinase) family protein.	SGN-U577565	BE354939	This study
39	Aspartyl protease family protein.	SGN-U574299	AW035081	This study
45	Ripening regulated protein-like, homologous to *Arabidopsis* oxidoreductase.	SGN-U579609	BG127104	This study
51	Auxin responsive protein, homologous to Arabidopsis auxin-responsive GH3, which encodes an IAA-amido synthase that conjugates Ala, Asp, Phe, and Trp to auxin.	SGN-U567051	AI775892	This study
52	Auxin induced protein, homologous to *Arabidopsis* indoleacetic acid-induced protein 16 (IAA16).	SGN-U579568	AI773435	This study

Table 2.7. (Continued).

APR N°[1]	BLAST Annotation from SOL Genome Network (SGN) / Gene name	SGN Unigene ID	GenBank Accession N°[2]	Source of VIGS clone
53	Auxin and ethylene responsive GH3-like protein.	SGN-U573533	AI489187	This study
54	Auxin regulated protein, homologous to *Arabidopsis* AA-amido synthases.	SGN-U585261	AY125870	This study
57	Enolase (2-phosphoglycerate dehydratase).	SGN-U579393	AW032518	This study
58	Oxophytodienoate reductase, involved in jasmonic acid biosynthesis.	SGN-U566794	BG130377	This study
60	Oxophytodienoate reductase, involved in jasmonic acid biosynthesis, homologous to *Arabidopsis* OPR3.	SGN-U576938	AI486721	This study
65	Acyl-CoA thioesterase family protein.	SGN-U576973	AY125884	This study
67	Homologous to *Arabidopsis* gibberelin 3 beta-hydroxylase.	SGN-U584326	AB010991	This study
69	Glutathione synthetase (GSH2).	SGN-U575017	BF112801	This study
72	Lipase-like protein.	SGN-U584528	BF114236	This study
75	Gamma hydroxybutyrate dehydrogenase.	SGN-U583712	AW039535	This study
76	Histidine decarboxylase.	SGN-U578638	AI484867	This study
80	Chorismate mutase, prephenate dehydratase.	SGN-U573964	AI772786	This study
81	Embryonic abundant protein EMB20, homologous to *Arabidopsis* prephenate dehydrogenase family protein.	SGN-U586965	AI486555	This study
90	No significant match.	SGN-U563853	AY125875	This study

Table 2.7. (Continued).

APR N°[1]	BLAST Annotation from SOL Genome Network (SGN) / Gene name	SGN Unigene ID	GenBank Accession N°[2]	Source of VIGS clone
95	No significant match.	SGN-U583479	AI486098	This study
96	Homologous to *Arabidopsis* F-box family protein.	SGN-U585684	AW154856	This study
97	WD-40 repeat family protein, homologous to *Arabidopsis* transducin family protein.	SGN-U572067	BE353168	This study
98	No significant match.	SGN-U579770	AY125868	This study
99	RING zinc finger-type transcription factor.	SGN-U568090	AY125873	This study
100	No significant match.	SGN-U577093	AY125883	This study
109	Homologous to *Arabidopsis* phototropic-responsive protein.	SGN-U574291	AW092525	This study
118	Pyridine nucleotide-disulfide oxidoreductase.	SGN-U576144	AW399697	This study
119	NADH nitrate reductase.	SGN-U579543	X14060	This study
127	Tospovirus resistance protein C.	SGN-U586997	AW979731	This study
129	Cytochrome P450 family protein.	SGN-U581118	AW030489	This study
130	Multicystatin, protease inhibitor.	SGN-U577197	AI486326	This study
134	Calcium-binding protein CAST.	SGN-U569581	AW219487	This study
141	Harpin inducing protein.	SGN-U574797	AI780237	This study
142	Lignin forming anionic peroxidase.	SGN-U579084	AI778712	This study
144	Harpin-induced protein-related / HIN1-related protein.	SGN-U571427	AI483954	This study
145	Dirigent protein, homologous to *Arabidopsis* disease resistance response protein.	SGN-U585771	AI488935	This study

Table 2.7. (Continued).

APR N°[1]	BLAST Annotation from SOL Genome Network (SGN) / Gene name	SGN Unigene ID	GenBank Accession N°[2]	Source of VIGS clone
146	TMV response-related gene product.	SGN-U579566	AY125890	This study
150	RSH-like protein, homologous to *Arabidopsis* RELA/SPOT HOMOLOG 3, involved in guanosine tetraphosphate metabolic process.	SGN-U570231	AI483664	This study
151	Cytochrome P450-like protein.	SGN-U575858	AW616143	This study
153	NAC domain protein, transcription factor.	SGN-U583008	AI486492	This study
154	U-box protein.	SGN-U582344	AI485996	This study
158	Phox homolog, gp91, homologous to *Arabidopsis* respiratory burst oxidase protein D (RbohD).	SGN-U579691	AW032624	This study
159	4-coumarate-CoA ligase.	SGN-U580976	AI775436	This study
162	Cinnamic acid 4-hydroxylase.	SGN-U581122	AI484136	This study
167	Phenylalanine ammonia-lyase.	SGN-U572140	AI773899	This study
168	4-coumarate-CoA ligase-like protein.	SGN-U569499	AI486465	This study
170	NADPH-cytochrome P450 oxidoreductase.	SGN-U573215	AY125879	This study
171	Phenylalanine ammonia-lyase (PAL).	SGN-U577677	AI777483	This study
187	Probable glutathione S-transferase (Pathogenesis-related protein 1).	SGN-U579357	AI772726	This study
188	Zinc finger transcription factor, homologous to *Arabidopsis* LSD1.	SGN-U568731	BI206715	This study
190	Putative 2-Hydroxyisoflavanone dehydratase.	SGN-U568021	AI778741	This study

Table 2.7. (Continued).

APR N°[1]	BLAST Annotation from SOL Genome Network (SGN) / Gene name	SGN Unigene ID	GenBank Accession N°[2]	Source of VIGS clone
193	Clp-like protease, homologous to *Arabidopsis* ATP-dependent Clp protease proteolytic subunit.	SGN-U579128	AI486961	This study
208	Putative ascorbate oxidase.	SGN-U581990	AW034131	This study
211	Phospho-2-dehydro-3-deoxyheptonate aldolase 1, DAHP synthase.	SGN-U566921	AI779054	This study
212	Ser/Thr protein kinase, homologous to *Arabidopsis* CTR1.	SGN-U566677	AF096250	This study
213	Cysteine protease, homologous to *Arabidopsis* calcium-binding EF hand family protein.	SGN-U572289	BE434992	This study
217	Putative phosphate-induced protein.	SGN-U564308	AY125859	This study
221	Cyclin C-like protein.	SGN-U579830	AW932726	This study
223	Homologous to *Arabidopsis* lipase class 3-family protein.	SGN-U565676	AY125865	This study
225	Calcium-dependent protein kinase, homologous to *Arabidopsis* CDPK32.	SGN-U572209	AY125862	This study
226	Homologous to *Arabidopsis* casein kinase 1-like protein 2.	SGN-U566822	AI484998	This study
228	Homologous to *Arabidopsis* protein tyrosine phosphatase.	SGN-U576520	AI895652	This study
229	MAP3K-like protein kinase.	SGN-U576543	AI894448	This study
237	Protein kinase, similar to Avr9/Cf-9 rapidly elicited protein 216 from tobacco, homologous to *Arabidopsis* CIPK11.	SGN-U569122	AI488151	This study

Table 2.7. (Continued).

APR N°[1]	BLAST Annotation from SOL Genome Network (SGN) / Gene name	SGN Unigene ID	GenBank Accession N°[2]	Source of VIGS clone
238	Protein kinase, homologous to *Arabidopsis* clathrin adaptor complexes medium subunit family protein/ APK1B.	SGN-U566665	AW030687	This study
239	CBL-interacting protein kinase, homologous to *Arabidopsis* CIPK6.	SGN-U583600	AI482686	This study
240	Protein kinase.	SGN-U579369	AI487007	This study
242	Shaggy-related protein kinase, homologous to *Arabidopsis* ASK-eta (ASK7).	SGN-U578819	BG631260	This study
243	Homologous to *Arabidopsis* S-locus lectin protein kinase family protein.	SGN-U599100	BG131401	This study
244	Protein kinase, homologous to *Arabidopsis* leucine-rich repeat receptor-like protein kinase.	SGN-U564935	AI781281	This study
246	Putative receptor-like serine-threonine protein kinase.	SGN-U563386	AW030463	This study
250	Protein kinase family protein.	SGN-U577235	AW398400	This study
253	Alternative oxidase 1B.	SGN-U589545	AI780606	This study
260	Homologous to *Arabidopsis* DNAJ heat shock protein.	SGN-U592388	AW622783	This study
261	J-domain protein, homologous to *Arabidopsis* DNAJ heat shock N-terminal domain-containing protein.	SGN-U585728	BG125954	This study
281	MYB-like transcription factor.	SGN-U576253	AI486576	This study
283	Scarecrow-like transcription factor, GRAS4.	SGN-U575365	BG130997	This study

Table 2.7. (Continued).

APR N°[1]	BLAST Annotation from SOL Genome Network (SGN) / Gene name	SGN Unigene ID	GenBank Accession N°[2]	Source of VIGS clone
284	Putative SCARECROW transcription factor, homologous to *Arabidopsis* phytochrome a signal transduction 1 (PAT1).	SGN-U567397	AW222024	This study
285	Putative scarecrow gene regulator.	SGN-U567396	AI489958	This study
287	Scarecrow-like transcription factor, GRAS6.	SGN-U569734	BI209421	This study
292	WRKY transcription factor, homologous to *Arabidopsis* AtWRKY40.	SGN-U566776	AI484501	This study
293	WRKY transcription factor, homologous to *Arabidopsis* AtWRKY33.	SGN-U577212	AW217158	This study
294	WRKY transcription factor, homologous to *Arabidopsis* AtWRKY40.	SGN-U566777	AW933891	This study
295	YABBY-like transcription factor, homologous to *Arabidopsis* YABBY1.	SGN-U583546	AW623191	This study
297	Zinc finger transcription factor, homologous to *Arabidopsis* zinc finger (AN1-like) family protein.	SGN-U585267	AI486585	This study
299	Homologous to *Arabidopsis* haloacid dehalogenase-like hydrolase family protein.	SGN-U604017	AY125871	This study
303	Homologous to *Arabidopsis* mitochondrial phosphate transporter.	SGN-U583149	AW092307	This study
305	Homologous to *Arabidopsis* putative Ran-binding protein 1.	SGN-U581660	AW621846	This study
307	Hexose transporter.	SGN-U579712	AJ010942	This study

Table 2.7. (Continued).

APR N°[1]	BLAST Annotation from SOL Genome Network (SGN) / Gene name	SGN Unigene ID	GenBank Accession N°[2]	Source of VIGS clone
312	Nodule membrane protein, homologous to *Arabidopsis* NOD26-like intrinsic protein 4, NIP4.	SGN-U569106	AW649858	This study
314	Homologous to *Arabidopsis* multidrug resistance P-glycoprotein 11, with ATPase activity.	SGN-U598239	AY125863	This study
315	Polyubiquitin UBQ10.	SGN-U578847	AW037748	This study
316	Ubiquitin activating enzyme, homologous to *Arabidopsis* SUMO activating enzyme 1b (SAE1b).	SGN-U586274	AI483239	This study
319	Homologous to *Arabidopsis* ATP-binding-cassette transporter.	SGN-U572828	AI775862	This study
324	Homologous to *Arabidopsis* wound-responsive family protein.	SGN-U582542	BE449927	This study
332	Homologous to *Arabidopsis* jasmonate-ZIM-domain protein 1, JAZ1, involved in jasmonate signaling.	SGN-U579837	AI485282	This study
333	Homologous to *Arabidopsis* jasmonate-ZIM-domain protein 1, JAZ1, involved in jasmonate signaling.	SGN-U581573	AW032315	This study
335	Putative membrane protein, homologous to *Arabidopsis* auxin-responsive family protein.	SGN-U581879	AI774937	This study
336	Weakly similar to *S. tuberosum* proteasome 26S ATPase subunit 1 variant.	SGN-U573521	AI484715	This study

Table 2.7. (Continued).

APR N°[1]	BLAST Annotation from SOL Genome Network (SGN) / Gene name	SGN Unigene ID	GenBank Accession N°[2]	Source of VIGS clone
337	Homologous to *Arabidopsis* pyridine nucleotide-disulphide oxidoreductase family protein.	SGN-U580395	AI485302	This study
341	Homologous to *Arabidopsis* BTB and TAZ domain protein, acts redundantly with BT2 and BT3 during female gametophyte development.	SGN-U583989	AW219850	This study
344	Homologous to *Arabidopsis* calmodulin-binding family protein.	SGN-U572885	AY125860	This study
347	No significant match.	SGN-U590718	BF098301	This study
371	No significant match.	SGN-U583644	AI484527	This study
372	No significant match.	SGN-U575183	AI484548	This study
373	Homologous to *Arabidopsis* calmodulin-binding family protein.	SGN-U572885	AI894665	This study
	Pti5 transcription factor (Tomato).		LOC544042	This study
	Pti6 transcription factor (Tomato)		LOC544043	This study
	3-phosphoinositide-dependent protein kinase 1, PDK1 (Tomato)		AY849915.1	This study
	NPR1/NIM1 (*N. tabacum*).			Ekengren *et al.* 2003
	EDS1 (*N. tabacum*).	SGN-U423107	AF480489.1	Ekengren *et al.* 2003
	RAR1 (*N. tabacum*).			Ekengren *et al.* 2003
	WRKY1 transcription factor (*N. benthamiana*).			Ekengren *et al.* 2003
	WRKY2 transcription factor (*N. benthamiana*).			Ekengren *et al.* 2003
	WRKY3 transcription factor (*N. benthamiana*).			Ekengren *et al.* 2003

Table 2.7. (Continued).

APR N°[1]	BLAST Annotation from SOL Genome Network (SGN) / Gene name	SGN Unigene ID	GenBank Accession N°[2]	Source of VIGS clone
	SIPKK (*N. benthamiana*).			Ekengren *et al.* 2003
	MEK2 (*N. tabacum*).			Ekengren *et al.* 2003
	MEK1 (*N. tabacum*).			Ekengren *et al.* 2003
	COI1 (*N. benthamiana*).			Ekengren *et al.* 2003
	NDR1 (*N. benthamiana*)			Ekengren *et al.* 2003
	MAPKKKα (*N. benthamiana*).		AY500155	del Pozo *et al.* 2004
	Calnexin (*N. benthamiana*).	SGN-U516661		del Pozo *et al.* 2004
	Calreticulin (*N. benthamiana*).			del Pozo *et al.* 2004
	Osmotin-like protein (*N. benthamiana*).	SGN-U515157		del Pozo *et al.* 2004
	Lipase (*N. benthamiana*).			del Pozo *et al.* 2004
	SGT1 (*N. benthamiana*).		AF494083.1	Peter Moffett, see Peart *et al.* 2002

The APR genes are from tomato while the source of the other genes is given in parenthesis after the gene name. [1]The APR number indicates the gene ID given during a transcriptional profiling analysis of the defense response of tomato to *P.s.* pv. *tomato* (Mysore *et al.* 2002). The genes that showed strong induction during the host defense response were selected for the screen. [2]For the APR genes, the GenBank IDs are from Mysore *et al.* (2002).

judged by replicated experiments and Fisher's exact test ($\alpha = 0.05$; Table 2.8). The identified genes encode proteins with putative functions in defense signaling, energy metabolism, protein stability, secondary metabolism and cell wall lignification.

Plants silenced for 4 genes display morphological alterations

Four out of the 14 genes identified from the screens caused morphological alterations in plants upon silencing (Figure 2.5). Plants silenced for the *cyclophilin* gene showed slightly curved and elongated leaf morphology, whereas *cytochrome C*-silenced plants were mildly chlorotic. Silencing of *anionic peroxidase* or *ubiquitin-activating enzyme* genes resulted in abnormal leaf morphologies and dwarf stature. None of the remaining 10 genes identified in the screen caused abnormal morphology when silenced. *BAK1*-silenced plants had a dwarf stature and crinkled leaves (Figure 2.5), as has been reported earlier in *Arabidopsis* and *N. benthamiana* (Chinchilla *et al.* 2007; Heese *et al.* 2007).

Plants silenced for aldehyde dehydrogenase, HCBT or ubiquitin-activating enzyme show reduced production of flg22-induced reactive oxygen species (ROS)

One of the early responses during the activation of PTI is the production of ROS (Boller and Felix 2009). In order to determine if any of the identified candidate genes plays a role in PTI-associated ROS production, we measured flg22-

Table 2.8. Percentage of plants in which PTI was compromised when candidate genes from the immunity-induced gene collection were silenced and evaluated using the cell-death-based assay.

Gene silenced	Category	Pf/DC	Pp/DC	Pf/Q1-1	Agro/Ptab
TRV2		0%	0%	0%	0%
Alternative oxidase	Energy metabolism	20%	13%	**40%**	7%
Anionic peroxidase	Cell wall protein	**42%**	**47%**	**47%**	5%
CA4H	Secondary metabolism	**43%**	21%	**50%**	**29%**
EDS1	Defense signaling	**27%**	**40%**	**27%**	7%
Proteasome 26S subunit	Protein stability	**36%**	27%	0%	9%
Transducin	Signaling	8%	8%	15%	**46%**
Ubiquitin activating enzyme	Protein stability	12%	18%	**29%**	25%

A minimum of 11 plants was evaluated for each assay. Percentages in bold represent those combinations where PTI was compromised as determined by pairwise comparisons of the TRV2 control with each of the candidate genes with a Fisher's exact test ($\alpha = 0.05$). Abbreviations: CA4H = Cinnamic acid 4-hydroxylase

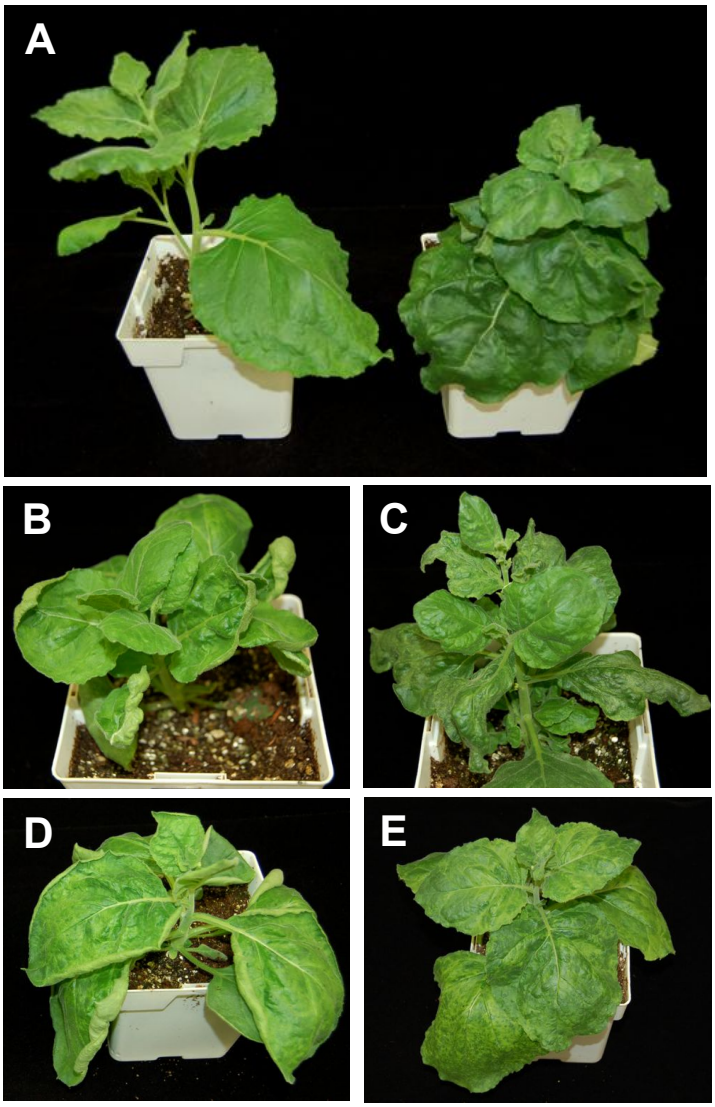

Figure 2.5. Morphological alterations of plants silenced for PTI-associated genes. A, Control TRV2 (left) and *BAK1*-silenced (right) plants. Plants silenced with a cDNA fragment from genes encoding the following: **B,** *anionic peroxidase*; **C,** *ubiquitin activating enzyme*; **D,** *cyclophilin*; and **E,** *cytochrome C*. Photographs were taken 4 weeks after VIGS was initiated.

induced ROS in plants silenced for each of the 14 genes. Plants silenced for *aldehyde dehydrogenase, HCBT* or *ubiquitin-activating enzyme* showed statistically significant lower levels of ROS production compared to non-silenced plants (Figure 2.6). None of the other 11 genes showed this reduction, and results with two of these are also shown in Figure 2.6. Plants silenced for *FLS2* predictably showed drastically reduced ROS levels in these experiments.

Silencing of the PTI candidate genes does not enhance a general cell death response to the challenger inoculations

It was possible that some of the genes we identified act as negative regulators of plant cell death. If that were the case, their silencing might lead to faster or stronger cell death in response to the challenger inoculation and be misinterpreted as being due to a breakdown of PTI in our assay. In order to examine this possibility, we infiltrated the challengers *Pst* DC3000 or *Pst* DC3000 Δ*hopQ1-1* at three different concentrations each into *N. benthamiana* leaves that were silenced for a subset of the candidate genes derived from the screen (see Methods). We did not include *P. s.* pv. *tabaci* 11528 as no break-down of PTI for these seven genes was observed for the *Agrobacterium*/*P. s.* pv. *tabaci* combination in the cell-death-based assay. For this and subsequent experiments described in the paper, we focused on the 7 genes derived from the VIGS library.

The progression of cell death in response to the challengers was monitored in the leaves and compared to non-silenced TRV-only control plants (Table 2.9;

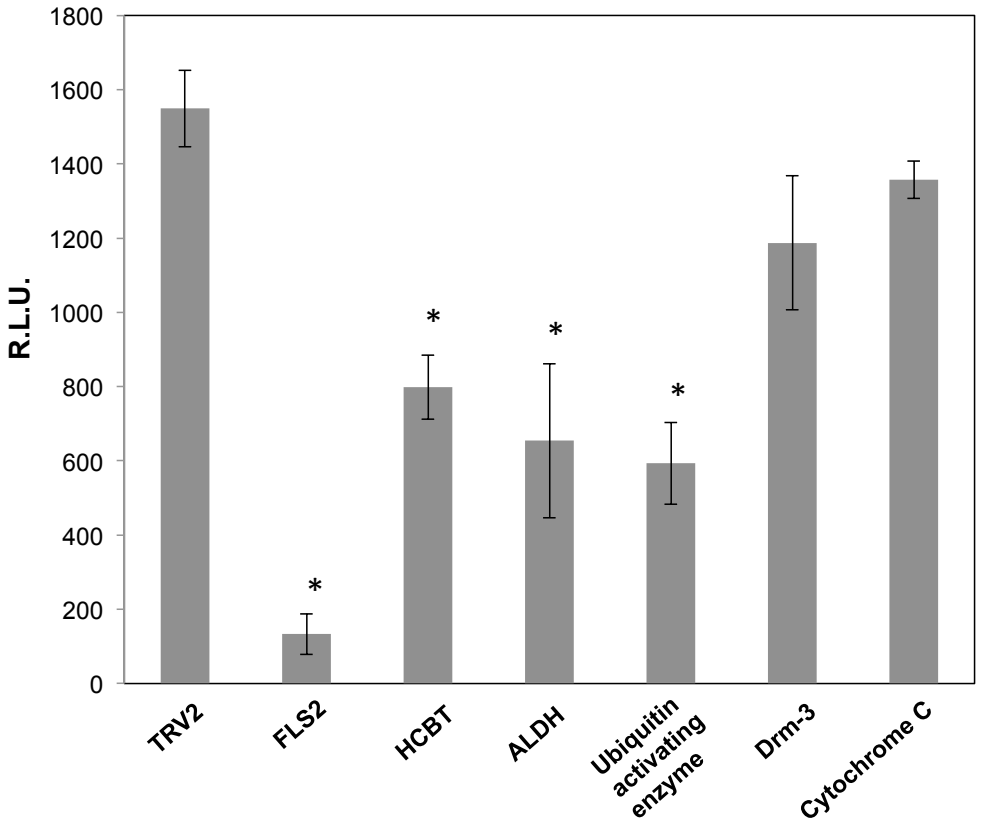

Figure 2.6. Production of flg22-induced ROS in plants silenced for some of the genes identified from the screen. Leaf discs from silenced plants were treated with 100 nM flg22 and ROS production was measured. The level of ROS at 20 minutes post-induction is shown as relative light units (R.L.U.), and the names of the genes silenced are indicated. Non-silenced TRV2 plants served as the control. At least 3 silenced plants were tested for each gene, and the average R.L.U. with SEM is shown. The experiment was repeated twice with similar results. An asterisk (*) indicates significantly lower ROS levels than TRV2, $p<0.001$. Abbreviations: ALDH: aldehyde dehydrogenase, HCBT: anthranilate N-hydroxycinnamoyl/ benzoyltransferase.

Table 2.9. Extent of cell death caused by inoculation of different challengers in plants silenced for the candidate genes from the VIGS library. **(A)** Inoculation with *P. s.* pv. *tomato* (*Pst)* DC3000 (~6 x 10^6 CFU/ml). **(B)** Inoculation with *Pst* DC3000 Δ*hopQ1-1* (~3 x 10^5 CFU/ml). An asterisk (*) indicates significantly faster cell death than the control (Fisher's exact test, α=0.05).

(A)

Gene silenced	Extent of cell death		
	Full	**Partial**	**None**
TRV2	8	3	1
BAK1	1	3	4
FLS2	8	3	1
Aldehyde dehydrogenase	7	3	2
Cathepsin B	5	4	3
Cyclophilin	4	5	3
Cytochrome C	6	4	2
Drm-3	7	2	3
HCBT	2	5	5
Plastocyanin	4	6	2

Table 2.9. (Continued).

(B)

Gene silenced	Extent of cell death		
	Full	**Partial**	**None**
TRV2	2	1	5
*BAK1**	4	4	0
FLS2	2	1	5
Aldehyde dehydrogenase	3	2	3
Cathepsin B	2	3	3
Cyclophilin	2	4	1
Cytochrome C	2	2	4
Drm-3	0	2	6
HCBT	0	4	4
Plastocyanin	2	2	4

and data not shown). A Fisher's exact test (α = 0.05) was used to determine that none of the genes showed significantly faster cell death than TRV-only control plants. *BAK1*-silenced plants were the only exception, since they showed faster cell death than control plants in response to *Pst* DC3000 Δ*hopQ1-1* (Table 2.9.B). These results indicate that the phenotypes we observed in our assays were due to compromised PTI upon gene silencing and not to a general promotion of the cell death response.

Interestingly, cell death in response to some bacterial concentrations actually developed at a slower rate in plants silenced for certain genes. This occurred, for example, in plants silenced for *cathepsin B, Drm-3, HCBT* (anthranilate N-hydroxycinnamoyl/benzoyltransferase) and *plastocyanin* at some *Pst* DC3000 or DC3000 Δ*hopQ1-1* titers that were tested (Table 2.9; and data not shown). It is possible these genes are also involved in host pathways that are involved in cell death associated with ETI or disease. This is consistent with earlier indications that host responses during PTI, ETI and disease may share some components, but differ in timing and amplitude (Boller and Felix 2009).

flg22-induced responses are compromised in plants silenced for *aldehyde dehydrogenase, cyclophilin* or *HCBT*

In order to determine if any of the candidate genes is involved specifically in FLS2-dependent responses other than ROS production, we performed the cell-death-based assay using flg22 as the inducer and *Pst* DC3000 as the

challenger in plants silenced for the seven genes derived from the VIGS library screen. A compromised PTI phenotype was seen in plants silenced for genes encoding *aldehyde dehydrogenase*, *cyclophilin* or *HCBT* (Table 2.10), suggesting that these three genes act downstream of flg22 perception and are involved in the FLS2-mediated PTI pathway. Note that both *aldehyde dehydrogenase* and *HCBT* were also observed to be involved in flg22-induced ROS production (Figure 2.6). Cyclophilin may play a role in PTI downstream to or independent of flg22-mediated ROS production.

Discussion

We have identified 14 genes that function in diverse cellular processes in order to promote host PTI. A summary of their putative roles is shown in Figure 2.7. PTI likely involves a series of interdependent responses and it is perhaps not surprising that there are so many steps at which this immune response can be attenuated. Early signaling events that involve PRRs, kinase cascades and transcription factors are activated upon perception of PAMPs (Asai *et al.* 2002). Some of these early responses may be PAMP-specific and the reliance of our screen on live bacteria (a source of diverse PAMPs) may explain why we did not identify genes involved in these initial PTI events. However, we did identify genes potentially involved in several PTI responses including the production of ROS and antimicrobial compounds, protein stabilization and degradation, cell wall lignification and hormone signaling. Understanding the role of each of the 14 candidate genes in PTI will require much further study. However, previous

Table 2.10. Percentage of plants in which PTI was compromised when candidate genes from the VIGS library were silenced and evaluated in the cell-death-based assay using 50 μM flg22 as the inducer and *Pst* DC3000 as the challenger.

Gene silenced	flg22/DC3000
TRV2	0%
BAK1	**70%**
FLS2	**75%**
Aldehyde dehydrogenase	**27%**
Cathepsin B	6%
Cyclophilin	**30%**
Cytochrome C	7%
Drm-3	15%
HCBT	**35%**
Plastocyanin	19%

A minimum of 15 plants was evaluated for each assay. Percentages in bold represent those instances where PTI was compromised as determined by pairwise comparisons of the TRV2 control with each of the candidate genes with a Fisher's exact test ($\alpha = 0.05$).

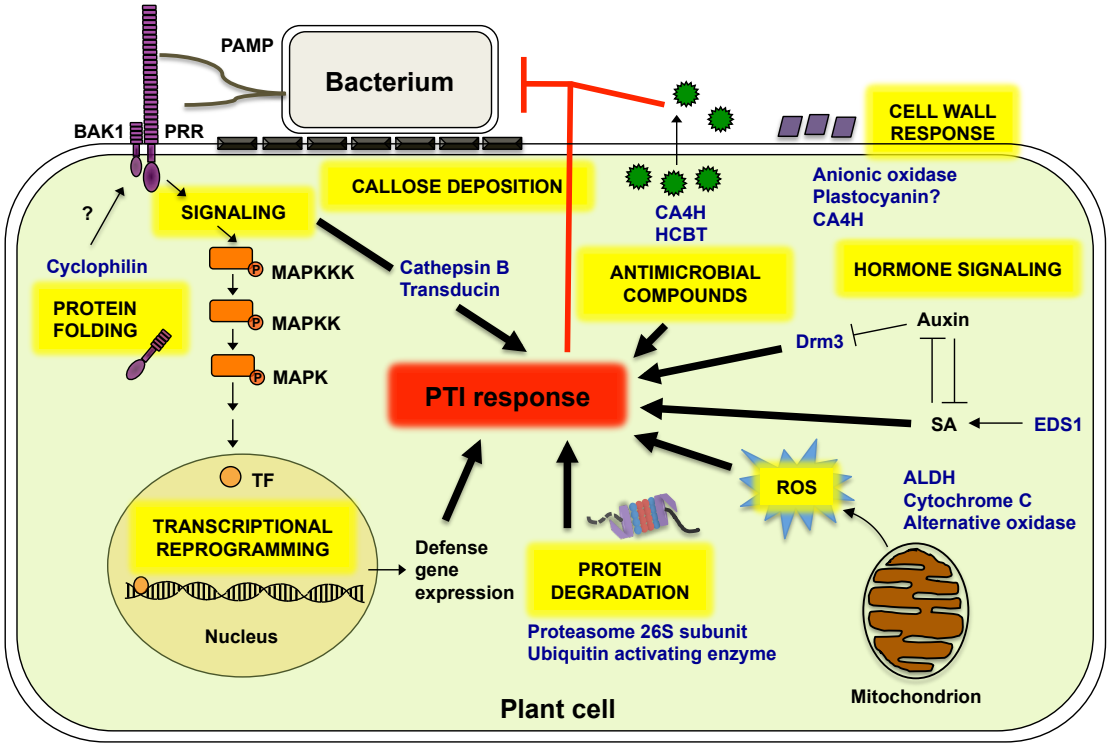

Figure 2.7. **A model summarizing the possible roles of the genes identified in PAMP-triggered immunity.** The model depicts some of the major cellular processes that are known to be involved upon PAMP perception (yellow boxes), and the genes identified in this study (blue). Note that CA4H may play a role in the production of antimicrobial compounds during secondary metabolism as well as in lignin biosynthesis, which is part of the cell wall response. Abbreviations: ALDH: aldehyde dehydrogenase, CA4H: cinnamic acid 4-hydroxylase, HCBT: anthranilate N hydroxycinnamoyl/ benzoyltransferase, SA: salicylic acid, TF: transcription factor.

data available for some of the genes or gene classes is discussed below and may provides important starting points for future work.

One of the genes from our screen, *cathepsin B,* has been shown previously to play a role in plant programmed cell death (PCD; Gilroy *et al.* 2007). The hypersensitive response to *Pst* DC3000 in leaves of *N. benthamiana* was compromised in plants silenced for *cathepsin B* (Gilroy *et al.* 2007) similar to what we observed when using a DC3000 inoculum level of 3 x 10^6 CFU/mL (data not shown). In addition, cathepsin B was also involved in controlling the progression of senescence, another form of PCD. Furthermore, an *Arabidopsis* plant carrying mutations in all three of the *cathepsin B* orthologs was more susceptible to virulent *Pst* DC3000 infection (McLellan *et al.* 2009). The role of *cathepsin B* in both PTI and ETI supports the occurrence of shared components in these two immune responses and we plan to use each of the 14 genes identified in this study to further examine that issue in the future.

EDS1 is another gene obtained from the screen for which previous evidence for a role in defense signaling exists. EDS1 is required for salicylic acid (SA) accumulation and the function of many resistance genes in restricting pathogen growth during ETI (Wiermer *et al.* 2005). SA has been shown to be important for the response against PAMPs from *Phytophthora* and bacterial flg22 (Tsuda *et al.* 2008; Halim *et al.* 2009). Therefore, it is possible that EDS1 functions in both ETI and PTI by its effect on SA accumulation.

Cyclophilins have peptidyl prolyl isomerase activity that facilitates protein folding. An *Arabidopsis* cyclophilin was previously shown to be involved in the

activation of the type III effector AvrRpt2, which was required for its virulence functions and for its recognition by the plant immune system (Coaker *et al.* 2005). It is tempting to speculate that the cyclophilin we identified here could modulate the stability of PRRs, as has been shown for ER-QC components associated with EFR (Li *et al.* 2009), or other host proteins involved in PTI signaling.

HCBT (anthranilate N-hydroxycinnamoyl/benzoyltransferase) catalyzes the first committed step in phytoalexin biosynthesis (Yang *et al.* 1997). Phytoalexins have long been implicated in the defense response against bacterial and fungal pathogens (Thomma *et al.* 1999; Qiu *et al.* 2008). It has also been shown that PGN induces the production of the phytoalexin camalexin in *Arabidopsis* (Gust *et al.* 2007). It is therefore conceivable that HCBT can function in PTI via its role in phytoalexin biosynthesis.

Drm3 shows similarity to a pea gene whose expression is down-regulated by auxin and associated with dormancy (Stafstrom *et al.* 1998). It is known that auxin and salicylic acid (SA) signaling pathways act antagonistically during the host response to pathogens with the former promoting disease susceptibility and the latter increasing disease resistance (Wang *et al.* 2007). Flg22-induced signaling is known to repress the transcription of auxin receptor genes through an RNAi mechanism leading to an increase in resistance (Navarro *et al.* 2006). The repression of a *Drm3* homolog by auxin and our observation here of a loss-of-function phenotype associated with this gene may indicate that Drm3 acts

as a positive regulator of PTI that is de-repressed when the auxin response is inhibited during PTI.

Ubiquitination is increasingly being found to contribute to PTI and our identification of two genes involved in this process, a putative proteasome 26S subunit homolog and a ubiquitin activating enzyme, provide further support for a role of this post-translational modification in plant immunity (Craig *et al.* 2009). The expression of several genes involved in protein degradation was induced upon flg22 treatment in *Arabidopsis* (Navarro *et al.* 2004). An E3 ligase U-box triple mutant in *Arabidopsis* displayed de-repression of PAMP responses and higher resistance to bacterial and oomycete pathogens, suggesting negative regulation of PTI by E3 ubiquitin ligases (Trujillo *et al.* 2008). The loss-of-function phenotype we observed here suggests that some ubiquitination components play an important role as positive regulators of PTI.

The combination of VIGS and a cell-death-based assay proved to be a highly effective approach to screen a large number of genes for possible involvement in PTI. Other experimental approaches to identify PTI-associated genes have been reported previously. These methods typically have employed purified PAMPs and measure early events such as the oxidative burst, alkalinization of cell culture medium, gene induction and MAPK activation, and later responses like callose deposition at the cell wall and inhibition of seedling growth (Boller and Felix 2009). Some of these methods are not amenable to a high-throughput screen, or are specific to a certain PTI pathway, whereas others

measure responses that occur within minutes of microbial recognition and may not uncover important downstream events.

The cell-death-based assay we used is based on earlier work by Klement *et al.* (2003) which was further optimized by Oh and Collmer (2005). It relies on non-pathogenic bacteria as a source of PAMPs and various challengers that cause either disease- or immunity-associated cell death. The genes identified by this approach may therefore play a role in responsiveness to a wide array of different PAMPs.

Data from our experiments on ROS production, and using flg22 as the inducer in the cell death assay also support the hypothesis that some of the genes identified are not exclusively regulated by the FLS2 pathway, but may be acting downstream of other PRRs (Figure 2.6 and Table 2.10). There is previous evidence that subtle differences exist in plant responses to different PAMPs. For example, defense gene *PR-1* expression, transcriptional changes and phytoalexin production were differently induced by flg22, chitin and PGN in *Arabidopsis* (Gust *et al.* 2007).

An advantage, therefore, of the combined cell death assays/VIGS approach is that it can be easily modified to target specific PTI pathways and to increase the efficiency of gene identification. For example, individual PAMPs such as PGN, EF-Tu, lipopolysaccharide (LPS) and others could be used as the inducer of PTI to identify host genes involved in recognition of these molecules. In addition, as the percentage of candidates identified from our *P. syringae*-induced genes was ~20-fold higher than that identified from the general library

screen (5.1% vs. 0.23%), it may be worthwhile to conduct preliminary transcriptional profiling with the specific PAMPs of interest in order to enrich for relevant PTI-associated genes.

It is important to note that we still have a poor understanding of why bacteria fail to grow in leaf tissue protected by PTI. Our data suggest that the barriers against bacterial growth are highly multifactorial and that compromising a single downstream component of PTI is insufficient to permit or enhance substantial bacterial growth. Our screen for cell death following bacterial challenge involved relatively high levels of inoculum. Thus, to reveal a VIGS-induced defect in PTI, the bacteria primarily had to succeed in deploying the type III secretion system (T3SS) and deliver functional effectors. The notion that PTI-protected tissue does not support delivery of effectors by challenge bacteria is supported by a concurrent study documenting the failure of *P. syringae* pv. *tomato* DC3000 to deliver into such tissue the AvrPto-Cya translocation reporter, which can be assayed for adenylate cyclase activity in plant cells rather than elicitation of cell death (Oh *et al.* 2010). However, the mechanism for this inhibition has not been determined, and it could be a secondary consequence of anti-bacterial stresses in PTI-protected tissue. The genes found in this screen may be useful in future work in understanding how PTI impacts T3SS function as well as inhibiting general bacterial growth.

We identified 14 genes from a screen of >3,200 and it can be asked whether this is a reasonable number to expect from a screen such as this. It is important to point out certain aspects of our screen that may have affected the

number of genes identified. First, the library we used was derived from leaf tissues exposed to a variety of elicitors and not specifically to PAMPs. It is possible that PAMP treatment would have enriched the library more for PTI-associated genes (note that our screen of 133 immunity-associated genes likely was enriched for genes involved in PTI). Second, we initially silenced one plant per gene and discovered only later that, because of the experimental variability of the assay, silencing of 3 plants with each gene gave a higher likelihood of observing PTI breakdown. Third, we required that silencing of a gene had to compromise PTI in at least three independent experiments to be considered further. This cut-off excluded some genes that may in fact have a more subtle effect on PTI. Finally it is important to consider that we screened only 3,200 gene fragments (and not all of these were unique). The total number of genes expressed in *N. benthamiana* leaves is unknown but, based on tomato, another Solanaceous species, is estimated to be ~16,500 (Lukas Mueller, pers. comm.). Hence, our screen was not a saturating one and it is possible that additional genes involved in PTI could be identified by this method.

Suboptimal efficiency of gene silencing is another factor that may have prevented us from obtaining a larger number of genes from the screen, and stronger phenotypes in our follow-up assays. While the degree of silencing achieved for the genes analyzed was good (Figure 2.4), we did not obtain complete silencing of the genes; this is to be expected since we used VIGS and not gene-knockout backgrounds. We also found that the silencing constructs for 2 out of the 14 genes, *cyclophilin* and *EDS1*, might knock down expression

of related, off-target genes (Table 2.11). We performed RT-PCR for a predicted off-target of *cyclophilin*, which we call *cyclophilin homolog* TC9299, and found that the transcript abundance of this gene was indeed reduced in silenced plants (Figure 2.4). TC9299 also encodes a cyclophilin and the observed phenotypes with the *cyclophilin* construct could therefore be due to the combined silencing of both of these genes.

We observed that silencing of four of the fourteen PTI-associated genes also caused defects in plant growth or development. These results add to several previous observations where disruption of a gene involved in immunity also affects plant morphology. For example, the receptor-like kinase *ERECTA* that is involved in plant development, and the *COPINE1/BONZAI1* genes from *Arabidopsis* were shown to have roles in immunity to bacterial, fungal and oomycete pathogens, and plants with mutations in these genes have developmental defects (Godiard *et al.* 2003; Yang *et al.* 2006; Sanchez-Rodriguez *et al.* 2009). Similarly, BAK1 is now known to play a role in both a hormone-sensitive developmental pathway and in PTI (Kinoshita *et al.* 2005; Chinchilla *et al.* 2007). In our case, silencing of four genes caused stunting of *N. benthamiana* and, in one case, leaf chlorosis. It is interesting that similar observations have been made in *Drosophila* where the well-characterized Toll receptor plays a role in embryo development and in immunity and a recent screen revealed that RNAi silencing of some genes in the *immune-deficiency* (Imd) pathway caused developmental defects (Foley and O'Farrell 2004). Together, these examples suggest that eukaryotes have relied on certain

Table 2.11. Predicted off-targets for silencing, predicted using siRNA Scan, http://bioinfo2.noble.org/RNAiScan.htm. The sequences of the VIGS constructs were used as the query. The IDs of the actual intended target gene, and additional off-target genes predicted to be co-silenced are given.

Gene	Target genome searched	ID of target	Functional Annotation
Cyclophilin	*N. benthamiana*	TC7047	Homologue to UP|CYPH_LYCES (P21568) Peptidyl-prolyl cis-trans isomerase (PPIase) (Rotamase) (Cyclophilin) (Cyclosporin A-binding protein) , complete
		TC9299	Homologue to UP|CYPH_LYCES (P21568) Peptidyl-prolyl cis-trans isomerase (PPIase) (Rotamase) (Cyclophilin) (Cyclosporin A-binding protein) , complete
EDS1	*N. benthamiana*	CK296764	Similar to UP|Q9LJ45 (Q9LJ45) PREG1-like negative regulator-like protein (At3g21870), partial (24%)
		NP821070	GB|AF479625.1|AAL85347.1 EDS1-like protein [*Nicotiana benthamiana*]

conserved genes to evolve mechanisms related to both growth/development and immune responses.

RNAi screens also have been performed successfully in other eukaryotes to identify regulators of the innate immune response. Genes involved in signaling, proteolysis, intracellular protein transport, protein synthesis, transcriptional regulation and defense responses have been identified to be positive regulators of immunity in diverse species such as *Drosophila*, *C. elegans* and the mouse (Foley and O'Farrell 2004; Alper *et al.* 2008; Cronin *et al.* 2009). Silencing of 10,689 genes in *Drosophila* identified 790 (7.4%) that may play a role in resistance to *Serratia marcescens*, while another study that silenced 7,216 genes in *Drosophila* identified 49 (0.68%) to be involved in the LPS-induced *Imd* signaling pathway (Alper *et al.* 2008; Cronin *et al.* 2009). Some of the genes identified in our study are predicted to be involved in signaling and protein degradation, suggesting that these same processes are used in innate immunity by diverse eukaryotes.

It is not surprising that a large number of plant genes are involved in PTI considering the diversity of pathogenic and non-pathogenic microbes that plants encounter. Moreover, the large number of pathogen effectors that have evolved to undermine PTI points to a corresponding complexity of plant immune processes (Lewis *et al.* 2009). For example, AvrPto, AvrPtoB, HopM1, HopAI1, and HopU1 are bacterial effectors that have been found to interfere with either the formation of PRR complexes, MAPK cascades, callose deposition, secretory vesicle pathways, DNA/RNA processing or the chloroplast

during pathogenesis (Boller and He, 2009; Guo *et al.* 2009; Lewis *et al.* 2009). The genes we identified here highlight the potential importance of protein stability, secondary metabolism, and hormone signaling in PTI and raise the possibility that each of these processes is targeted by pathogen effectors. In the future it will be interesting to investigate which of these processes may be targeted by pathogen effectors and the underlying mechanisms involved. Such knowledge of the molecular basis of PTI may ultimately lead to manipulation of this important host response in order to develop crop plants with more durable resistance to pathogens.

Acknowledgments

We thank past and current members of the Martin lab for their help with assay infiltrations during the initial phase of the VIGS screen. We especially thank Elise Pasoreck, Sara Cohen, Hye-Sook Oh, Junchen Gu, Bridget Randall, Daniel Opel and Diane Dunham for technical assistance. We thank Sebastien Cunnac and Jesse Munkvold for critical comments on the manuscript. We also thank Simona Despa, Statistical Consulting Unit, Cornell University, Chang-Sik Oh and Jesse Munkvold for help in statistical analysis of the data. Funding for this work was from National Science Foundation grant no. DBI-0605059 (ACV and GBM).

REFERENCES

Alper S., Laws R., Lackford B., Boyd W.A., Dunlap P., Freedman J.H., and Schwartz D.A. 2008. Identification of innate immunity genes and pathways using a comparative genomics approach. Proc Natl Acad Sci U S A 105:7016-7021.

Asai T., Tena G., Plotnikova J., Willmann M.R., Chiu W.L., Gomez-Gomez L., Boller T., Ausubel F.M., and Sheen J. 2002. MAP kinase signalling cascade in *Arabidopsis* innate immunity. Nature 415:977-983.

Badel J.L., Shimizu R., Oh H.S., and Collmer A. 2006. A *Pseudomonas syringae* pv. *tomato avrE1/hopM1* mutant is severely reduced in growth and lesion formation in tomato. Mol Plant Microbe Interact 19:99-111.

Bent A.F., and Mackey D. 2007. Elicitors, effectors, and R genes: the new paradigm and a lifetime supply of questions. Annu Rev Phytopathol 45:399-436.

Boller T., and Felix G. 2009. A renaissance of elicitors: perception of microbe-associated molecular patterns and danger signals by pattern-recognition receptors. Annu Rev Plant Biol 60:379-406.

Boller T., and He S.Y. 2009. Innate immunity in plants: an arms race between pattern recognition receptors in plants and effectors in microbial pathogens. Science 324:742-744.

Chakravarthy S., Velasquez A.C., and Martin G.B. 2009. Assay for pathogen-associated molecular pattern (PAMP)-triggered immunity (PTI) in plants. J Vis Exp 31 DOI: 10.3791/1442

Chinchilla D., Bauer Z., Regenass M., Boller T., and Felix G. 2006. The *Arabidopsis* receptor kinase FLS2 binds flg22 and determines the specificity of flagellin perception. Plant Cell 18:465-476.

Chinchilla D., Zipfel C., Robatzek S., Kemmerling B., Nurnberger T., Jones J.D., Felix G., and Boller T. 2007. A flagellin-induced complex of the receptor FLS2 and BAK1 initiates plant defence. Nature 448:497-500.

Coaker G., Falick A., and Staskawicz B. 2005. Activation of a phytopathogenic bacterial effector protein by a eukaryotic cyclophilin. Science 308:548-550.

Craig A., Ewan R., Mesmar J., Gudipati V., and Sadanandom A. 2009. E3 ubiquitin ligases and plant innate immunity. J Exp Bot 60:1123-1132.

Cronin S.J., Nehme N.T., Limmer S., Liegeois S., Pospisilik J.A., Schramek D., Leibbrandt A., Simoes R deM., Gruber S., Puc U., Ebersberger I., Zoranovic T., Neely G.G., von Haeseler A., Ferrandon D., and Penninger J.M. 2009. Genome-wide RNAi screen identifies genes involved in intestinal pathogenic bacterial infection. Science 325:340-343.

Cuppels D.A. 1986. Generation and Characterization of Tn5 Insertion Mutations in *Pseudomonas syringae* pv. *tomato*. Appl Environ Microbiol 51:323-327.

del Pozo O., Pedley K.F., and Martin G.B. 2004. MAPKKKalpha is a positive regulator of cell death associated with both plant immunity and disease. EMBO J 23:3072-3082.

Foley E., and O'Farrell P.H. 2004. Functional dissection of an innate immune response by a genome-wide RNAi screen. PLoS Biol 2:e203.

Gilroy E.M., Hein I., van der Hoorn R., Boevink P.C., Venter E., McLellan H., Kaffarnik F., Hrubikova K., Shaw J., Holeva M., Lopez E.C., Borras-Hidalgo O., Pritchard L., Loake G.J., Lacomme C., and Birch P.R. 2007. Involvement of cathepsin B in the plant disease resistance hypersensitive response. Plant J 52:1-13.

Gimenez-Ibanez S., Hann D.R., Ntoukakis V., Petutschnig E., Lipka V., and Rathjen J.P. 2009. AvrPtoB targets the LysM receptor kinase CERK1 to promote bacterial virulence on plants. Curr Biol 19:423-429.

Godiard L., Sauviac L., Torii K.U., Grenon O., Mangin B., Grimsley N.H., and Marco Y. 2003. ERECTA, an LRR receptor-like kinase protein controlling development pleiotropically affects resistance to bacterial wilt. Plant J 36:353-365.

Goodin M.M., Zaitlin D., Naidu R.A., and Lommel S.A. 2008. *Nicotiana benthamiana*: its history and future as a model for plant-pathogen interactions. Mol Plant Microbe Interact 21:1015-1026.

Guo M., Tian F., Wamboldt Y., and Alfano J.R. 2009. The majority of the type III effector inventory of *Pseudomonas syringae* pv. *tomato* DC3000 can suppress plant immunity. Mol Plant Microbe Interact 22:1069-1080.

Gust A.A., Biswas R., Lenz H.D., Rauhut T., Ranf S., Kemmerling B., Gotz F., Glawischnig E., Lee J., Felix G., and Nurnberger, T. 2007. Bacteria-derived peptidoglycans constitute pathogen-associated molecular patterns triggering innate immunity in *Arabidopsis*. J Biol Chem 282:32338-32348.

Halim V.A., Altmann S., Ellinger D., Eschen-Lippold L., Miersch O., Scheel D., and Rosahl S. 2009. PAMP-induced defense responses in potato require both salicylic acid and jasmonic acid. Plant J 57:230-242.

Hann D.R., and Rathjen J.P. 2007. Early events in the pathogenicity of *Pseudomonas syringae* on *Nicotiana benthamiana*. Plant J 49:607-618.

Heese A., Hann D.R., Gimenez-Ibanez S., Jones A.M., He K., Li J., Schroeder J.I., Peck S.C., and Rathjen J.P. 2007. The receptor-like kinase SERK3/BAK1 is a central regulator of innate immunity in plants. Proc Natl Acad Sci U S A 104:12217-12222.

Holsters M., Silva B., Van Vliet F., Genetello C., De Block M., Dhaese P., Depicker A., Inze D., Engler G., Villarroel R., van Montagu M., and Schell J. 1980. The functional organization of the nopaline *A. tumefaciens* plasmid pTiC58. Plasmid 3:212-230.

Huang H.C., Schuurink R., Denny T.P., Atkinson M.M., Baker C.J., Yucel I., Hutcheson S.W., and Collmer A. 1988. Molecular cloning of a *Pseudomonas syringae* pv. *syringae* gene cluster that enables *Pseudomonas fluorescens* to elicit the hypersensitive response in tobacco plants. J Bacteriol 170:4748-4756.

Kinoshita T., Cano-Delgado A., Seto H., Hiranuma S., Fujioka S., Yoshida S., and Chory J. 2005. Binding of brassinosteroids to the extracellular domain of plant receptor kinase BRI1. Nature 433:167-171.

Klement Z., Bozso Z., Kecskes M.L., Besenyei E., Arnold C., and Ott P.G. 2003. Local early induced resistance of plants as the first line of defence against bacteria. Pest Manag Sci 59:465-474.

Kvitko B.H., Park D.H., Velasquez A.C., Wei C.F., Russell A.B., Martin G.B., Schneider D.J., and Collmer A. 2009. Deletions in the repertoire of *Pseudomonas syringae* pv. *tomato* DC3000 type III secretion effector genes reveal functional overlap among effectors. PLoS Pathog 5:e1000388.

Lewis J.D., Guttman D.S., and Desveaux D. 2009. The targeting of plant cellular systems by injected type III effector proteins. Semin Cell Dev Biol 20:1055-1063.

Li J., Zhao-Hui C., Batoux M., Nekrasov V., Roux M., Chinchilla D., Zipfel C., and Jones J.D. 2009. Specific ER quality control components required for biogenesis of the plant innate immune receptor EFR. Proc Natl Acad Sci U S A. 106:15973-15978.

Lu R., Malcuit I., Moffett P., Ruiz M.T., Peart J., Wu A.J., Rathjen J.P., Bendahmane A., Day L., and Baulcombe D.C. 2003. High throughput virus-induced gene silencing implicates heat shock protein 90 in plant disease resistance. EMBO J 22:5690-5699.

McBride K.E., and Summerfelt K.R. 1990. Improved binary vectors for *Agrobacterium*-mediated plant transformation. Plant mol biol 14:269-276.

McLellan H., Gilroy E.M., Yun B.W., Birch P.R., and Loake G.J. 2009. Functional redundancy in the *Arabidopsis cathepsin B* gene family contributes to basal defence, the hypersensitive response and senescence. New Phytol 183:315-326.

Miya A., Albert P., Shinya T., Desaki Y., Ichimura K., Shirasu K., Narusaka Y., Kawakami N., Kaku H., and Shibuya N. 2007. CERK1, a LysM receptor kinase, is essential for chitin elicitor signaling in *Arabidopsis*. Proc Natl Acad Sci U S A 104:19613-19618.

Mysore K.S., Crasta O.R., Tuori R.P., Folkerts O., Swirsky P.B., and Martin G.B. 2002. Comprehensive transcript profiling of Pto- and Prf-mediated host defense responses to infection by *Pseudomonas syringae* pv. *tomato*. Plant J 32:299-315.

Navarro L., Zipfel C., Rowland O., Keller I., Robatzek S., Boller T., and Jones J.D. 2004. The transcriptional innate immune response to flg22. Interplay and overlap with *Avr* gene-dependent defense responses and bacterial pathogenesis. Plant Physiol 135:1113-1128.

Navarro L., Dunoyer P., Jay F., Arnold B., Dharmasiri N., Estelle M., Voinnet O., and Jones J.D. 2006. A plant miRNA contributes to antibacterial resistance by repressing auxin signaling. Science 312:436-439.

Nelson K.E., Weinel C., Paulsen I.T., Dodson R.J., Hilbert H., Martins dos Santos V.A., Fouts D.E., Gill S.R., Pop M., Holmes M., Brinkac L., Beanan M., DeBoy R.T., Daugherty S., Kolonay J., Madupu R., Nelson W., White O., Peterson J., Khouri H., Hance I., Chris Lee P., Holtzapple E., Scanlan D., Tran K., Moazzez A., Utterback T., Rizzo M., Lee K., Kosack D., Moestl D., Wedler H., Lauber J., Stjepandic D., Hoheisel J., Straetz M., Heim S., Kiewitz C., Eisen J.A., Timmis K.N., Dusterhoft A., Tummler B., and Fraser C.M. 2002. Complete genome sequence and comparative analysis of the metabolically versatile *Pseudomonas putida* KT2440. Environ Microbiol 4:799-808.

Oh H.S., and Collmer A. 2005. Basal resistance against bacteria in *Nicotiana benthamiana* leaves is accompanied by reduced vascular staining and suppressed by multiple *Pseudomonas syringae* type III secretion system effector proteins. Plant J 44:348-359.

Oh H.S., Park D.H., and Collmer A.C. 2010. Components of the *Pseudomonas syringae* type III secretion system can elicit and suppress plant innate immunity MPMI:in revision.

Peart J.R., Mestre P., Lu R., Malcuit I., and Baulcombe D.C. 2005. NRG1, a CC-NB-LRR protein, together with N, a TIR-NB-LRR protein, mediates resistance against tobacco mosaic virus. Curr Biol 15:968-973.

Qiu J.L., Fiil B.K., Petersen K., Nielsen H.B., Botanga C.J., Thorgrimsen S., Palma K., Suarez-Rodriguez M.C., Sandbech-Clausen S., Lichota J., Brodersen P., Grasser K.D., Mattsson O., Glazebrook J., Mundy J., and Petersen M. 2008. *Arabidopsis* MAP kinase 4 regulates gene expression through transcription factor release in the nucleus. EMBO J 27:2214-2221.

Ron M., and Avni A. 2004. The receptor for the fungal elicitor ethylene-inducing xylanase is a member of a resistance-like gene family in tomato. Plant Cell 16:1604-1615.

Saijo Y., Tintor N., Lu X., Rauf P., Pajerowska-Mukhtar K., Haweker H., Dong X., Robatzek S., and Schulze-Lefert P. 2009. Receptor quality control in the endoplasmic reticulum for plant innate immunity. EMBO J. 28:3439-3449.

Sanchez-Rodriguez C., Estevez J.M., Llorente F., Hernandez-Blanco C., Jorda L., Pagan I., Berrocal M., Marco Y., Somerville S., and Molina A. 2009. The ERECTA receptor-like kinase regulates cell wall-mediated resistance to pathogens in *Arabidopsis thaliana*. Mol Plant Microbe Interact 22:953-963.

Schwessinger B., and Zipfel C. 2008. News from the frontline: recent insights into PAMP-triggered immunity in plants. Curr Opin Plant Biol 11:389-395.

Stafstrom J.P., Ripley B.D., Devitt M.L., and Drake B. 1998. Dormancy-associated gene expression in pea axillary buds. Cloning and expression of *PsDRM1* and *PsDRM2*. Planta 205:547-552.

Thilmony R., Underwood W., and He S.Y. 2006. Genome-wide transcriptional analysis of the *Arabidopsis thaliana* interaction with the plant pathogen *Pseudomonas syringae* pv. *tomato* DC3000 and the human pathogen *Escherichia coli* O157:H7. Plant J 46:34-53.

Thomma B.P., Nelissen I., Eggermont K., and Broekaert W.F. 1999. Deficiency in phytoalexin production causes enhanced susceptibility of *Arabidopsis thaliana* to the fungus *Alternaria brassicicola*. Plant J 19:163-171.

Trujillo M., Ichimura K., Casais C., and Shirasu K. 2008. Negative regulation of PAMP-triggered immunity by an E3 ubiquitin ligase triplet in *Arabidopsis*. Curr Biol 18:1396-1401.

Tsuda K., Sato M., Glazebrook J., Cohen J.D., and Katagiri F. 2008. Interplay between MAMP-triggered and SA-mediated defense responses. Plant J 53:763-775.

Velasquez A.C., Chakravarthy S., and Martin G.B. 2009. Virus-induced gene silencing (VIGS) in *Nicotiana benthamiana* and tomato. J Vis Exp 28 DOI: 10.3791/1292.

Wang D., Pajerowska-Mukhtar K., Culler A.H., and Dong X. 2007. Salicylic acid inhibits pathogen growth in plants through repression of the auxin signaling pathway. Curr Biol 17:1784-1790.

Wei C.F., Kvitko B.H., Shimizu R., Crabill E., Alfano J.R., Lin N.C., Martin G.B., Huang H.C., and Collmer A. 2007. A *Pseudomonas syringae* pv. *tomato* DC3000 mutant lacking the type III effector HopQ1-1 is able to cause disease in the model plant *Nicotiana benthamiana*. Plant J 51:32-46.

Wiermer M., Feys B.J., and Parker J.E. 2005. Plant immunity: the EDS1 regulatory node. Curr Opin Plant Biol 8:383-389.

Yang Q., Reinhard K., Schiltz E., and Matern U. 1997. Characterization and heterologous expression of hydroxycinnamoyl/benzoyl-CoA:anthranilate N-hydroxycinnamoyl/benzoyltransferase from elicited cell cultures of carnation, *Dianthus caryophyllus* L. Plant Mol Biol 35:777-789.

Yang S., Yang H., Grisafi P., Sanchatjate S., Fink G.R., Sun Q., and Hua J. 2006. The BON/CPN gene family represses cell death and promotes cell growth in *Arabidopsis*. Plant J 45:166-179.

Zipfel C. 2009. Early molecular events in PAMP-triggered immunity. Curr Opin Plant Biol 12:414-420.

Zipfel C., Robatzek S., Navarro L., Oakeley E.J., Jones J.D., Felix G., and Boller T. 2004. Bacterial disease resistance in *Arabidopsis* through flagellin perception. Nature 428:764-767.

Zipfel C., Kunze G., Chinchilla D., Caniard A., Jones J.D., Boller T., and Felix G. 2006. Perception of the bacterial PAMP EF-Tu by the receptor EFR restricts *Agrobacterium*-mediated transformation. Cell 125:749-760.

CHAPTER III

TOMATO LYSM-RECEPTOR-LIKE KINASES ARE INVOLVED IN IMMUNITY AGAINST BACTERIA[3]

Introduction

To deal with an ever-changing environment, plants have evolved inducible defenses to protect themselves against potential threats. Recognition of non-self in order to mount those defenses is of prime importance for a plant in order to survive. Plant immune systems recognize epitopes of conserved molecules in microorganisms, referred to as Pathogen- or Microbe-associated molecular patterns (PAMPs or MAMPs), using plasma membrane-localized Pattern-recognition receptors (PRRs). This recognition event prevents the establishment of a potential pathogen by eliciting PAMP-triggered immunity (PTI; Jones and Dangl 2006). The mechanism used by PTI to inhibit pathogen colonization is still unknown. As part of their virulence mechanisms, plant pathogenic microorganisms are adapted to suppress PTI using secreted effectors and toxins. For instance, bacteria secrete dozens of protein effectors through their type III secretion machinery in order to dampen plant defenses (Buell *et al.* 2003; Thieme *et al.* 2005). Plant resistance (R) proteins recognize the effectors or their activity inside plant cells and elicit Effector-triggered immunity (ETI) to stop the advance of the potential threat. A hallmark of ETI is

[3] Part of this chapter has been published in the journal The Plant Journal (Volume 69, 2012, pp. 92 - 103) by Lirong Zeng, André C. Velásquez, Kathy R. Munkvold, Jingwei Zhang and Gregory B. Martin.

the onset a type of programmed cell death (PCD) known as the hypersensitive response (HR) throughout the cells where effector recognition occurred (Thomma *et al.* 2011).

There is a wide variety of PAMPs being recognized by the plant immune system, including bacterial cold-shock protein (CSP), translation elongation factor Tu (EF-Tu), lipopolysaccharide (LPS) and peptidoglycan (PGN); fungal chitin; and oomycete INF1 protein (Kamoun *et al.* 1998; Newman *et al.* 2002; Felix and Boller 2003; Kunze *et al.* 2004; Gust *et al.* 2007; Miya *et al.* 2007). The archetype of plant PAMP perception is flagellin, which is recognized in plants as diverse as *Arabidopsis thaliana*, *Nicotiana benthamiana*, tomato and rice (Felix *et al.* 1999; Hann and Rathjen 2007; Takai *et al.* 2008). The epitope of flagellin recognized by the plant immune system is a 22-amino acid region in the N-terminus of the protein (Felix *et al.* 1999), although a second epitope of flagellin, flgII-28, has also been shown to trigger immune responses in the Solanaceae (Cai *et al.* 2011). The PRR responsible for flagellin detection is FLS2, a single-pass transmembrane protein with an extracellular leucine-rich repeat (LRR) region for flg22 binding and an intracellular kinase domain to relay the signal (Gómez-Gómez and Boller 2000; Chinchilla *et al.* 2006). The flagellin recognition PRR complex requires a second plasma membrane LRR receptor-like kinase (RLK), BAK1, which is also involved in brassinosteroid perception (Chinchilla *et al.* 2007). BAK1 is not only involved in flagellin perception but also in several other PAMP perception systems (Heese *et al.*

2007). There appears to be some redundancy in BAK1 function, as a closely related LRR RLK, BKK1, has a similar role in immunity (Roux *et al.* 2011).

Chitin, a polymer of N-acetylglucosamine and the major constituent of fungal cell walls, acts as an elicitor of plant immunity responses (Miya *et al.* 2007). Chitin is recognized in rice by a PRR complex composed of Lysin motif (LysM) receptor-like protein (RLP) OsCEBiP and LysM-RLK OsCERK1 (Shimizu *et al.* 2010). OsCEBiP is responsible for chitin binding in the monocot rice (Kaku *et al.* 2006) while in the dicot *A. thaliana* no LysM RLP has been shown to be involved in chitin perception. However, *Arabidopsis* AtCERK1 has been shown to bind chitin *in vitro* (Petutschnig *et al.* 2010) and is indispensable for chitin signaling (Miya *et al.* 2007; Wan *et al.* 2008). Interestingly, AtCERK1 is also involved in immunity against bacterial pathogens, as *cerk1-2* mutant plants are more susceptible than wild-type plants to *Pseudomonas syringae* (Gimenez-Ibanez *et al.* 2009a). The absence of transcriptional responses to PGN in *AtCERK1* mutant plants could be the reason for this increased bacterial susceptibility (Willmann *et al.* 2011). Interestingly, similar to the involvement of a LysM RLP in chitin perception in rice, two LysM RLPs (AtLym1 and AtLym3) are responsible for PGN binding while in both cases the respective CERK1 protein is probably involved in subsequent signaling transduction events (Willmann *et al.* 2011).

In this study, the potential roles of peptidoglycan in plant immunity and of tomato LysM-RLKs in immunity against bacteria and in chitin perception were investigated. Specifically, reactive oxygen species (ROS) production, mitogen-

activated protein kinase (MAPK) activation, transcriptional gene upregulation, and protection from disease by PAMP pre-treatment were among the immunity responses measured. Due to the presence of an intracellular kinase domain in LysM-RLKs, the importance of phosphorylation of these proteins in immunity was also examined.

Materials and Methods

Bacterial strains

Bacterial strains are listed on Table 3.1. *Agrobacterium tumefaciens* strains were routinely grown on LB or IM (Induction medium – 50 mM MES, 27.8 mM glucose, 18.7 mM NH_4Cl, 2 mM NaH_2PO_4, 2 mM KCl, 1.2 mM $MgSO_4$, 90 µM $CaCl_2$, 9 µM $FeSO_4$, pH 5.6) media at 30 °C while *Pseudomonas syringae* strains were grown on KB or SOC at room temperature or 30 °C. Antibiotic concentrations used were 10 µg/mL for gentamicin, 50 µg/mL for kanamycin, 100 µg/mL for rifampicin and 100 µg/mL for spectinomycin.

Elicitors

LPS-free *Escherichia coli* and *Staphylococcus aureus* peptidoglycan (PGN) were bought from InvivoGen (San Diego, CA). *Xanthomonas campestris* pv. *campestris* (*Xcc*) PGN and muropeptides were a kind gift from Dr. Mari Anne Newman. Chitin was purchased from Sigma-Aldrich Co, LLC (St. Louis, MO). Flg22 and csp22 peptides were synthesized by GenScript USA Inc. (Piscataway, NJ) or Biomatik USA, LLC (Wilmington, DE).

Table 3.1. Strains used in this study. The features column lists the plasmids that the strains harbor or the genes that have been deleted in the corresponding strain.

Species	Strain	Features	Reference
Agrobacterium tumefaciens	GV3101	pER8	Zuo *et al.* 2000
Agrobacterium tumefaciens	GV3101	pER8::*SlBti9_1a*	This study
Agrobacterium tumefaciens	GV3101	pER8::*SlBti9_1a K349N*	This study
Agrobacterium tumefaciens	GV2260	pER8::*SlBti9_1b*	This study
Agrobacterium tumefaciens	GV2260	pER8::*SlBti9_1b K355N*	This study
Agrobacterium tumefaciens	GV3101	pER8::*Slyk10*	This study
Agrobacterium tumefaciens	GV3101	pER8::*Slyk10 K360N*	This study
Agrobacterium tumefaciens	GV3101	pER8::*Slyk13*	This study
Agrobacterium tumefaciens	GV3101	pER8::*Slyk13 K328N*	This study
Agrobacterium tumefaciens	GV2260	p35S::*P1/HC-PRO*	Kasschau and Carrington 2001
Agrobacterium tumefaciens	Unknown	pTA7002::*BAX*	Kawai-Yamada *et al.* 2001
Agrobacterium tumefaciens	Unknown	p35S::*INF1*	Kamoun *et al.* 2003
Agrobacterium tumefaciens	GV3101	pYL192	Liu *et al.* 2002b
Agrobacterium tumefaciens	GV3101	pYL279	Liu *et al.* 2002a
Agrobacterium tumefaciens	GV2260	pYL279::*SlBti9*	This study
Agrobacterium tumefaciens	GV2260	pYL279::*NbBAK1*	Chakravarthy *et al.* 2010

Table 3.1. (Continued)

Species	Strain	Features	Reference
Agrobacterium tumefaciens	GV3101	pYL279::*SlFLS2*	Chakravarthy *et al.* 2010
Agrobacterium tumefaciens	GV2260	pYL156::*NbSIPK*	Ekengren *et al.* 2003
Agrobacterium tumefaciens	GV2260	pYL156::*NbWIPK*	Ekengren *et al.* 2003
Agrobacterium tumefaciens	GV3101	pYL156::*NtMEK1*	Ekengren *et al.* 2003
Agrobacterium tumefaciens	GV3101	pYL156::*NtMEK2*	Ekengren *et al.* 2003
Agrobacterium tumefaciens	GV2260	pYL279::*NbMAPKKKa*	del Pozo *et al.* 2004
Agrobacterium tumefaciens	GV2260	pYL156::*NtEDS1*	Liu *et al.* 2002b
Agrobacterium tumefaciens	GV2260	pYL156::*NtRAR1*	Liu *et al.* 2002b
Agrobacterium tumefaciens	GV3101	pTV00::*NbSGT1*	Peart *et al.* 2002
Agrobacterium tumefaciens	GV3101	pYL279::*Transducin*	Chakravarthy *et al.* 2010
Agrobacterium tumefaciens	Unknown	pYL279::*Cyclophilin*	Chakravarthy *et al.* 2010
Agrobacterium tumefaciens	Unknown	pYL279::*Drm-3*	Chakravarthy *et al.* 2010
Agrobacterium tumefaciens	Unknown	pYL279::*ALDH*	Chakravarthy *et al.* 2010
Agrobacterium tumefaciens	GV3101	pYL279::*Alternative oxidase*	Chakravarthy *et al.* 2010
Agrobacterium tumefaciens	GV3101	pYL279::*Anionic peroxidase*	Chakravarthy *et al.* 2010
Agrobacterium tumefaciens	GV3101	pYL279::*CA4H*	Chakravarthy *et al.* 2010
Agrobacterium tumefaciens	Unknown	pYL279::*Cytochrome C*	Chakravarthy *et al.* 2010
Agrobacterium tumefaciens	Unknown	pYL279::*HCBT*	Chakravarthy *et al.* 2010

Table 3.1. (Continued)

Species	Strain	Features	Reference
Agrobacterium tumefaciens	Unknown	pYL279::*Plastocyanin*	Chakravarthy *et al.* 2010
Agrobacterium tumefaciens	Unknown	pYL279::*Cathepsin B*	Chakravarthy *et al.* 2010
Agrobacterium tumefaciens	GV3101	pYL279::*26S*	Chakravarthy *et al.* 2010
Agrobacterium tumefaciens	GV3101	pYL279::*Ubiquitin/ SUMO*	Chakravarthy *et al.* 2010
Pseudomonas syringae pv. *tomato*	DC3000	Δ*avrPto* Δ*avrPtoB*	Lin and Martin 2005
Pseudomonas syringae pv. *tomato*	DC3000	Δ*avrPto* Δ*avrPtoB* Δ*hopQ1-1* Δ*fliC*	Kvitko *et al.* 2009
Pseudomonas syringae pv. *tomato*	DC3000	Δ*fliC*	Collmer lab - Cornell University
Pseudomonas syringae pv. *tomato*	DC3000	Δ*hrcC* Δ*cfa*	Collmer lab - Cornell University

Abbreviations: ALDH = Aldehyde dehydrogenase. CA4H = Cinnamic acid 4-hydroxyalse. HCBT = Anthranilate N-hydroxycinnamoyl/benzoyltransferase. 26 S = Proteasome 26 S subunit. Ubiquitin/SUMO = Ubiquitin-/SUMO-activating enzyme.

Sonicated *Pseudomonas syringae* pv. *tomato* (*Pst*) DC3000 Δ*fliC* bacterial extracts were prepared by growing a single colony of *Pst* Δ*fliC* in SOC media overnight at 220 rpm and room temperature. The bacterial culture was harvested by centrifuging at 3000 x g for 10 minutes and then resuspended in water to a final $O.D._{600}$ of 50. Cultures were sonicated with a Branson Sonifier 250 (Emerson Electric Co.; Danbury, CT) using ten 15 second pulses with 15 seconds pauses in between the pulses (Output = 3.5, Constant duty cycle).

Bacterial inoculations

Bacterial strains were grown on KB agar plates with appropriate antibiotics at 30 °C for two days. Strains were resuspended to the required $O.D._{600}$ in 10 mM $MgCl_2$ with 0.002 % Silwet L-77 as a surfactant agent and vacuum infiltrated into 3 ½ - 4-week old tomato plants. The attenuated strain *Pst* DC3000 Δ*avrPto* Δ*avrPtoB* Δ*hopQ1-1* Δ*fliC* and the non-pathogenic *Pst* DC3000 Δ*hrcC* Δ*cfa* were used at inocula of 4×10^4 CFU/mL and 1.5×10^5 CFU/mL, respectively. Plants were placed in a growth chamber with 50 - 60 % RH, 16 hour day length and 21 - 24 °C after inoculation.

For the PAMP protection experiments, 100 µg/mL of *E. coli* or *S. aureus* PGN, 100 µg/mL chitin, 2.5 µM flg22, 10 mM $MgCl_2$ or water were syringe infiltrated into fully expanded tomato leaflets of 4-week old plants. Plants were kept under constant lights and twenty hours after infiltration, vacuum infiltration of *Pst* DC3000 Δ*avrPto* Δ*avrPtoB* (at a inoculum of 1 - 1.5 x 10^4 CFU/mL) was carried out as described above.

Virus-induced gene silencing

Virus-induced gene silencing (VIGS) was performed as described in Velásquez *et al.* (2010). *Nicotiana benthamiana* plants were kept in a growth chamber with 50 - 60 % RH, 16 hour day length and 20 - 22 °C for approximately 3 - 4 weeks after silencing before being used for experiments.

Reactive oxygen species production

Leaf discs from 4-week old tomato plants were placed adaxial-side up in white polypropylene 96-well plates (Nunc, Thermo Fisher Scientific Inc.; Hanover Park, IL) and floated in 200 µL of water for 16 hours. Water was removed from the plate and a 100 µL solution containing the elicitor at the proper concentration plus 34 µg/mL luminol and 10 µg/mL horseradish peroxidase (HRP) type VI-A (both from Sigma-Aldrich Co, LLC; St. Louis, MO) was added to the leaf discs. Luminescence was recorded in a Synergy™ 2 multi-mode microplate reader (BioTek® Instruments, Inc.; Winoosky, VT). Elicitors were used at 100 µg/mL for *E. coli* PGN, 200 µg/mL for *Xcc* PGN, and 100 nM for both flg22 and csp22. Each sample was done in triplicate.

RNA extraction, cDNA synthesis and Reverse transcription-PCR

RNA extraction, cDNA synthesis and Reverse transcription-PCR (RT-PCR) was performed as described in Chakravarthy *et al.* (2010). RT-PCR of *SlBti9_1a* used primers SlBti9_1a-f and SlBti9-r while that of its spliceform, *SlBti9_1b*, used SlBti9_1b-f and SlBti9-r. Primers are described in Table 3.2.

Quantitative Real Time PCR

Quantitative Real Time PCR (qRT-PCR) was performed as described in Nguyen *et al.* (2010) but using the following qRT-PCR cycling conditions: 50 °C for 2 minutes; 95 °C for 10 minutes; and 40 cycles of 95 °C for 30 seconds, 55 °C for 30 seconds and 72 °C for 30 seconds. To evaluate gene transcriptional upregulation, 4-week old tomato plants were syringe-infiltrated with water, 100 µg/mL of PGN or 100 µg/mL of chitin. Six hours after infiltration, tissue was harvested for RNA extraction, cDNA preparation and qRT-PCR. Fold-induction of each gene was estimated from qRT-PCR data using *SlEF1α* as a normalization control. The ratio of expression sets as 1.0 as the normalized expression of the respective gene in water-treated plants.

To calculate the degree of gene silencing, tissue was collected from 4-week old tomato plants. The relative ratio of expression sets as 1.0 as the normalized expression of each gene in wild-type plants (using *SlEF1α* for normalization). Primers and their concentrations are described in Table 3.2.

Agrobacterium-mediated protein overexpression in Nicotiana benthamiana

A. tumefaciens primary cultures were grown in LB with appropriate antibiotics at 30 °C and 220 rpm overnight. The next day, cultures were harvested by centrifugation at 3000 x g for 10 minutes. Cultures were resuspended in an equal volume of Induction medium (IM) and the wash step was repeated. A one in ten dilution of the washed culture was inoculated into IM with the appropriate antibiotics and grown overnight at 30 °C and 220 rpm. The

Table 3.2. Primer sequences used in this study. The DNA sequence of the primer and the concentration of the primer used for qRT-PCR (if applicable) is shown.

Primer name	Sequence	Primer concentration (nM)
SlATPase qRT-f	5'-TTGCTGAAGCCTTGGCTCTTTACG-3'	200
SlATPase qRT-r	5'-ACCAGCGCGAGAAGAAAGGATGAT-3'	200
SlBti9 qRT-f	5'-AGACCACCTCCATCAGTATGGTCA-3'	100
SlBti9 qRT-r	5'-TGCCTGAAAGCACTGGAGAATTGC-3'	100
SlBti9_1a qRT-f	5'-TTGACGTATGTGACGGCGACAATG-3'	100
SlBti9_1a qRT-r	5'-ATAAATGATCCCTTCTCCGGCACG-3'	100
SlBti9_1b qRT-f	5'-TCTTGTGGCGAGGAACTACTCTGA-3'	25
SlBti9_1b qRT-r	5'-ACAGGGTACGTCACAAACAACCCA-3'	25
SlEF1α qRT-f	5'-TCCAAAGATGGTCAGACCCGTGAA-3'	200
SlEF1α qRT-r	5'-ATACCTAGCCTTGGAGTACTTGGG-3'	200
SlLyk3 qRT-f	5'-TTGAGGGATGGCCTGGCAACTAAA-3'	100
SlLyk3 qRT-r	5'-AGTTCCTCAGAGCTGCCAGCATAA-3'	100
SlLyk10 qRT-f	5'-AGCAATCAGCAGAGAGGCCTAAGA-3'	200
SlLyk10 qRT-r	5'-TGGACAATCTCCTCAGCTTCACCT-3'	200
SlLyk11 qRT-f	5'-GGGCTTGTTGGATTGTTTGAGGATG-3'	100
SlLyk11 qRT-r	5'-TGGCAAGAAGAGCCACATTCCAGA-3'	100
SlLyk12 qRT-f	5'-AGTGGTGGTGCTAGAGAAGGGTTA-3'	200
SlLyk12 qRT-r	5'-TGGACCTCATGCTAGGTCTCAACT-3'	200
SlLyk13 qRT-f	5'-AGTCCTGGCCTTTCAGGCATACAT-3'	400
SlLyk13 qRT-r	5'-ATTGCTGCTTTCTTTCCTCGCAGC-3'	400
Solyc07g055560 qRT-f	5'-GGATTGGGCCAAAGCCTATGGTAT'-3'	150
Solyc07g055560 qRT-r	5'-AGTCCTTGTGCTAGCAACTTGGTG-3'	150
Solyc08g029000 qRT-f	5'-GGAAACGCGTGTCTTTGCAGTTGA-3'	150
Solyc08g029000 qRT-r	5'-TCCTGTAGTGAGCCACTTCTCCAA-3'	150

Table 3.2. (Continued)

Primer name	Sequence	Primer concentration (nM)
Solyc08g080640 qRT-f	5'-TCTCAATCGAGGCCAAACATGGGT-3'	50
Solyc08g080640 qRT-r	5'-ACATGTACCTCTGCCTGCAGCATT-3'	50
Solyc09g089930 qRT-f	5'-ATCCGAAACAGTCACATCGCATCG-3'	150
Solyc09g089930 qRT-r	5'-TTCTCCTTCGCCGGTATTGCTTCA-3'	150
Solyc10g083690 qRT-f	5'-ACCCTATGAGTTTCAAGCCCGAGA-3'	50
Solyc10g083690 qRT-r	5'-GCGAAATGCATCATTCGATGGCCT-3'	50
Solyc12g005720 qRT-f	5'-ACACCTCCAACAGGGTTCTCAACA-3'	150
Solyc12g005720 qRT-r	5'-TGCTTGTAACATCGCCGCGACATA-3'	150
Solyc12g100240/ Solyc12g100260 qRT-f	5'-CAACGCGATTAAGCCATTGCTAGG-3'	150
Solyc12g100240/ Solyc12g100260 qRT-r	5'-TGCACTCCTTTGTATCCCTCCACA-3'	150
SlBti9_1a-f	5'-ATGTTTGAATCCAGGCCAAGAAG-3'	-
SlBti9_1b-f	5'-ATGTTGAACTTATCCCTTTTCTT'-3'	-
SlBti9-r	5'-CTACCTTCCAGACATGAGGTTTATC-3'	-

following day, the cultures were washed twice in 10 mM MES (pH 5.5) and10 mM $MgCl_2$ and their density was adjusted to the required $O.D._{600}$ (between 0.075 to 0.4). Finally, acetosyringone was added to a final concentration of 200 µM. For LysM-RLK overexpression experiments, strains were mixed in a 1 to 1 ratio with an *A. tumefaciens* strain harboring a plasmid for P1/HC-Pro expression, an RNAi suppressor from tobacco etch virus (TEV; Kamoun *et al.* 2003). Bacterial suspensions were infiltrated with a needleless syringe on 6 - 7 week-old fully-expanded leaves of *N. benthamiana* plants and kept at 22 - 24 °C, 60 % RH with constant lights for the duration of the experiment. Forty-eight hours after agroinfiltration, 1 µM β-estradiol (for strains carrying pER8 plasmids) or 3 µM dexamethasone (for pTA7002::*BAX*) were applied when needed on infiltrated areas to induce protein expression.

Electrolyte leakage assays

Samples from silenced *N. benthamiana* plants that had been previously agroinfiltrated with *A. tumefaciens* GV2260 pER8::*SlBti9_1b* were collected 40 hours after 1 µM β-estradiol treatment. Leaf discs were floated in 2 mL of water for 2 hours at room temperature with shaking at 80 rpm, after which they were removed and water conductivity was measured using an Acorn CON 5 conductivity meter (Oakton Instruments; Vernon Hills, IL). Each sample was done in duplicate.

Protein extraction and phosphatase treatments

N. benthamiana tissue was collected, frozen and ground to a fine powder. Samples were incubated in extraction buffer (10 % glycerol, 100 mM Tris HCl – pH 7.5, 100 mM NaCl, 0.75 % Triton X-100, 10 mM DTT, 5 mM EDTA – pH 8.0, 5 mM EGTA – pH 8.0, 1X Protease inhibitor cocktail for plant cell and tissue extracts from Sigma-Aldrich, 10 mM β-glycerophosphate, 10 mM NaF and 1 mM Na_3VO_4) for 10 minutes at 4 °C and centrifuged for 10 minutes at 16000 x g. The supernatant was collected and the protein concentration of the samples was determined using the Bio-Rad protein Assay (Bio-Rad Laboratories, Inc.; Hercules, CA).

Samples lacking phosphatase inhibitors did not have β-glycerophosphate, NaF or Na_3VO_4 in their extraction buffer. Samples that were separated in Mn^{2+}-Phos-tag™ AAL-107 did not have EDTA or EGTA, since this reagent would chelate the Mn^{2+} ions necessary for Phos-tag™ PAGE.

Dephosphorylation of 56 µg of *N. benthamiana* proteins was performed with 600 U of λ-phosphatase (New Englands BioLabs, Inc.; Ipswich, MA) in 1X Reaction buffer (100mM NaCl, 50 mM HEPES, 2 mM DTT, 0.01% Brij 35, pH 7.5) supplemented with 1 mM $MnCl_2$ in a 45 µL reaction volume.

Immunoblotting and Polyacrylamide gel electrophoresis.

The protein samples were separated on 10 % polyacrylamide gels or 25 µM Mn^{2+}-Phos-tag™ AAL-107 8 % polyacrylamide gels (Wako Chemicals USA; Richmond, VA). Mn^{2+}-Phos-tag™ gels allow better resolution of phosphorylated

proteins since the Phos-tag™ reagent binds to and retards the movement of phosphorylated proteins. After the PAGE, samples were transferred to polyvinylidene difluoride (PVDF) membranes using an electroblotter (Bio-Rad).

Immunoblotting was done with anti-HA or anti-HA conjugated to HRP antibodies (clone 3F10 from rat, Roche Applied Science; Indianapolis, IN) at a 1 in 5000 dilution. Goat anti-rat IgG conjugated to HRP (Santa Cruz Biotechnology, Inc., Santa Cruz, CA) was used at a 1 in 25000 dilution to detect rat anti-HA antibodies. Sample chemiluminescence was detected using the Amersham ECL Plus or Amersham ECL Prime Western blotting detection systems (GE Healthcare Life Sciences; Piscataway, NJ).

Protoplast isolation and Mitogen-activated protein kinase (MAPK) activation assays

Protoplast isolation from Rio Grande *PtoS* tomato plants was essentially carried out as described in Nguyen *et al.* (2010) except that protoplast recovery on ice was only for 45 minutes and that the final protoplast concentration was 5 x 10^5 protoplasts/mL. After protoplasts (1 x 10^5 protoplasts) were resuspended in 1 mL of WI buffer (0.5 M mannitol, 4 mM MES pH 5.7 and 20 mM KCl), elicitors were added and samples were incubated for 15 minutes with shaking at 50 rpm. Elicitors were used at 1, 10, 100 or 250 µg/mL for chitin; 250 µg/mL for *Xcc*, *S. aureus* or *E. coli* PGN; 50 µg/mL for *Xcc* muropeptides; 50 nM for flg22; and 40 µL for sonicated *Pst* DC3000 Δ*fliC* bacterial extracts ($O.D._{600}$ = 50; about 2.9 x 10^9 CFU per sample).

After protein extraction with 75 µL of extraction buffer (see above), 10 µL of each sample was loaded into PAGE gels. Proteins were detected with rabbit polyclonal anti-pERK antibody (1 in 2500 dilution in 5 % Bovine serum albumin – BSA) from Cell Signaling Technology, Inc. (Danvers, MA). Anti-pERK antibodies detect phosphorylated threonines and/or tyrosines from the conserved TEY (Thr-Glu-Tyr) phosphorylation motif of MAPK kinases. Tomato MAPKs detected in an immunoblot with anti-pERK antibodies are SlMPK1 and SlMPK2 (both migrate as a 48 kDa band) and SlMPK3 (which belongs to the 45 kDa band; Hind *et al.* 2010).

Phylogenetic and statistical analyses

Alignments and phylogenetic trees were generated using CLUSTAL W algorithm in MegAlign (Lasergene 10.0.0, DNASTAR Inc.; Madison, WI). Statistical analyses (Tukey-Kramer HSD tests and Student's T tests) were performed in JMP software version 9.0.2 (SAS Institute Inc.; Cary, NC). Fisher's exact tests were performed using a website from Kirkman (1996; http://www.physics.csbsju.edu/stats/).

Results

Peptidoglycan induces transcriptional activation but not any other immune responses in tomato

Peptidoglycan (PGN) constitutes a Pathogen-associated molecular pattern (PAMP) that is recognized by the *Arabidopsis thaliana* immune system (Gust *et*

al. 2007; Erbs *et al.* 2008). In *A. thaliana*, PGN induces a variety of archetypal immune responses including production of reactive oxygen species (ROS) and nitric oxide (NO), activation of mitogen-activated protein kinases (MAPK), transcriptional reprogramming and phytoalexin production (Gust *et al.* 2007; Erbs *et al.* 2008). The recognition systems for certain PAMPs are widely distributed in plants, as is for example flagellin recognition, which is detected in Brassicaceae, Solanaceae and Poaceae (Felix *et al.* 1999; Takai *et al.* 2008). However, recognition of some other PAMPs is limited to only a few species, as is elongation factor Tu (EF-Tu) detection that has only been reported to occur in the Brassicaceae (Kunze *et al.* 2004). Peptidoglycan is widely present in most bacteria and its peripheral location makes it an excellent potential target for plant immune recognition systems. It is possible, therefore, that plants in the Solanaceae also have a system for PGN detection (having evolved independently or not from the Brassicaceae).

The production of reactive oxygen species in response to PGN as an elicitor was assayed in tomato leaf discs (Figure 3.1). No ROS production was observed for either *Xanthomonas campestris pv. campestris* or *E. coli* PGN, with values indistinguishable from the negative water control. On the contrary, a positive control, flg22 (a 22-amino acid epitope from flagellin which is recognized by the plant immune system; Felix *et al.* 1999) gave a strong ROS production in tomato leaves, as has been reported before (Robatzek *et al.* 2007).

MAPK activation is another typical response of the plant immune system. MAPK activation was assayed after PGN perception at concentrations higher

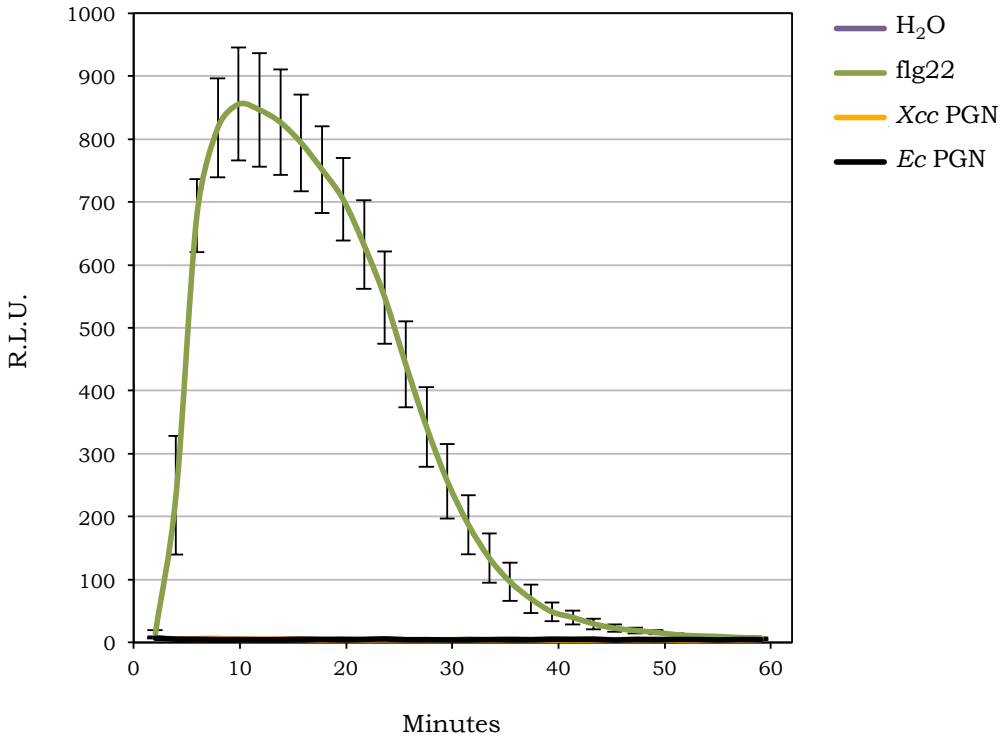

Figure 3.1. Peptidoglycan does not induce reactive oxygen production in tomato. Reactive oxygen species (ROS) production in tomato cv. Rio-Grande *prf3* plants after 200 µg/mL *Xanthomonas campestris* pv. *campestris* (*Xcc)* and 100 µg/mL *Escherichia coli* (*Ec*) peptidoglycan (PGN) treatment. Also shown as positive and negative controls are 100 nM flg22 and water (H_2O) treatments. Average relative light units (R.L.U.) of leaf discs taken from 4 plants are shown as a function of time, with the standard error of the mean (σ^E) indicated. This experiment was repeated twice with similar results.

than those that had been used previously for *A. thaliana* (Gust *et. al* 2007). No MAPK response in tomato protoplasts was seen with PGN from Gram negative (*E. coli* and *Xanthomonas campestris* pv. *campestris*; the weak response observed for the latter was not reproducible and was probably due to sample to sample variation) or Gram positive (*S. aureus*) bacteria or with muropeptides derived from them (Figure 3.2A). In contrast, a potent MAPK activation was seen with chitin (a PAMP which is present in the cell wall of plant pathogenic fungi), flg22 or bacterial extracts lacking flagellin (Pst Δ*fliC*; Figure 3.2B).

Pre-treatment with PAMPs causes immune defense activation that can protect the plant from subsequent bacterial infections for several hours after the initial pre-treatment (Newman *et al.* 2002; Kunze *et al.* 2004; Zipfel *et al.* 2004). PGN from both Gram positive and Gram negative bacteria failed to provide any protection from subsequent infections with hypovirulent *Pseudomonas syringae* pv. *tomato* (*Pst*) DC3000 Δ*avrPto* Δ*avrPtoB* (Figure 3.3). Previous observations of PGN protection from bacterial infections in tomato are probably due to impure preparations of commercial PGN (Nguyen *et al.* 2010). In contrast, chitin did provide such protection, manifested as a 100-fold reduction in bacterial growth and the absence of bacterial specks in leaflets pre-treated with this PAMP (Figure 3.3). Even though chitin is a PAMP derived from fungi, the defenses being activated in PTI seem to be broadly conserved for different classes of PAMPs (Wan *et al.* 2008), and therefore, chitin pre-treatment was able to protect from subsequent bacterial infections.

Figure 3.2. Peptidoglycan does not activate Mitogen-activated protein kinases cascades in tomato. (**A**) Mitogen-activated protein kinase (MAPK) activation in tomato cv. Rio Grande *PtoS* protoplasts after treatment for 15 minutes with various concentrations of chitin (1 - 250 µg/mL); 250 µg/mL of peptidoglycan (PGN) from *Xanthomonas campestris* pv. *campestris* (*Xcc*), *Staphylococcus aureus* (*Sa*) or *Escherichia coli* (*Ec*); or 50 µg/mL of muropeptides from *Xcc*. (**B**) MAPK activation in tomato cv. Rio Grande *PtoS* protoplasts after treatment for 15 minutes with 50 nM flg22 or 40 µL of sonicated *Pst* DC3000 Δ*fliC* bacterial extracts ($O.D._{600}$ = 50).

A Ponceau S stain shows similar loading between lanes. In both images, phosphorylated MAPKs were detected using the polyclonal anti-pERK antibody from Cell Signaling Technology. These experiments were repeated twice with similar results.

A

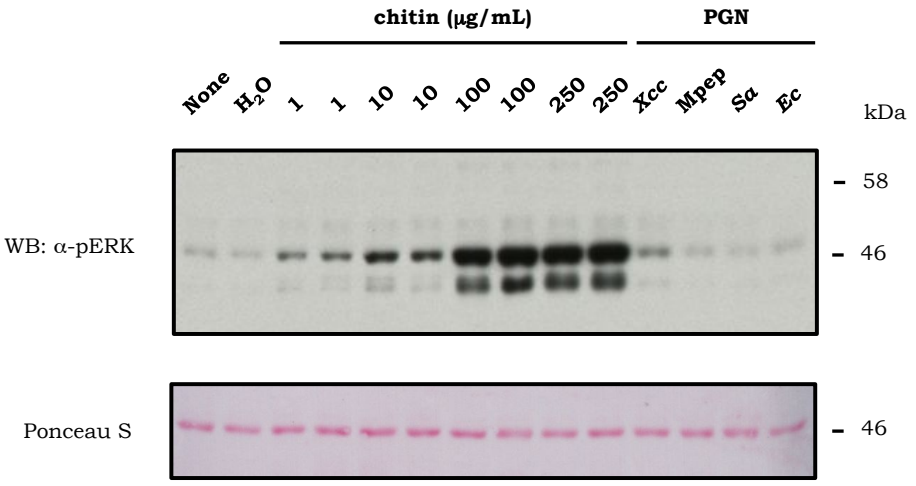
chitin (µg/mL)
PGN
None
H2O
1
1
10
10
100
100
250
250
Xcc
Mpep
Sa
Ec
kDa
WB: α-pERK
58
46
Ponceau S
46

B

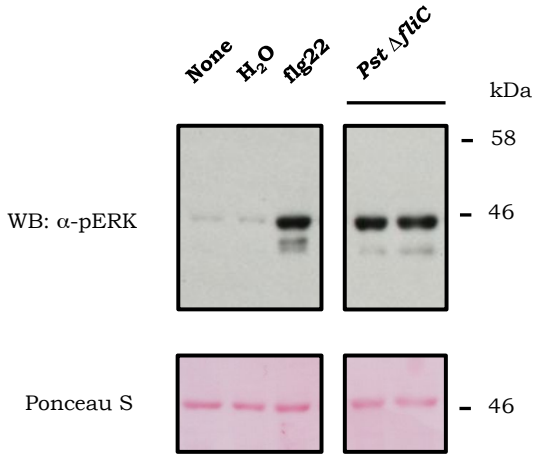
None
H2O
flg22
Pst ΔfliC
kDa
WB: α-pERK
58
46
Ponceau S
46

Figure 3.3. Pre-treatment with peptidoglycan does not confer disease protection in tomato. (**A**) Bacterial populations in tomato plants that were pre-treated with 100 μg/mL *Escherichia coli* (*Ec*) or *Staphylococcus aureus* (*Sa*) peptidoglycan (PGN), 100 μg/mL chitin or 10 mM $MgCl_2$ twenty hours before vacuum infiltration of *Pst* DC3000 Δ*avrPto* Δ*avrPtoB* (1 x 10^4 CFU/mL). Each elicitor and its corresponding $MgCl_2$ control were infiltrated in half of the same leaflet of a plant. Bars represent the average of 4 plants with the standard error of the mean (σ^E) indicated. Means with different letters were significantly different based on a Tukey-Kramer HSD test (α = 0.05). (**B**) Bacterial disease symptoms of leaflets pre-treated with the above mentioned elicitors and their corresponding $MgCl_2$ controls. Notice the absence of specks in the area of the leaflet infiltrated with chitin. Photographs were taken 4 days after vacuum-infiltration of the bacterial strain. These experiments were performed twice with similar results.

A

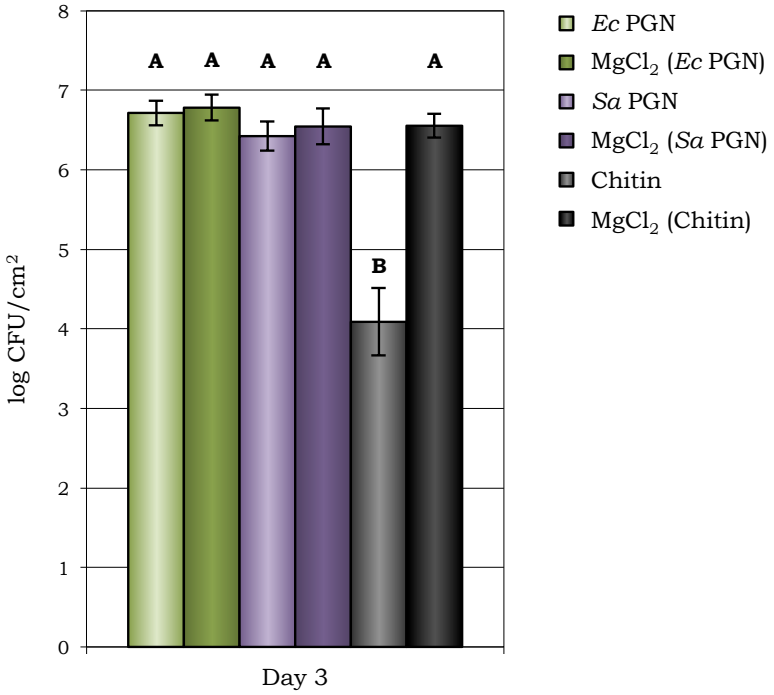
8
7
6
5
4
3
2
1
0
log CFU/cm²
A
A
A
A
B
A
Day 3
Ec PGN
MgCl2 (Ec PGN)
Sa PGN
MgCl2 (Sa PGN)
Chitin
MgCl2 (Chitin)

B

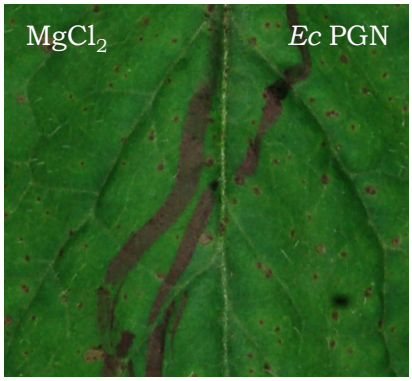
MgCl2
Ec PGN

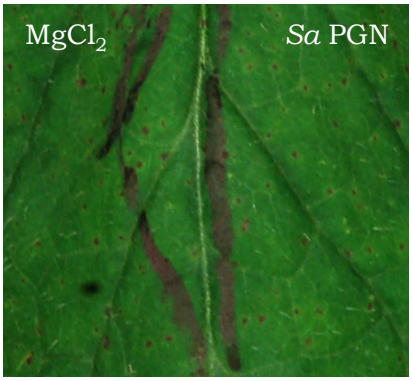
MgCl2
Sa PGN

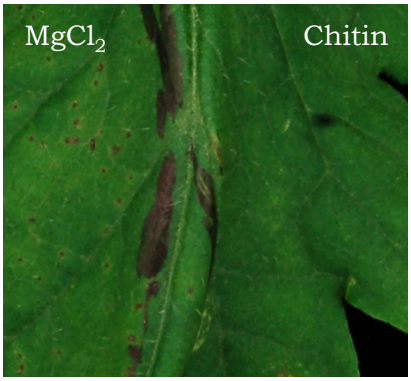
MgCl2
Chitin

Massive transcriptional reprogramming has been reported to occur in plants after PAMP detection (Navarro *et al.* 2004; Zipfel *et al.* 2006; Wan *et al.* 2008). Seven genes were selected from data derived from the tomato transcriptional response after PAMP treatment (H. Rosli and G. Martin, unpublished). These genes were selected since they showed the highest level of induction after PGN treatment in the RNA-seq dataset. Quantitative Real-time PCR (qRT-PCR) on those genes confirmed their induction by PGN (Table 3.3). The induction of three of these genes was analyzed more thoroughly and is shown on Figure 3.4. Transcriptional upregulation was the only immune response to PGN that was detected in tomato. Since PGN offered no ROS production, no MAPK activation and importantly, no protection from bacterial infections, PGN seems to be at most, only a modest inducer of PTI in tomato.

LysM receptor-like kinases in tomato

A LysM receptor-like kinase (LysM-RLK or Lyk), SlBti9 (for AvrPtoB tomato interacting protein 9), was discovered to interact with the *Pst* DC3000 effector AvrPtoB in a yeast two-hybrid (Y2H) screen (Zeng *et al.* 2012). The interaction between the effector and the LysM-RLK, inhibited SlBti9 kinase activity *in vitro* (Zeng *et al.* 2012). Since virulence targets of bacterial effectors are probably directly involved in immunity, SlBti9 was further characterized.

SlBti9 encodes a protein with three extracellular Lysin motifs (LysM), a single pass transmembrane domain and an intracellular kinase domain (Figure 3.5).

Table 3.3. Transcriptionally upregulated genes after peptidoglycan (PGN) and chitin treatment in tomato. The gene identification number and description, along with the approximate fold-induction six hours after each treatment is shown. Fold-induction was estimated from qRT-PCR using *SlEF1α* as a normalization control. The normalized expression of each gene in water-treated plants was set to 1.0.

Gene	Description	Aproximate fold-induction	
		PGN	Chitin
Solyc07g055560.2.1	G-type lectin S-receptor-like protein	20	2
Solyc08g029000.2.1	Lipoxygenase	160	600
Solyc08g080640.1.1	Osmotin-like protein	12	3
Solyc09g089930.1.1	Ethylene-responsive transcription factor 1a	6	7
Solyc10g083690.2.1	Cytochrome P450	40	6
Solyc12g005720.1.1	Cysteine-rich receptor-like protein kinase	16	12
Solyc12g100240.1.1 *Solyc12g100260.1.1*	Fatty acid desaturase	80	140

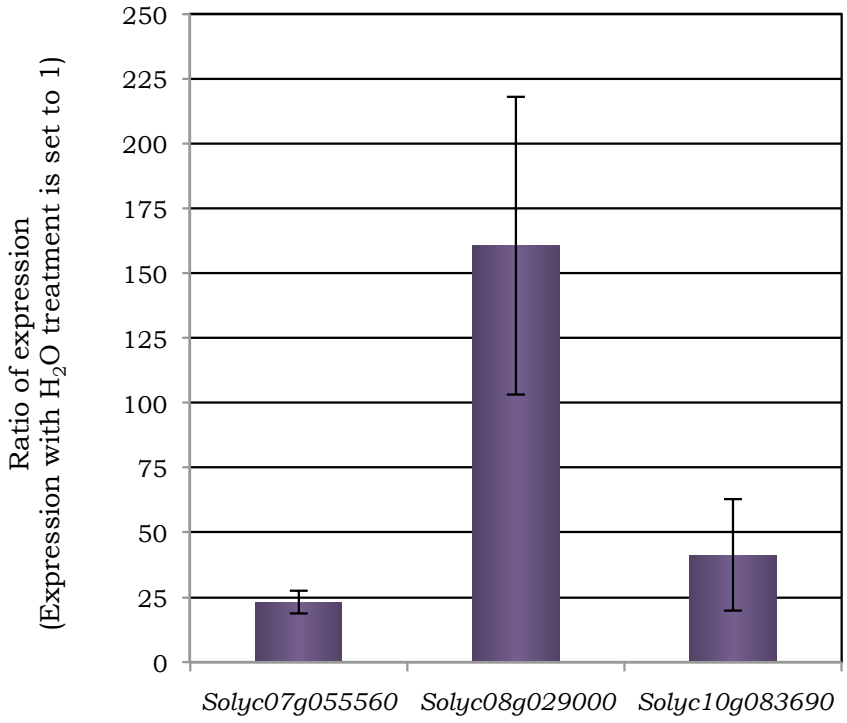

Figure 3.4. Peptidoglycan induces gene expression in tomato. *Solyc07g055560* (a G-type lectin S-receptor-like protein), *Solyc08g029000* (a lipoxygenase) and *Solyc10g083690* (a cytochrome P450) transcript induction six hours after 100 µg/mL *Escherichia coli* peptidoglycan treatment. Bars represent the average of 6 plants with the standard error of the mean (σ^E) indicated. Expression was analyzed by qRT-PCR using *SlEF1α* as a normalization control. The normalized expression of each gene in water-treated plants was set to 1.0.

Figure 3.5. Domain organization and amino acid sequence of the SlBti9_1b protein. (**A**) Schematic representation of different domains of the SlBti9_1b protein. SP, signal peptide; LysM, Lysin motif; TMD, transmembrane domain; kinase, Serine/threonine kinase domain. Also indicated is the location of the fragment used for the hairpin-Bti9 (hpBti9) construct. Numbers indicate the amino acid positions to which these domains correspond. (**B**) Amino acid sequence of SlBti9_1b protein domains. Amino acids that are conserved in LysM domains are indicated in red (using the LysM domain consensus in Buist *et al.* 2008). Lysine 355 within the kinase domain is also highlighted in red and corresponds to the putative ATP binding site.

A

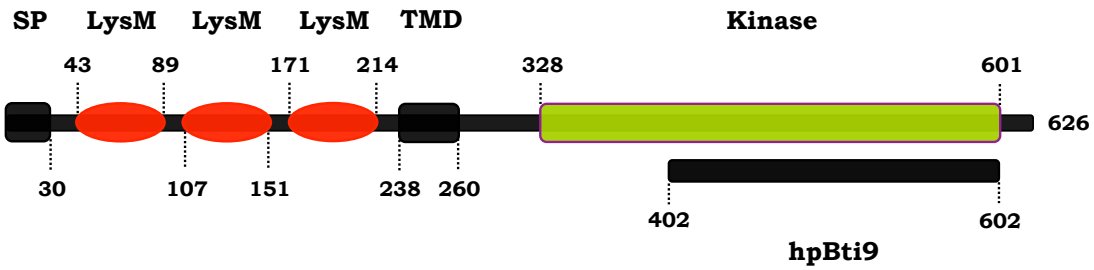

B

1	MFESRPRSVLSLGVFVILVYLSSVPLPVNS	SP
31	QCNRGCDLALAS	
43	FYVWRGSNLTLISEMFSTSIADIVSYNNRDNIPNQDSVIAGTRINIP	LysM
90	FRCDCLNDGEVLGHAFP	
107	YRVKSGDTYDLVARNYSDLTTAQWMMKFNSYPENNIPNTVNLSVV	LysM
152	VNCSCGNSDVSKDFGLFVT	
171	YPVRAEDNLTSVASAANVSEDIIRRYNPAAVSILDIGQGIIYIP	LysM
215	GRDRNGNFPPLPTSTDGLSGGAK	
238	AGISIGAIGVVLLLAGLVYVGCY	TMD
261	RNKTRKISLLRSEDHLHQYGHGPEGSTTVKAADSGRLADGNSPVLSGITVDK SVEFTYEELATATND	
328	FSIANKIGQGGFGAVYYAELRGEKAAIKKMDMEATREFLAELKVLTNVHHLN LVRLIGYCVEGSLFLVYEYVENGHIGQHLRGTGRDPLPWSKRVQIALDSARGL EYIHEHTVPVYIHRDIKTANILIDKNFHAKVADFGLTKLTEVGSSSLQTRLVGT FGYMPPEYAQYGDVSPKVDVYAFGVVLYELISAKEAIVKPNGSVTESKGLVAL FEEVLNQPDPDEDLRQLVDPRLGDDYPLDSVRKMAQLAKACTHENPLIRPSM RSIVVALMTL	KD
602	SSSTEDWDVGSFYGNQGMINLMSGR	

In the recently sequenced tomato genome (Sol Genomics Network – SGN; http://solgenomics.net/), there is a predicted gene (*Solyc07g049190*) encoding a protein with 3 LysM domains that is located about 2.5 kb from *SlBti9*. Since the first exon of *SlBti9* also codes for the three extracellular LysM domains (Figure 3.6B), it is possible that this predicted gene is part of a splicing variant of *SlBti9*. An RT-PCR with primers that aligned to the first codon of *Solyc07g049190* and to the last codon of *SlBti9* confirmed that this was indeed the case (Figure 3.6A). Therefore, *Solyc07g049190* was renamed as exon 1a of *SlBti9*, and the splicing variant it codes for, *SlBti9_1a*; while the originally identified *SlBti9* was renamed as *SlBti9_1b*. The transcript abundance of *SlBti9_1b* is between 4 and 40 times higher than that of *SlBti9_1a*, depending on the gene induction treatment being compared (H. Rosli and G. Martin, unpublished).

LysM domains have been shown to function as carbohydrate binding domains (Buist *et al.* 2008). For example, the structure of the extracellular domain of *A. thaliana* CERK1 bound to chitopentaose was recently solved (Liu *et al.* 2012). A comparison of the amino acid sequence of both spliceforms revealed that most of the variation was within the signal peptide domain and the three LysM domains (Figure 3.7). Amino acids conserved amongst LysM domains in SlBti9_1b (Figure 3.5B) were for the most part also conserved in SlBti9_1a (Figure 3.7). However, the variation within the LysM domains might confer a yet uncharacterized functional divergence to these two splicing variants.

Figure 3.6. *SlBti9* has two splicing variants in tomato. (**A**) Agarose gel electrophoresis of Reverse-transcription (RT) PCR to show the transcription of both *SlBti9* splicing variants, (1) *SlBti9_1a* and (2) *SlBti9_1b*, in tomato cv. Rio Grande *prf3*. (**B**) Genomic organization of the *SlBti9* locus (*Solyc07g049180* and *Solyc07g049190*; the latter corresponds to exon 1a) showing *SlBti9_1a* and *SlBti9_1b*, the two splicing variants of *SlBti9* which differ in their first exon. Also shown are the shared 11 exons present in each mature transcript. Exons are represented as horizontal bars (with the arrow of the last exon showing the direction of transcription) while introns are represented as lines. Dashed lines depict the two different splicing events.

A

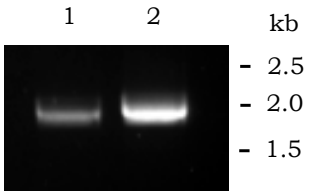
1
2
kb
2.5
2.0
1.5

B

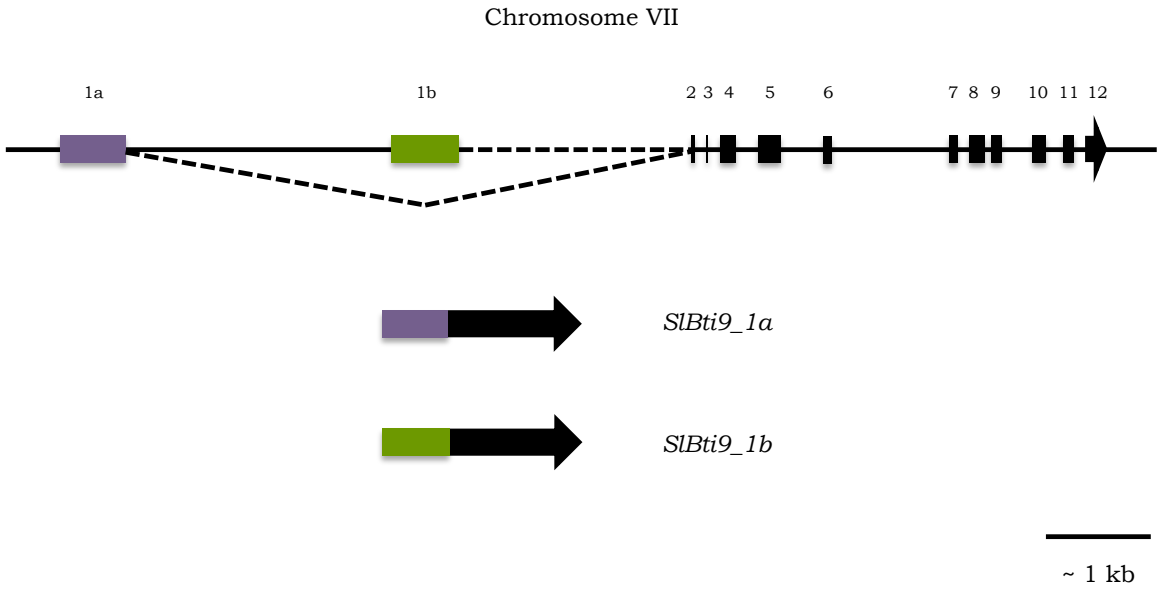
Chromosome VII
1a
1b
2 3 4
5
6
7 8 9
10 11 12
SlBti9_1a
SlBti9_1b
~ 1 kb

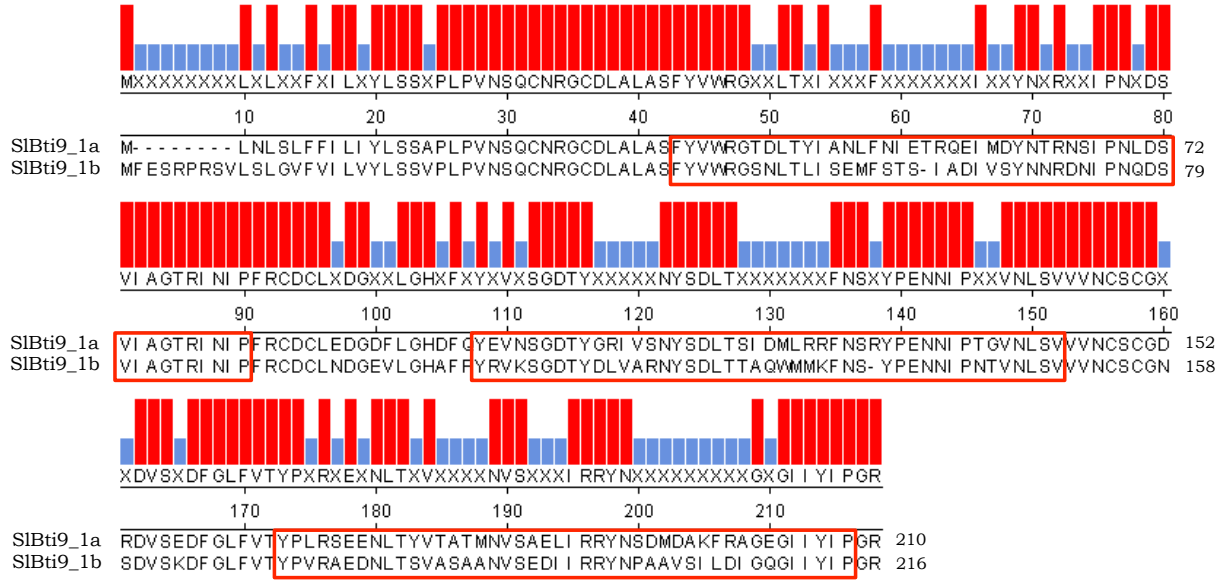

Figure 3.7. Comparison between the N-terminal regions of the two splicing variants of *SlBti9*. Amino acid alignment between transcribed exons 1a and 1b of *SlBti9*. The red boxes indicate the three LysM domains encoded by both exons. Alignment was generated using CLUSTAL W algorithm in MegAlign (DNAstar Inc.). Red bars indicate amino acids that are identical.

A search for LysM-RLKs in the tomato genome revealed that there were 14 that could be identified (counting the two *SlBti9* spliceforms as one; Figure 3.8 and Table 3.4), compared to only 5 in *Arabidopsis thaliana* (Wan *et al.* 2008). All tomato LysM-RLKs have a predicted signal peptide, a single pass transmembrane domain and an intracellular serine/threonine protein kinase. The extracellular regions of most tomato LysM-RLKs have three clearly distinguishable LysM subdomains, except for those of SlLyk3, SlLyk13 and SlLyk14. However, the presence of two conserved Cys-X-Cys motifs in all extracellular domains of tomato LysM-RLKs suggests that there could be three LysM domains in all tomato LysM-RLKs (Arrighi *et al.* 2006).

The tomato LysM-RLK family has 6 members that have an RD kinase (an arginine precedes the conserved aspartate that is the proton acceptor in the catalytic domain of the kinase) while the other 8 are non-RD. All the non-RD kinase LysM-RLKs cluster in the phylogenetic tree and are characterized by being encoded by 1 to 3 exons. The RD kinase LysM-RLKs are encoded by 10 to 13 exons and include the clade where SlBti9 resides (Figure 3.8). All non-RD kinases lacked the glycine-rich region that comprises the P-loop (phosphate binding group) while several of them (SlLyk2, SlLyk6, SlLyk7 and SlLyk15) were also lacking the invariant aspartate of the His-X-Asp (HXD) motif in the catalytic loop. The DFG motif (Asp-Phe-Gly), a motif that is N-terminal from the activation segment (Kornev *et al.* 2006), was also missing in all non-RD kinases while the activation loop itself was missing for SlLyk2 and SlLyk10. All this suggests that most likely, all the non-RD kinase LysM-RLKs have either

Figure 3.8 Phylogenetic tree of tomato LysM receptor-like kinase proteins. The phylogenetic tree is based on the amino acid sequences of SlBti9 and other LysM-receptor-like kinases (Lyk) from tomato, *Arabidopsis* and other plant species. Proteins that have been shown to be involved in Nod-factor perception are shown in orange. Shown in blue is SlLyk14, for which there is no evidence for transcription in the SOL Genomics Network (SGN) database. SlSerk3A was used as an outgroup for the analysis. The alignment and phylogenetic tree were generated using CLUSTAL W algorithm in MegAlign (DNAStar Inc.). Bootstrap values are indicated next to each branch (bootstrap trials = 1000; seed 111). The red box highlights the Bti9 clade while two brackets show the RD and non-RD kinase LysM-RLK groups. The tomato Lyk (SlLyk) proteins were named using a recommended nomenclature (Zhang *et al.* 2007) and are based on the closest *Arabidopsis* homolog using the full-length protein sequence.

Abbreviations: NA = Not applicable. At = *Arabidopsis thaliana*. Lj = *Lotus japonicus*. Mt = *Medicago truncatula*. Nb = *Nicotiana benthamiana*. Os = *Oryza sativa*. Pa = *Parasponia andersonii*. Sl = *Solanum lycopersicum*.

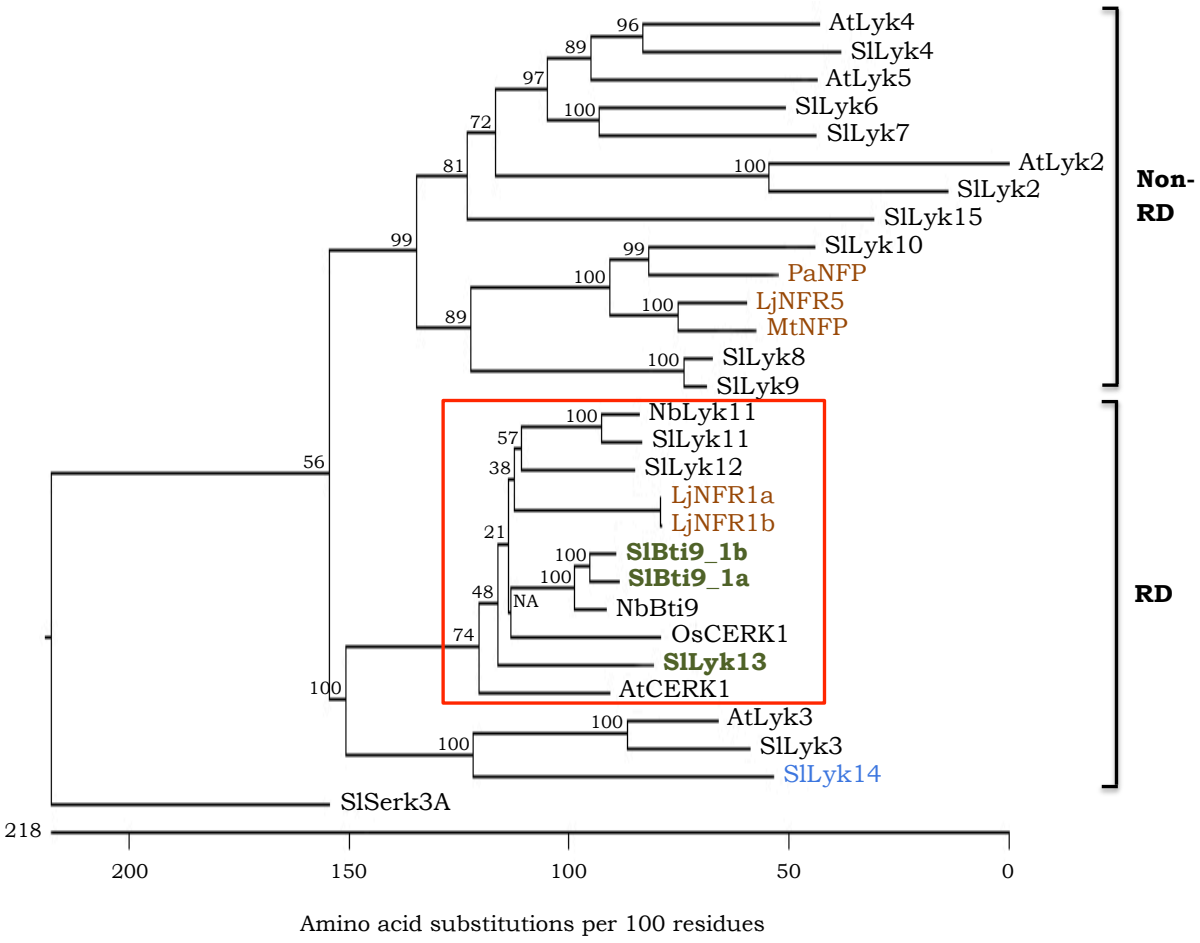
AtLyk4
SlLyk4
AtLyk5
SlLyk6
SlLyk7
AtLyk2
SlLyk2
SlLyk15
SlLyk10
PaNFP
LjNFR5
MtNFP
SlLyk8
SlLyk9
NbLyk11
SlLyk11
SlLyk12
LjNFR1a
LjNFR1b
SlBti9_1b
SlBti9_1a
NbBti9
OsCERK1
SlLyk13
AtCERK1
AtLyk3
SlLyk3
SlLyk14
SlSerk3A
Non-RD
RD
218
200
150
100
50
0
Amino acid substitutions per 100 residues

Table 3.4. Genbank accession and identification numbers for the genes and proteins used in this study.

	Genbank accession number	Gene ID number
AtCERK1	BAF92788	*At3g21630*
AtLyk2	Q9SGI7	*At3g01840*
AtLyk3	Q9FZA7	*At1g51940*
AtLyk4	O64825	*At2g23770*
AtLyk5	O22808	*At2g33580*
LjNFR1a	Q70KR8	
LjNFR1b	Q70KR7	
LjNFR5	Q70KR1	
MtNFP	ABF50224	
NbBti9	JN232974	
NbLyk11	JN232968	
OsCERK1		*Os08g42580*
PaNFP	AET97541	
SlSERK3A	AK328403	*Solyc10g047140*
SlBti9_1a	JN119874 / AK326822	*Solyc07g049190*
SlBti9_1b	HM208130	*Solyc07g049180*
SlLyk2		*Solyc02g094010*
SlLyk3	JN232969	*Solyc03g121050*
SlLyk4	AK327844	*Solyc02g089900*
SlLyk6	AK328052	*Solyc12g089020*
SlLyk7		*Solyc02g089920*
SlLyk8	AK325508	*Solyc09g083200*
SlLyk9		*Solyc09g083210*
SlLyk10	JN232970	*Solyc02g065520*
SlLyk11	JN232971	*Solyc02g081040*
SlLyk12	JN232972	*Solyc02g081050*
SlLyk13	JN232973	*Solyc01g098410*
SlLyk14		*Solyc06g069610*
SlLyk15		*Solyc11g069630*

reduced kinase activity or follow atypical catalytic mechanisms (Arrighi *et al.* 2006; Madsen *et al.* 2011).

There is evidence for transcription of all tomato LysM-RLKs except for *SlLyk14* in the SGN database (http://solgenomics.net/). Expression in leaves is absent for *SlLyk2* and *SlLyk15* while that of *SlLyk11* and *SlLyk12* is very low (H. Rosli and G. Martin, unpublished). Also, three pairs of LysM-RLKs cluster in the genome and are separated by less than 2 kb (*SlLyk4* and *SlLyk7*, *SlLyk8* and *SlLyk9*, and *SlLyk11* and *SlLyk12*). Of these 3 pairs, *SlLyk8* and *SlLyk9* seem to have arisen from a recent duplication event since there are more than 92 % identical at the nucleotide level.

Tomato LysM receptor-like kinases are involved in immunity

Arabidopsis CERK1 is a LysM-RLK that has been shown to be involved in immunity against bacteria (Gimenez-Ibanez *et al.* 2009a). The protein with the highest amino acid identity to AtCERK1 in tomato is SlBti9 (either splicing variant is equally similar), however, any of the other three LysM-RLKs in the clade in which SlBti9 resides could be the actual functional homolog of AtCERK1 in tomato (Figure 3.8). Two stable single-copy transgenic lines over-expressing a hairpin *SlBti9* fragment from the kinase domain (shared by both spliceforms; Figure 3.5) were generated (hpBti9-5 and hpBti9-26). Even though these 2 lines were predicted to target only *SlBti9*, *SlLyk12* and *SlLyk13* (based on the presence of at least 21 contiguous nucleotides identical to the hpBti9 transgene), transcriptional downregulation was also observed for *SlLyk11*

(Figures 3.9 and 3.10). This could have occurred due to transitive silencing (Voinnet 2008) since *SlLyk11* and *SlLyk12* share several stretches of more than 21 identical nucleotides. Two other LysM-RLKs, SlLyk3 and SlLyk10, were not downregulated by our hpBti9 transgene, showing the specificity of the RNAi hairpin construct (Figure 3.9).

Inoculation of hpBti9 plants with *Pst* DC3000 Δ*avrPto* Δ*avrPto* Δ*hopQ1-1* Δ*fliC* revealed that they were more susceptible to infection than an azygous control (an azygous line has lost the hpBti9 transgene by segregation during the establishment of the hpBti9 lines; Figure 3.11A). The strain lacked the *fliC* gene and therefore, it is unable to form a functional flagellum and does not elicit FLS2-mediated responses. The increase in bacterial growth was modest but reproducible in both hpBti9 lines (about a 2-fold increase) and lead to dramatic symptom differences (Figures 3.11A and 3.11B). To test if this increase in susceptibility could also be observed with a non-pathogenic bacterium, *Pst* DC3000 Δ*hrcC* Δ*cfa* was inoculated into tomato leaves. This strain does not carry a functional type III secretion system, and therefore, cannot translocate effectors into plant cells. Also, this strain is unable to synthesize the *Pst* DC3000 phytotoxin coronatine. Again, hpBti9 plants were more susceptible to bacterial colonization than azygous plants (a two-fold increase as was observed for *Pst* DC3000 Δ*avrPto* Δ*avrPto* Δ*hopQ1-1* Δ*fliC*, Figure 3.11C). These experiments support a role for one or more members of the Bti9 clade in tomato immunity against *Pst*.

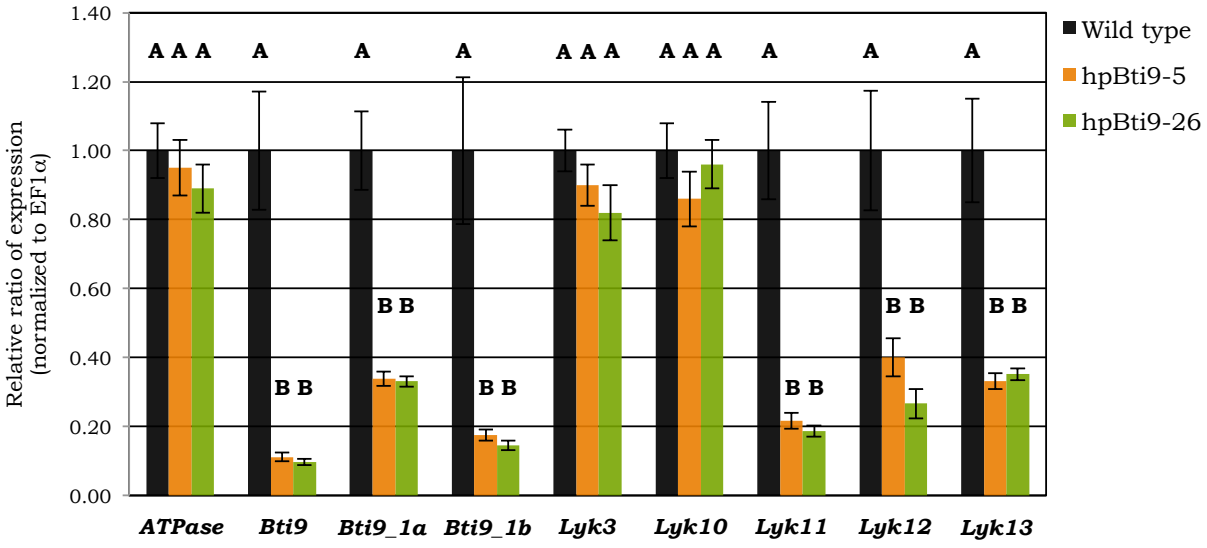

Figure 3.9. *SlBti9*, *SlLyk11*, *SlLyk12* and *SlLyk13* expression is reduced in hpBti9 lines. Transcript abundance of *SlBti9*, its two splicing variants and its three closest tomato homologues was reduced in hpBti9-5 and hpBti9-26 transgenic lines carrying the hpBti9 construct. Expression was analyzed by qRT-PCR using *SlEF1α* as a normalization control. Similar results were obtained using *SlATPase* normalization. The relative ratio of expression sets as 1.0 as the normalized expression of the gene in wild-type plants. Each bar represents the average of 8 plants with the standard error of the mean (σ^E) indicated. Means with different letters were significantly different based on a Tukey-Kramer HSD test ($\alpha = 0.05$).

Figure 3.10 Comparison of the DNA sequence spanning the hairpin Bti9 fragment with the corresponding region in *SlLyk11*, *SlLyk12, and SlLyk13*. (**A**) Comparison of nucleotide similarity between the fragment used for *Bti9* silencing (hpBti9) and *SlLyk11*. (**B**) Comparison of the nucleotide similarity between the fragment used for *Bti9* silencing (hpBti9) and *SlLyk12*. (**C**) Comparison of the nucleotide similarity between the fragment used for *Bti9* silencing (hpBti9) and *SlLyk13*. The red boxes highlight the only regions with more than 21 identical contiguous nucleotides in *SlLyk12 and SlLyk13* and based on this, only these two genes were originally predicted to be silenced by the hpBti9 construct. Alignments were generated using CLUSTAL W algorithm in MegAlign (DNAstar Inc.). Red bars indicate nucleotides that are identical.

A

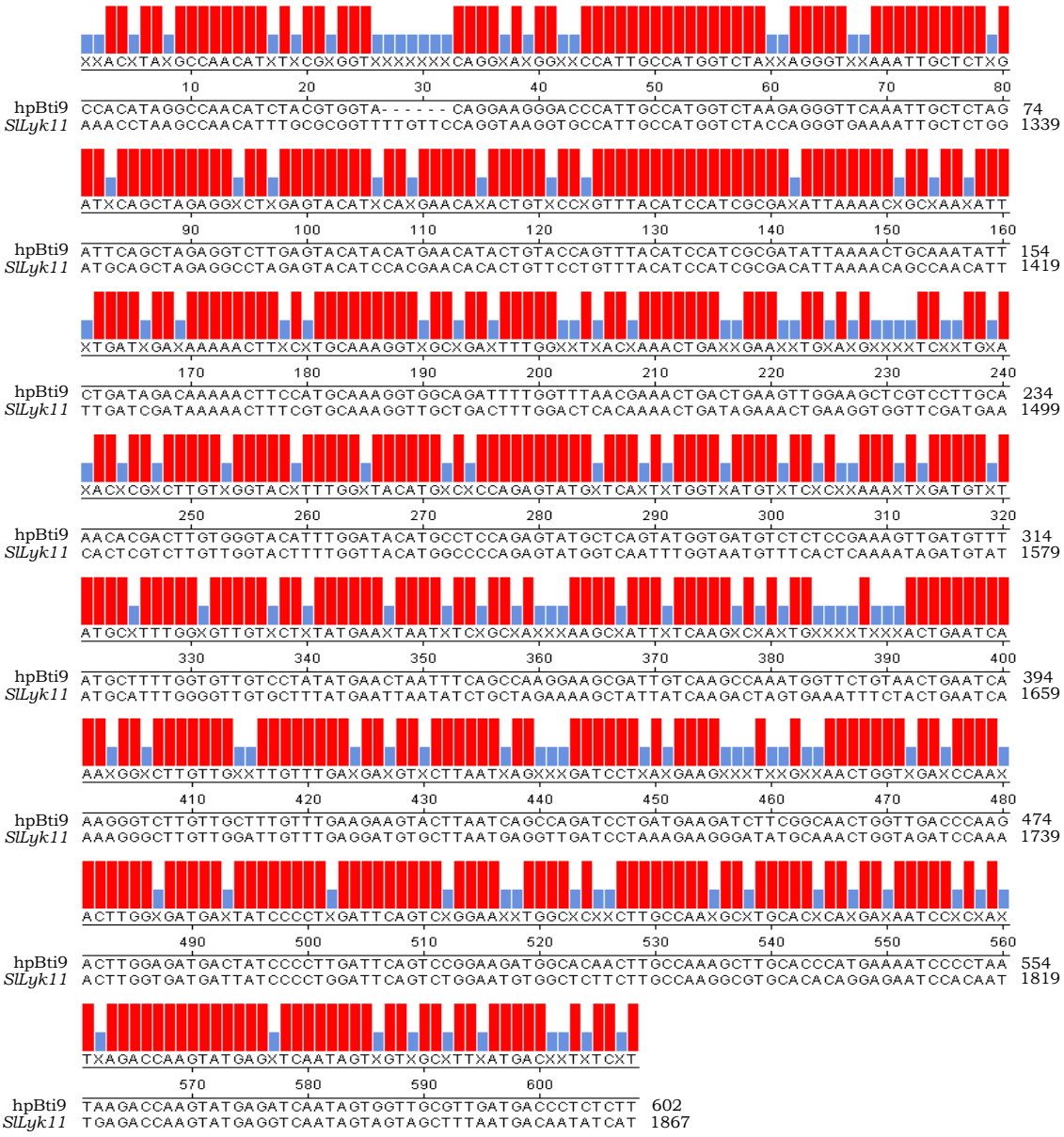
hpBti9 CCACATAGGCCAACATCTACGTGGTA------CAGGAAGGGACCCATTGCCATGGTCTAAGAGGGTTCAAATTGCTCTAG 74
SlLyk11 AAACCTAAGCCAACATTTGCGCGGTTTTGTTCCAGGTAAGGTGCCATTGCCATGGTCTACCAGGGTGAAAATTGCTCTGG 1339
hpBti9 ATTCAGCTAGAGGTCTTGAGTACATACATGAACATACTGTACCAGTTTACATCCATCGCGATATTAAAACTGCAAATATT 154
SlLyk11 ATGCAGCTAGAGGCCTAGAGTACATCCACGAACACACTGTTCCTGTTTACATCCATCGCGACATTAAAACAGCCAACATT 1419
hpBti9 CTGATAGACAAAAACTTCCATGCAAAGGTGGCAGATTTTGGTTTAACGAAACTGACTGAAGTTGGAAGCTCGTCCTTGCA 234
SlLyk11 TTGATCGATAAAAACTTTCGTGCAAAGGTTGCTGACTTTGGACTCACAAAACTGATAGAAACTGAAGGTGGTTCGATGAA 1499
hpBti9 AACACGACTTGTGGGTACATTTGGATACATGCCTCCAGAGTATGCTCAGTATGGTGATGTCTCTCCGAAAGTTGATGTTT 314
SlLyk11 CACTCGTCTTGTTGGTACTTTTGGTTACATGGCCCCAGAGTATGGTCAATTTGGTAATGTTTCACTCAAAATAGATGTAT 1579
hpBti9 ATGCTTTTGGTGTTGTCCTATATGAACTAATTTCAGCCAAGGAAGCGATTGTCAAGCCAAATGGTTCTGTAACTGAATCA 394
SlLyk11 ATGCATTTGGGGTTGTGCTTTATGAATTAATATCTGCTAGAAAAGCTATTATCAAGACTAGTGAAATTTCTACTGAATCA 1659
hpBti9 AAGGGTCTTGTTGCTTTGTTTGAAGAAGTACTTAATCAGCCAGATCCTGATGAAGATCTTCGGCAACTGGTTGACCCAAG 474
SlLyk11 AAAGGGCTTGTTGGATTGTTTGAGGATGTGCTTAATGAGGTTGATCCTAAAGAAGGGATATGCAAACTGGTAGATCCAAA 1739
hpBti9 ACTTGGAGATGACTATCCCCTTGATTCAGTCCGGAAGATGGCACAACTTGCCAAAGCTTGCACCCATGAAAATCCCCTAA 554
SlLyk11 ACTTGGTGATGATTATCCCCTGGATTCAGTCTGGAATGTGGCTCTTCTTGCCAAGGCGTGCACACAGGAGAATCCACAAT 1819
hpBti9 TAAGACCAAGTATGAGATCAATAGTGGTTGCGTTGATGACCCTCTCTT 602
SlLyk11 TGAGACCAAGTATGAGGTCAATAGTAGTAGCTTTAATGACAATATCAT 1867

B

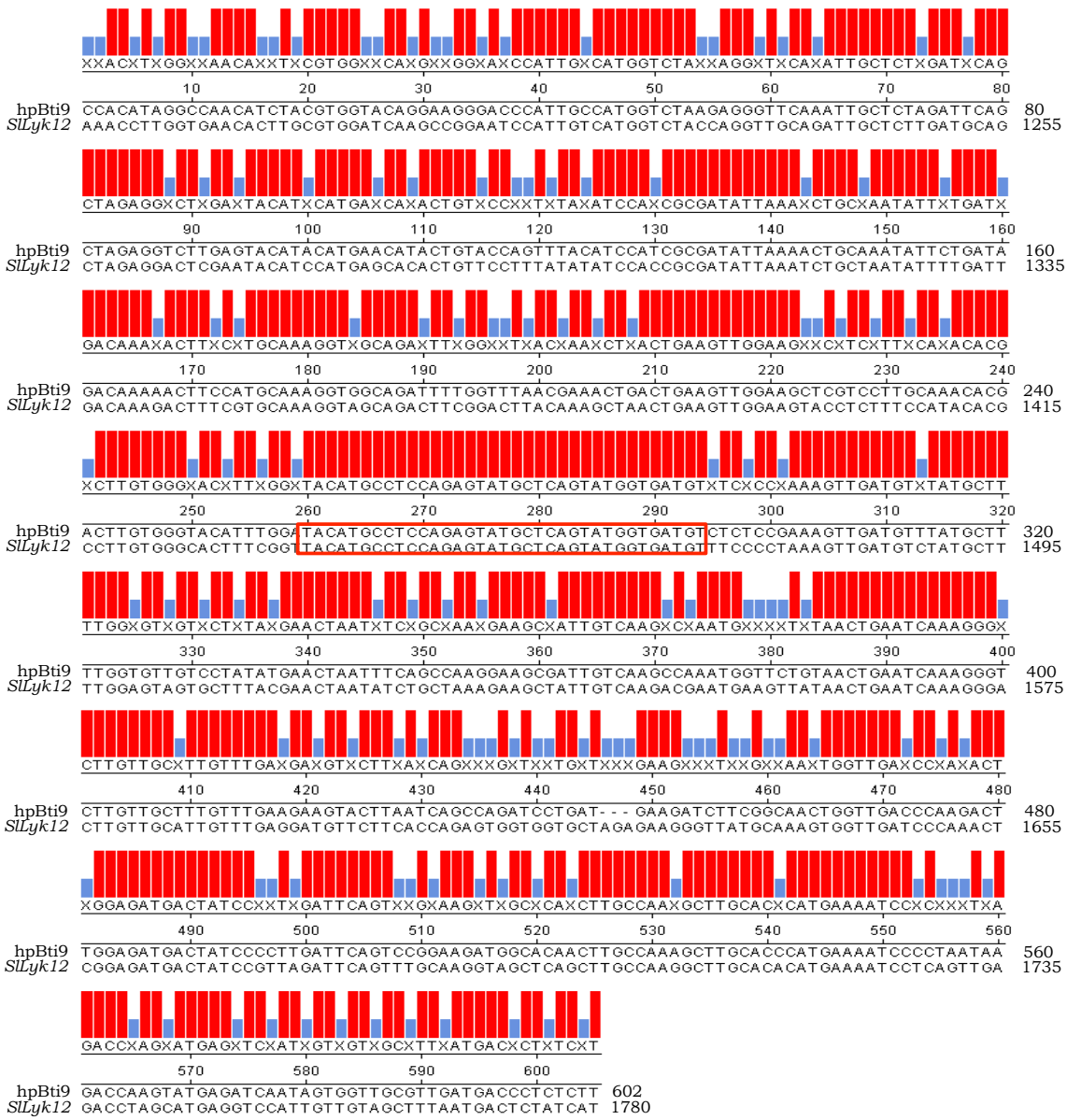
hpBti9
SlLyk12
80
1255
160
1335
240
1415
320
1495
400
1575
480
1655
560
1735
602
1780

C

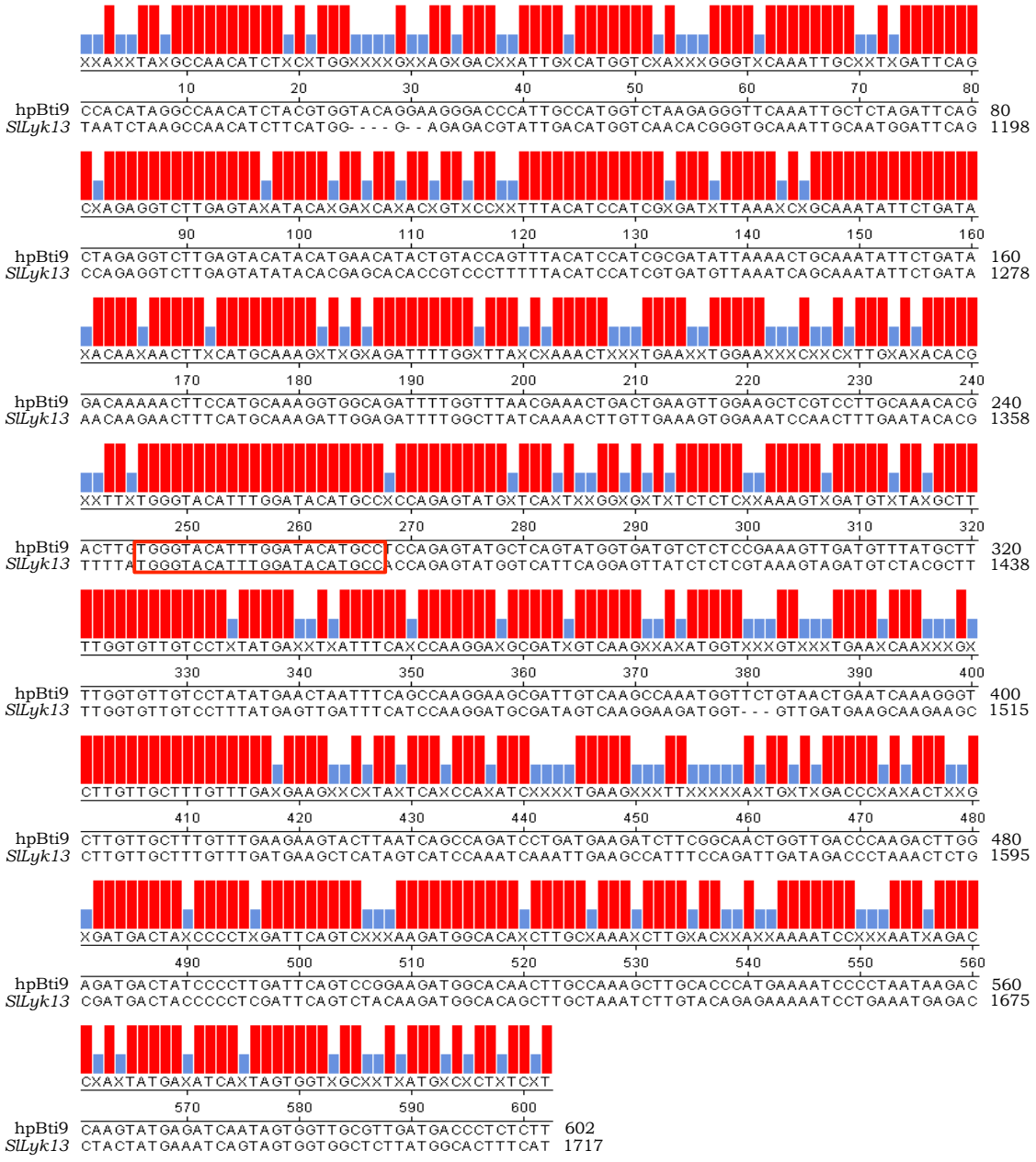
hpBti9 CCACATAGGCCAACATCTACGTGGTACAGGAAGGGACCCATTGCCATGGTCTAAGAGGGTTCAAATTGCTCTAGATTCAG 80
SlLyk13 TAATCTAAGCCAACATCTTCATGG- - - - G- - AGAGACGTATTGACATGGTCAACACGGGTGCAAATTGCAATGGATTCAG 1198
hpBti9 CTAGAGGTCTTGAGTACATACATGAACATACTGTACCAGTTTACATCCATCGCGATATTAAAACTGCAAATATTCTGATA 160
SlLyk13 CCAGAGGTCTTGAGTATATACACGAGCACACCGTCCCTTTTTACATCCATCGTGATGTTAAATCAGCAAATATTCTGATA 1278
hpBti9 GACAAAAACTTCCATGCAAAGGTGGCAGATTTTGGTTTAACGAAACTGACTGAAGTTGGAAGCTCGTCCTTGCAAACACG 240
SlLyk13 AACAAGAACTTTCATGCAAAGATTGGAGATTTTGGCTTATCAAAACTTGTTGAAAGTGGAAATCCAACTTTGAATACACG 1358
hpBti9 ACTTGTGGGTACATTTGGATACATGCCTCCAGAGTATGCTCAGTATGGTGATGTCTCTCCGAAAGTTGATGTTTATGCTT 320
SlLyk13 TTTTATGGGTACATTTGGATACATGCCACCAGAGTATGGTCATTCAGGAGTTATCTCTCGTAAAGTAGATGTCTACGCTT 1438
hpBti9 TTGGTGTTGTCCTATATGAACTAATTTCAGCCAAGGAAGCGATTGTCAAGCCAAATGGTTCTGTAACTGAATCAAAGGGT 400
SlLyk13 TTGGTGTTGTCCTTTATGAGTTGATTTCATCCAAGGATGCGATAGTCAAGGAAGATGGT- - - GTTGATGAAGCAAGAAGC 1515
hpBti9 CTTGTTGCTTTGTTTGAAGAAGTACTTAATCAGCCAGATCCTGATGAAGATCTTCGGCAACTGGTTGACCCAAGACTTGG 480
SlLyk13 CTTGTTGCTTTGTTTGATGAAGCTCATAGTCATCCAAATCAAATTGAAGCCATTTCCAGATTGATAGACCCTAAACTCTG 1595
hpBti9 AGATGACTATCCCCTTGATTCAGTCCGGAAGATGGCACAACTTGCCAAAGCTTGCACCCATGAAAATCCCCTAATAAGAC 560
SlLyk13 CGATGACTACCCCCTCGATTCAGTCTACAAGATGGCACAGCTTGCTAAATCTTGTACAGAGAAAAATCCTGAAATGAGAC 1675
hpBti9 CAAGTATGAGATCAATAGTGGTTGCGTTGATGACCCTCTCTT 602
SlLyk13 CTACTATGAAATCAGTAGTGGTGGCTCTTATGGCACTTTCAT 1717

Figure 3.11. The Bti9 clade is involved in tomato immunity against *P. syringae* pv. *tomato*. (**A**) Disease symptoms of leaflets where either hpBti9 was lost by segregation (termed "azygous") or where hpBti9 was present (lines hpBti9-5 and hpBti9-26). The photos were taken 3 days after vacuum infiltration of plants with the attenuated strain *Pst* DC3000 Δ*avrPto* Δ*avrPtoB* Δ*hopQ1-1* Δ*fliC* (4 x 10^4 CFU/mL). (**B**) Bacterial populations in leaves of azygous and hpBti9 tomato plants 3 days after inoculation with *Pst* DC3000 Δ*avrPto* Δ*avrPtoB* Δ*hopQ1-1* Δ*fliC*. Each bar represents the average of 4 plants with the standard error of the mean (σ^E) indicated. Means with different letters were significantly different based on a Tukey-Kramer HSD test ($\alpha = 0.05$). (**C**) Bacterial populations in leaves of azygous and hpBti9-26 tomato plants 4 days after inoculation with non-pathogenic *Pst* DC3000 Δ*hrcC* Δ*cfa* (1.5 x 10^5 CFU/mL). Each bar represents the mean of 4 plants with the standard error of the mean (σ^E) indicated. The asterisk denotes that the difference of bacterial populations in leaves of azygous and hpBti9-26 was significant as tested by a Student's T test ($\alpha = 0.05$). These experiments were performed three times with similar results.

A

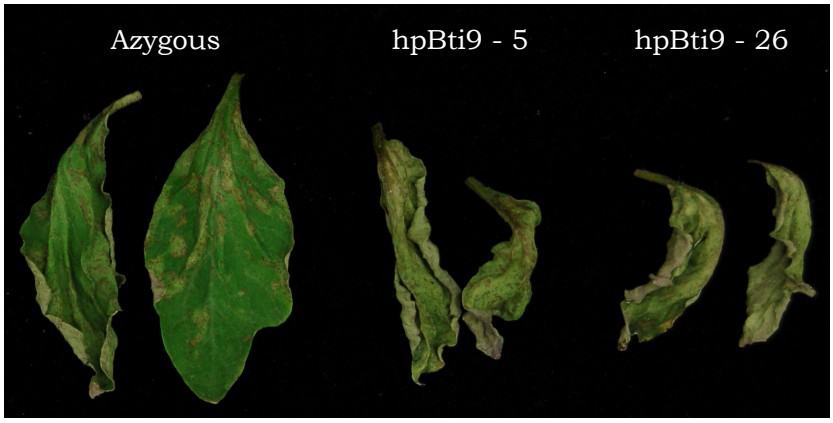
Azygous
hpBti9 - 5
hpBti9 - 26

B

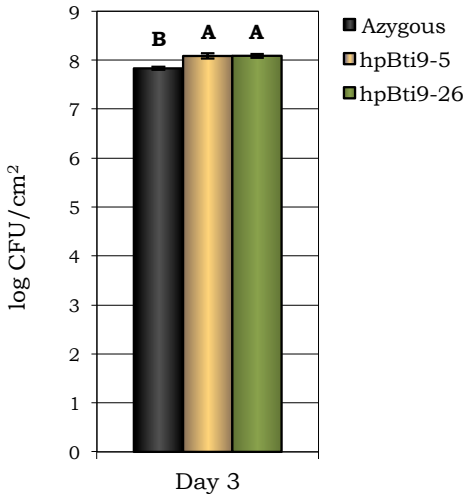
B
A
A
Azygous
hpBti9-5
hpBti9-26
log CFU/cm2
0
1
2
3
4
5
6
7
8
9
Day 3

C

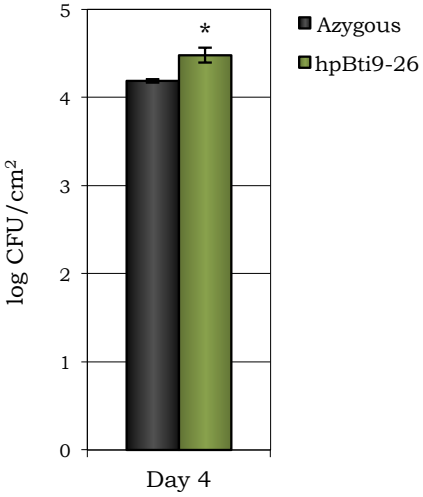
*
Azygous
hpBti9-26
log CFU/cm2
0
1
2
3
4
5
Day 4

It has been recently shown that AtCERK1 is involved in PGN perception in *Arabidopsis* (Willmann *et al.* 2011). However, since PGN is such a weak elicitor of PTI in tomato (Figures 3.1, 3.2 and 3.3), probably the enhanced bacterial susceptibility phenotype observed in hpBti9 plants (Figure 3.11) is not due to an involvement of PGN, if in fact there is any, in tomato immunity. To evaluate if the Bti9 clade has any role in known tomato PAMP perception systems, ROS production after flagellin (flg22) and cold-shock protein (csp22, the epitope being recognized in the Solanaceae; Felix and Boller 2003) recognition was evaluated. Unexpectedly, ROS production in hpBti9 plants was lower than the one observed for the azygous control, even though there was some variation within experiments between the two hpBti9 lines (Figure 3.12). Both ROS production and protection from subsequent *Pst* infections by flg22 was compromised in hpBti9 plants (Figure 3.13). The almost 20-fold decrease in bacterial growth observed in azygous plants pre-treated with flg22 was reduced to only a 4-fold decrease in hpBti9 plants. This loss of flagellin-induced immunity could be the cause of the increased susceptibility to non-pathogenic bacteria observed in hpBti9 plants, although in *A. thaliana*, there was no difference in gene upregulation after flg22 treatment between wild-type and *cerk1-2* plants (Wan *et al.* 2008).

Tomato LysM receptor-like kinases are involved in chitin perception

Arabidopsis CERK1 is also known to play a role in response against fungi by being part of the receptor complex that detects chitin, the major component of

Figure 3.12. Reactive oxygen species production after flagellin or cold-shock protein perception is slightly affected in hpBti9 plants. (**A**) Reactive oxygen species (ROS) production in azygous and hpBti9-5 and hpBti9-26 lines after 100 nM flg22 treatment. (**B**) ROS production in azygous and hpBti9-5 and hpBti9-26 lines after 100 nM csp22 treatment. Average relative light units (R.L.U.) of 7 - 8 plants are shown as a function of time, with the standard error of the mean (σ^E) indicated. Shown to at the bottom right of each figure is the average cumulative ROS produced for the experiment with the standard error of the mean (σ^E) indicated. Means with different letters were significantly different based on a Tukey-Kramer HSD test ($\alpha = 0.05$). These experiments were performed three times with similar results.

A

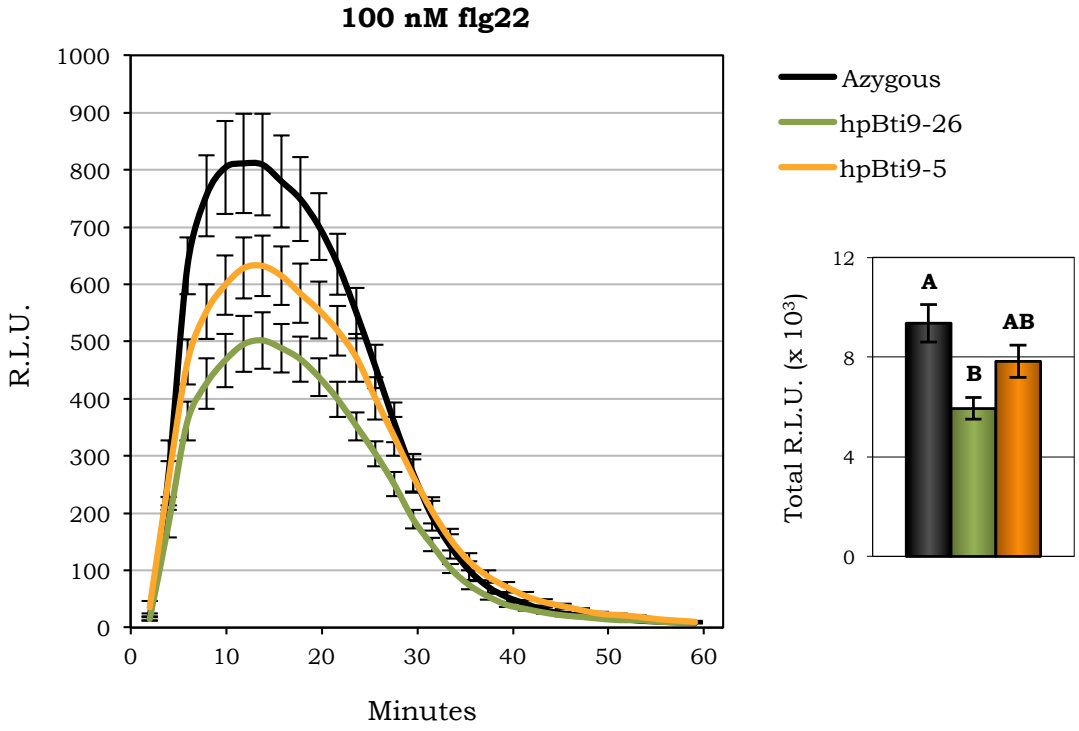
100 nM flg22
R.L.U.
Minutes
Azygous
hpBti9-26
hpBti9-5
Total R.L.U. (x 10³)
A
B
AB

B

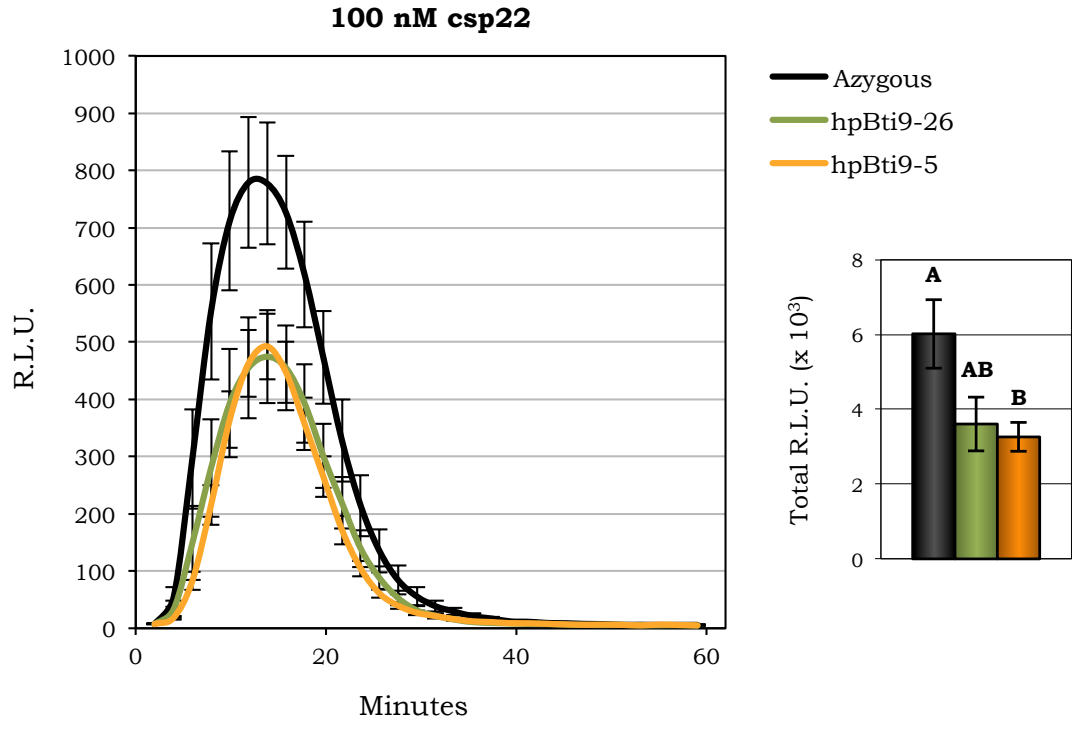
100 nM csp22
R.L.U.
Minutes
Azygous
hpBti9-26
hpBti9-5
Total R.L.U. (x 10³)
A
AB
B

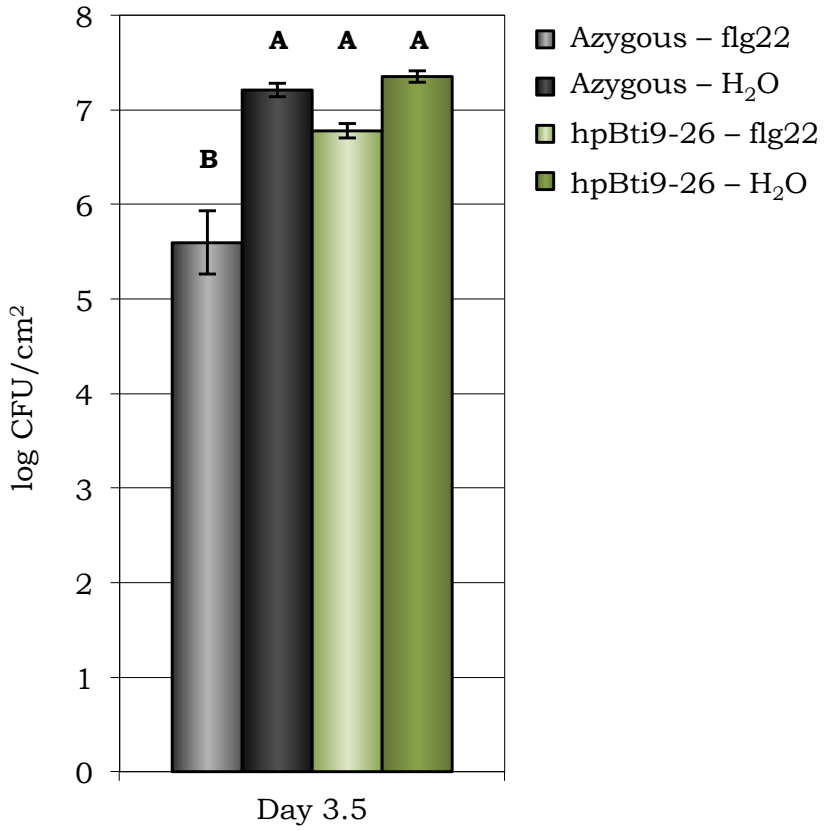

Figure 3.13. Flagellin pre-treatment does not confer disease protection in hpBti9 plants. Bacterial populations in azygous and hpBti9-26 plants that were pre-treated with water (H_2O) or 2.5 μM flg22 twenty hours before vacuum infiltration of *Pst* DC3000 Δ*avrPto* Δ*avrPtoB* (1.5 x 10^4 CFU/mL). Flg22 and its corresponding H_2O control were infiltrated in half of the same leaflet of a plant. Bars represent the average of 6 plants with the standard error of the mean (σ^E) indicated. Means with different letters were significantly different based on a Tukey-Kramer HSD test ($\alpha = 0.05$). This experiment was performed twice with similar results.

fungal cell walls (Miya *et al.* 2007; Wan *et al.* 2008; Petutschnig *et al.* 2010). Chitin treatment causes transcriptional gene upregulation in tomato (Table 3.3) and therefore, two genes were selected to evaluate if their expression was compromised in hpBti9 plants. Indeed, the induction of these genes was lower in hpBti9 plants, implicating the Bti9 clade in chitin signaling and possibly immunity against fungi (Figure 3.14).

As shown before, chitin induction of immune responses protects against subsequent *Pst* Δ*avrPto*Δ*avrPtoB* infections (Figure 3.3). This protection was partially lost in both hpBti9 lines, a 550-fold difference in bacterial growth between the water and chitin pre-treated wild-type plants was reduced to only a 70-fold difference (Figure 3.15), highlighting the importance of the Bti9 LysM-RLK clade in chitin signaling.

Over-expression of LysM receptor-like kinases in Nicotiana benthamiana causes cell death

SlBti9_1b overexpression under the control of an estradiol-inducible system in *N. benthamiana* caused cell death to quickly appear in the infiltrated area (Figure 3.16A). Cell death due to over-expression of LysM-RLKs had already been observed when two *Lotus japonicus* LysM-RLKs involved in Nod-factor perception, LjNFR1 and LjNFR5, were co-expressed in leaves (Madsen *et al.* 2011). A mutation of the lysine critical for ATP binding in the kinase domain of SlBti9_1b (K355N; in kinase subdomain II) abolished this cell death-inducing activity (Figure 3.16A). Lack of cell death in this case was not due to a

Figure 3.14. Chitin gene induction is compromised in hpBti9 plants. (**A**) *Solyc08g029000* (a lipoxygenase) transcript induction six hours after 100 µg/mL chitin treatment. (**B**) *Solyc12g100240*/*Solyc12g100260* (two fatty acid desaturases whose PCR product has identical sequence with the qRT-PCR primer pair used) transcript induction six hours after 100 µg/mL chitin treatment. Bars represent the average of 6 plants with the standard error of the mean (σ^E) indicated. Expression was analyzed by qRT-PCR using *SlEF1α* as a normalization control. The ratio of expression sets as 1.0 as the normalized expression of the marker gene in water treated plants. Means with different letters were significantly different based on a Tukey-Kramer HSD test (α = 0.05). These experiments were performed twice with similar results.

A

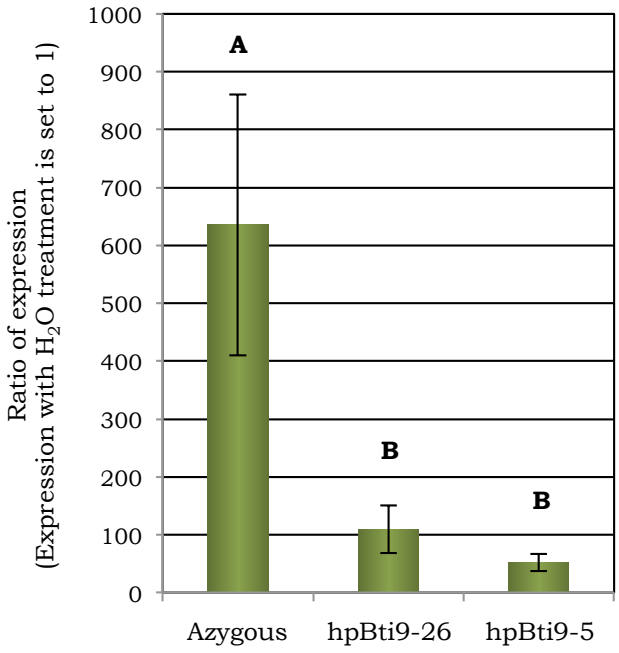
Ratio of expression
(Expression with H_2O treatment is set to 1)
1000
900
800
700
600
500
400
300
200
100
0
A
B
B
Azygous
hpBti9-26
hpBti9-5

B

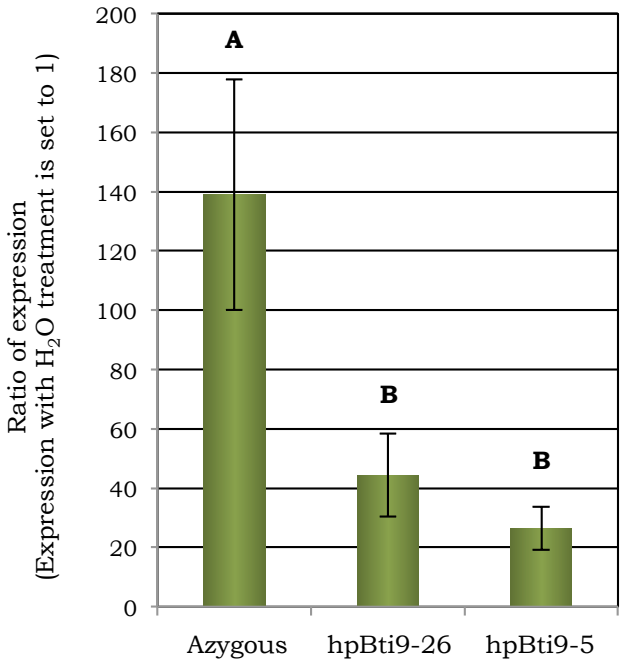
Ratio of expression
(Expression with H_2O treatment is set to 1)
200
180
160
140
120
100
80
60
40
20
0
A
B
B
Azygous
hpBti9-26
hpBti9-5

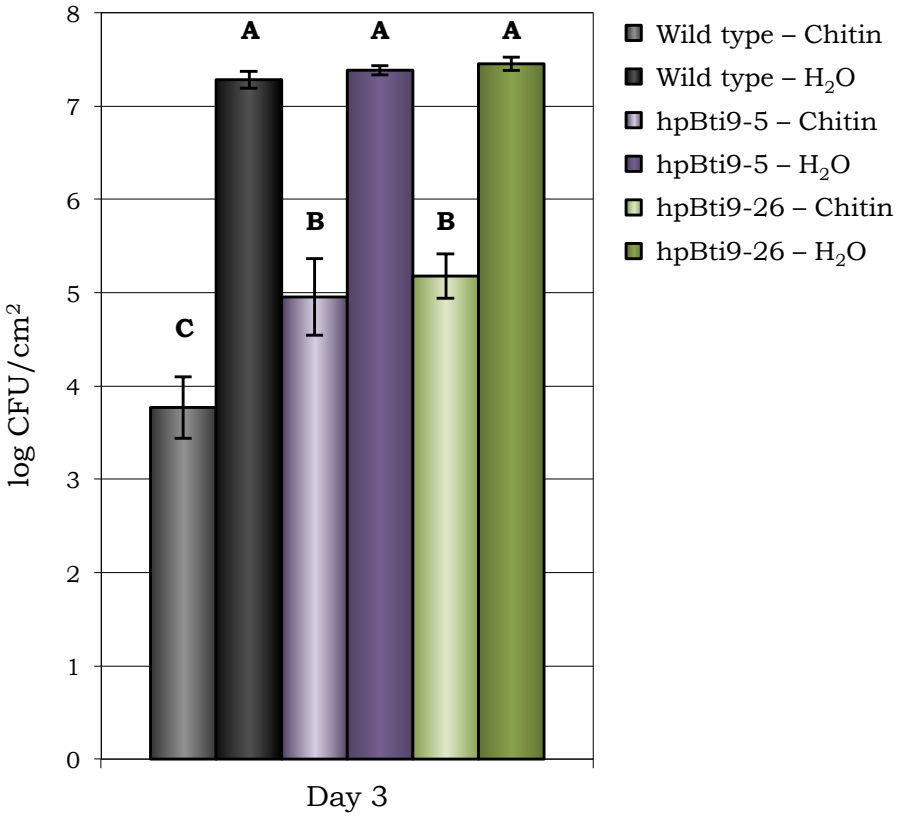

Figure 3.15. Chitin pre-treatment does not confer full disease protection in hpBti9 plants. Bacterial populations in wild-type and hpBti9 plants that were pre-treated with water (H_2O) or 100 µg/mL chitin twenty hours before vacuum infiltration of *Pst* DC3000 Δ*avrPto* Δ*avrPtoB* (1.5 x 10^4 CFU/mL). Chitin and its corresponding H_2O control were infiltrated in half of the same leaflet of a plant. Bars represent the average of 8 plants with the standard error of the mean (σ^E) indicated. Means with different letters were significantly different based on a Tukey-Kramer HSD test ($\alpha = 0.05$). This experiment was performed three times with similar results.

Figure 3.16. Over-expression of SlBti9_1b in *Nicotiana benthamiana*, but not of its kinase-mutant, causes cell death. (**A**) Over-expression of (1) SlBti9_1b, its kinase inactive mutant (2) SlBti9_1b K355N and of the (3) pER8 empty vector in *N. benthamiana*. Photograph was taken 48 hours after 1 μM β-estradiol treatment. Dotted blue lines show where strains that did not cause cell death were agroinfiltrated. (**B**) Immunoblot with anti-HA (α-HA) antibodies to show the protein accumulation of the above mentioned proteins in *N. benthamiana*. Samples were collected 24 hours after β-estradiol treatment. Twenty μg of total protein were loaded per lane. Note the relative mobility shift of SlBti9_1b as compared to its kinase inactive mutant, SlBti9_1b K355N.

A

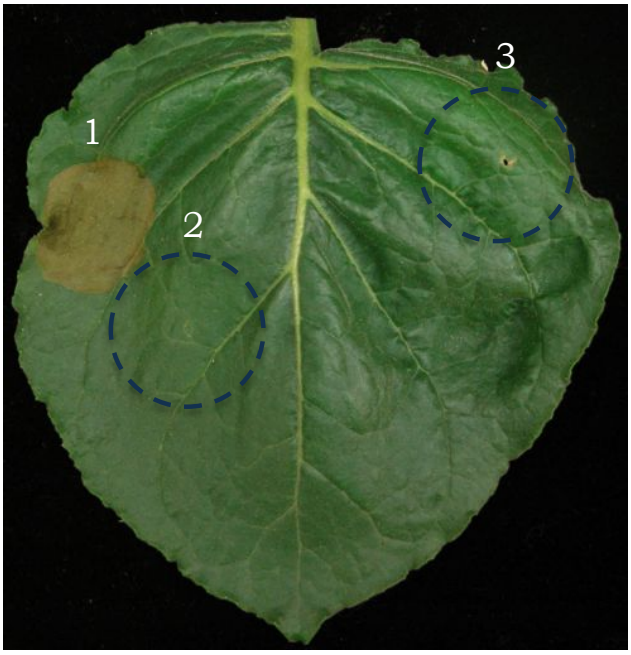

B

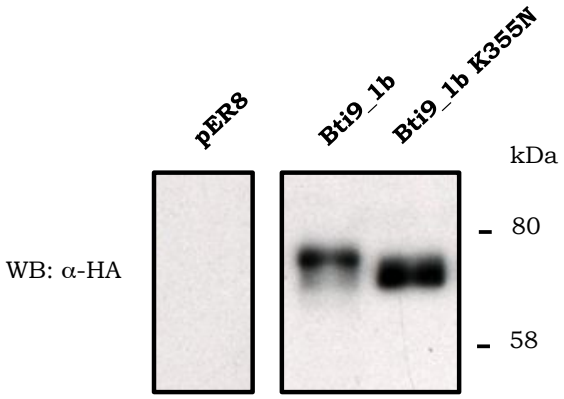

difference in protein expression since both SlBti9_1b and SlBti9_1b K355N proteins accumulated to similar levels (Figure 3.16B). Also, a mobility shift was observed in the immunoblot when comparing SlBti9_1b and its kinase inactive mutant suggesting differential post-translational modifications (e.g., phosphorylation) between these two proteins.

SlBti9_1b-mediated cell death could be due to activation of a signal transduction pathway leading to programmed cell death (PCD) or to toxicity (a non-specific process not genetically controlled). To distinguish between these two possibilities, SlBti9_1b was overexpressed in plants silenced for several genes known to be involved in immunity. If RNAi of these genes compromised SlBti9_1b-mediated cell death, this would indicate that overexpression of SlBti9_1b is likely activating a signaling pathway leading to PCD . Twenty-three different genes were silenced in *N. benthamiana* that were either part of a PRR complex or a MAPK cascade (e.g., *FLS2* or *MAPKKKα*), involved in downstream events of PTI (identified from a screen done by Chakravarthy *et al.* 2010), or involved in HR-mediated responses (e.g., *SGT1*). Three genes; *MEK1*, *MEK2* and *SGT1*; compromised the cell death caused by over-expression of SlBti9_1b (Table 3.5 and Figure 3.17A). Silencing *SGT1* also compromised the cell death caused by over-expression of INF1 and BAX, two well-characterized inducers of PCD. BAX-mediated cell death was also reduced in *MEK2*-silenced plants (Figure 3.17A; Peart *et al.* 2002; del Pozo *et al.* 2004; although in del Pozo *et al.* it was *MEK1* and not *MEK2*-silencing that compromised BAX-mediated cell death). Methanol, a non-specific cell death inducer, caused cell death in all of

Table 3.5. Cell death caused by SlBti9_1b over-expression is attenuated in plants silenced for *NbMEK1*, *NbMEK2* or *NbSGT1*. Number of infiltrated spots where cell death was evaluated as being absent (<10 %), partial (between 10 % - 75 %) or full (> 75 %) after agroinfiltration of *A. tumefaciens* GV2260 pER8::SlBti9_1b in *Nicotiana benthamiana* plants that had been previously silenced for each of the indicated genes. Pair-wise comparisons using a Fisher's exact test were performed between each gene silenced and the *TRV2* control (a Bonferroni correction was applied to the level of significance. $\alpha = 0.05/n$, where "n" equals the number of comparisons being made). Tests that were different from the *TRV2* control are highlighted in green.

Gene silenced	Cell death			Fisher's exact test (α = 0.0021)
	None	Partial	Full	
TRV2	7	16	46	-
Bti9	30	0	0	5.00E-19
BAK1	2	8	8	0.150
FLS2	8	9	16	0.110
SIPK	3	1	8	0.224
WIPK	4	2	6	0.113
MEK1	57	13	0	6.00E-24
MEK2	32	23	15	2.80E-08
MAPKKKa	8	3	7	0.004
EDS1	1	1	10	0.625
RAR1	0	0	4	0.712
SGT1	41	5	2	6.00E-18
Cyclophilin	0	2	10	0.683
Drm-3	2	2	8	0.778
Transducin	2	1	9	0.388
ALDH	2	4	6	0.458
Alt. oxidase	3	2	13	0.458
An. peroxidase	0	0	12	0.059
CA4H	2	1	9	0.388
Cytochrome C	1	2	9	0.888
HCBT	1	3	8	1.000
Plastocyanin	0	3	9	0.776
Cathepsin B	5	4	9	0.181
Proteasome 26S	1	2	9	0.888
Ubiquitin/SUMO	6	10	16	0.231

Abbreviations: ALDH = Aldehyde dehydrogenase. Alt. oxidase = Alternative oxidase. An. peroxidase = Anionic peroxidase. CA4H = Cinnamic acid 4-hydroxyalse. HCBT = Anthranilate N-hydroxycinnamoyl/benzoyltransferase. Proteasome 26 S = Proteasome 26 S subunit. Ubiquitin/SUMO = Ubiquitin/SUMO-activating enzyme.

Figure 3.17. SlBti9_1b over-expression is compromised in plants silenced for *NbMEK1*, *NbMEK2* or *NbSGT1*. (**A**) Leaves of silenced *Nicotiana benthamiana* plants were infiltrated with *Agrobacterium tumefaciens* strains over-expressing (1) SlBti9_1b, (2) the pER8 empty vector, (4) INF1 or (5) BAX. One area (3) was infiltrated with 40% methanol, a non-specific inducer of cell death. INF1 and BAX are two inducers of programmed cell death (PCD), from *Phytophthora infestans* and mouse, respectively. RNAi of *Bti9* should interfere with SlBti9_1b protein over-expression and as such, these plants were used as negative controls. Photographs were taken 53 hours after 1 μM β-estradiol or 3 μM dexamethasone treatment. The gene silenced in each plant is mentioned above each picture. Dotted blue lines show where strains that did not cause cell death were agroinfiltrated. (**B**) Electrolyte leakage assay in leaves of silenced plants for the above mentioned genes after over-expression of SlBti9_1b. Leaf discs were taken from plants 40 hours after 1 μM β-estradiol treatment, floated in water for 2 hours and conductivity was measured using an Acorn CON 5 conductivity meter (Oakton Instruments). Bars represent the average of 6 plants with the standard error of the mean (σ^E) indicated. Means with different letters were significantly different based on a Tukey-Kramer HSD test ($\alpha = 0.05$). This experiment was performed twice with similar results.

A

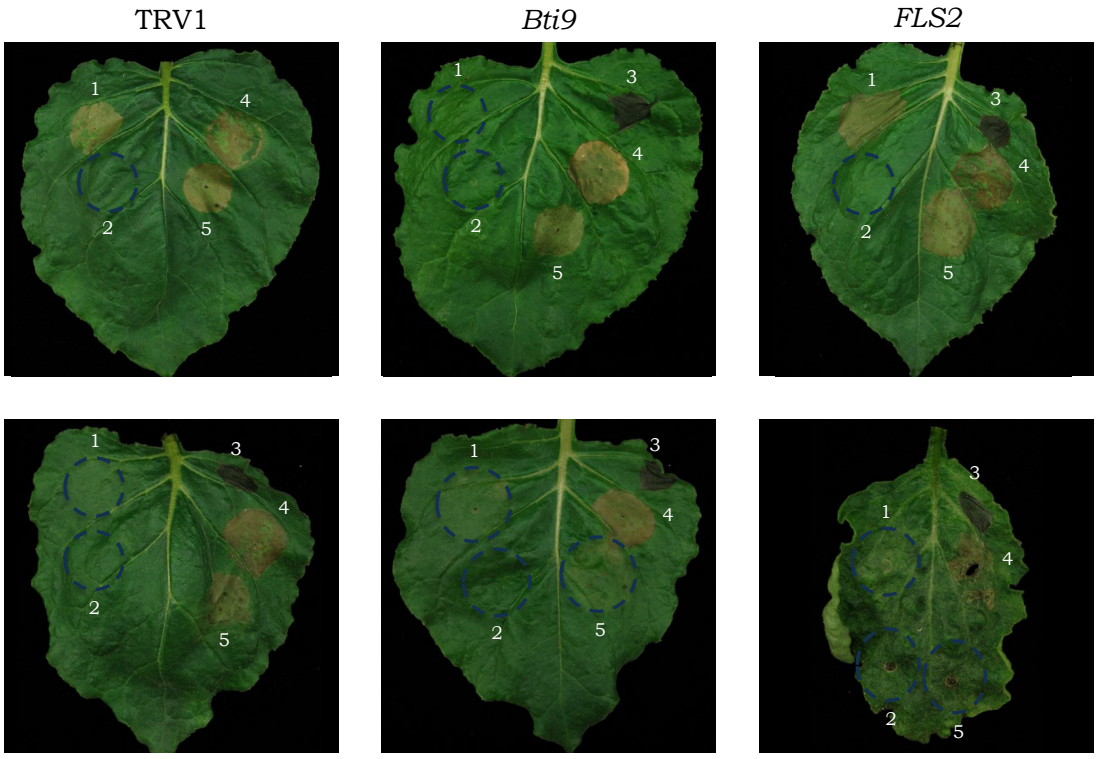
TRV1
Bti9
FLS2
MEK1
MEK2
SGT1

B

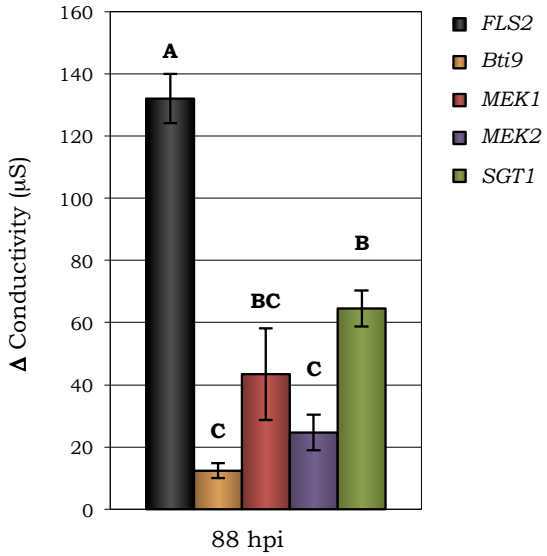
160
140
120
100
80
60
40
20
0
Δ Conductivity (µS)
A
C
BC
C
B
88 hpi
FLS2
Bti9
MEK1
MEK2
SGT1

the silenced plants (Figure 3.17A). *FLS2*-silencing did not compromise SlBti9_1b-mediated cell death and as such, FLS2 is probably not directly involved in SlBti9 signal transduction. An electrolyte leakage assay confirmed the results obtained visually for the suppression of SlBti9_1b-mediated cell death (Figure 3.17B). These results indicate that SlBti9_1b over-expression probably causes PCD and not toxicity-induced cell death.

It is possible that over-expression of other LysM-RLKs besides SlBti9_1b could induce cell death in *N. benthamiana*. SlBti9_1a and SlLyk13, two LysM-RLKs that reside in the Bti9 clade, were therefore overexpressed in *N. benthamiana* leaves. SlLyk11 and SlLyk12, the two other tomato LysM-RLKs present in the Bti9 clade, were not used for these experiments. *SlLyk12* transcript was barely detectable in leaves even after different PAMP treatments (H. Rosli and G. Martin, unpublished) while both SlLyk11 and SlLyk12 interacted with *Pst* effector AvrPtoB in a manner independent of phenylalanine 173 (Zeng *et al.* 2012). Phenylalanine 173 is an amino acid that has been shown to be necessary for AvrPtoB virulence activity (Xiao *et al.* 2007) and as such, it was expected that a LysM-RLK involved in immunity against bacteria would lose its interaction with AvrPtoB if this amino acid were mutated (while SlBti9 and SlLyk13 interaction with AvrPtoB required this amino acid; Zeng *et al.* 2012).

Initially, no cell death was observed by over-expression of any LysM-RLKs except for SlBti9_1b. Low levels of expression for SlBti9_1a and SlLyk13 might account for the lack of cell death with these proteins (data not shown). To

enhance protein expression, P1/HC-Pro, an RNAi-suppressor from Tobacco etch virus (TEV; Kasschau and Carrington 2001) was co-expressed with the abovementioned proteins. SlLyk10, which has a non-RD kinase domain, was also included in the experiments since it belongs to a different group of tomato LysM-RLKs (Figure 3.8) This time, cell death was observed when over-expressing SlBti9_1a and SlLyk13, although SlLyk13 cell death was delayed approximately 1 day when compared to that of SlBti9_1b while SlBti9_1a caused cell death in only approximately 60% of the infiltrated spots (Figure 3.18A). The difference in cell death strength is probably due to the disparity in protein expression in *N. benthamiana* between SlBti9_1b and both SlBti9_1a and SlLyk13 (Figure 3.18B). No cell death could be observed when over-expressing SlLyk10 even though its protein levels were similar to those observed for SlBti9_1b (Figure 3.18B). Also, as had been observed for SlBti9_1b K355N, putative kinase-inactive mutants, SlBti9_1a K349N and SlLyk13 K360N, did not cause cell death (Figure 3.18A). The effect of silencing *MEK1*, *MEK2* and *SGT1* on SlBti9_1a and SlLyk13-mediated cell death could not be evaluated since an RNAi suppressor was required for efficient expression of these proteins and this would have interfered with silencing of the aforementioned genes.

SlBti9_1b is auto-phosphorylated in planta

SlBti9_1b has been shown to have trans- and auto-phosphorylation activity *in vitro* (Zeng *et al.* 2012). Therefore, the PAGE mobility shift that had been

Figure 3.18. Over-expression of several tomato LysM receptor-like kinase proteins in *Nicotiana benthamiana* causes cell death. (**A**) Over-expression of (1) Bti9_1a, (2) Bti9_1a K349N, (3) Bti9_1b, (4) Bti9_1b K355N, (5) pER8 empty vector, (6) SlLyk13, (7) SlLyk13 K328N, (8) SlLyk10 and (9) SlLyk10 K360N in *N. benthamiana* 96 hours after 1 μM β-estradiol treatment. Each strain was mixed in a 1 to 1 ratio with P1/HC-Pro, an RNAi suppressor from tobacco etch virus (TEV), to enhance protein accumulation. Note that neither SlLyk10 nor none of the kinase inactive mutants (the lysine to asparagine mutations) caused cell death when over-expressed. Dotted blue lines show where strains that did not cause cell death were agroinfiltrated. (**B**) Immunoblot with anti-HA (α-HA) antibodies to show the protein accumulation of the above mentioned proteins in *N. benthamiana*. Note the relative mobility shift of SlBti9_1a, SlBti9_1b and SlLyk13 as compared to their respective kinase inactive mutants. Samples were collected 24 hours after β-estradiol treatment. The chemiluminescence film to which the immunoblot was exposed required 20 times longer exposure times for SlBti9_1a and SlLyk13 than for SlBti9_1b and SlLyk10, since the amount of protein over-expressed of the first two was much lower than that of the two latter LysM-RLKs. A Ponceau S stain shows that the wild-type and kinase-inactive LysM-RLK proteins were loaded with similar amounts of total protein.

A

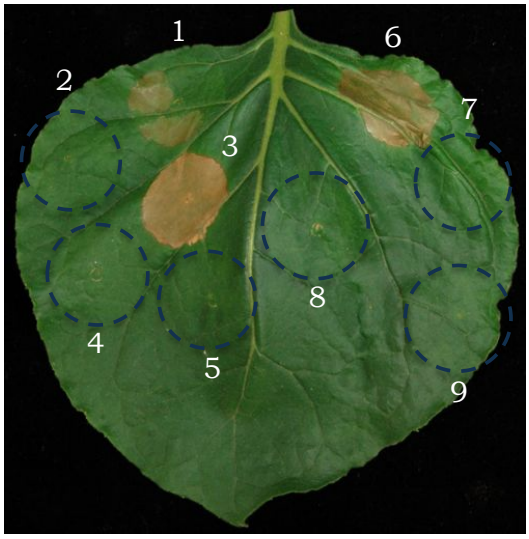
1
2
3
4
5
6
7
8
9

B

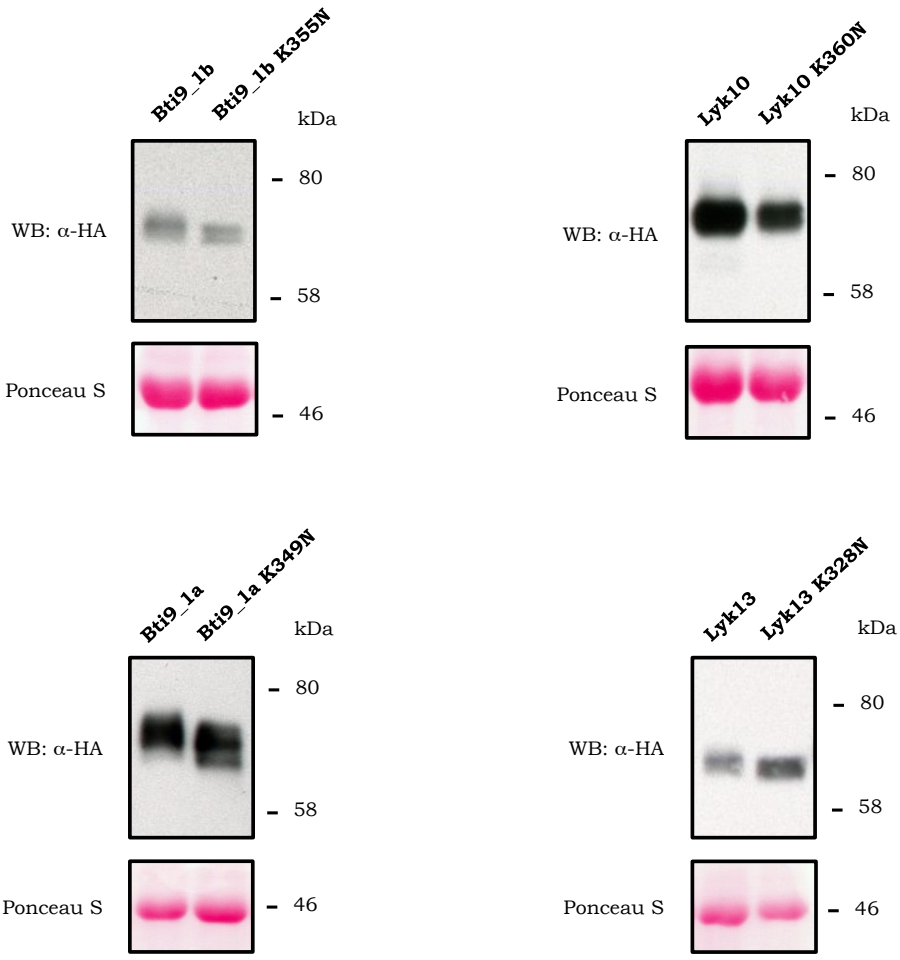
Bti9_1b
Bti9_1b K355N
kDa
80
58
WB: α-HA
Ponceau S
46
Lyk10
Lyk10 K360N
kDa
80
58
WB: α-HA
Ponceau S
46
Bti9_1a
Bti9_1a K349N
kDa
80
58
WB: α-HA
Ponceau S
46
Lyk13
Lyk13 K328N
kDa
80
58
WB: α-HA
Ponceau S
46

observed for SlBti9_1b when compared to its kinase inactive mutant could be the result of auto-phosphorylation (Figure 3.16B). Both SlBti9_1b andSlBti9_1b K355N proteins were separated on a Mn^{2+}-Phos-tag™ PAGE gel. Phos-tag™ in the gel matrix specifically retards the migration of phosphorylated proteins by reversibly binding to phosphate groups and allowing a better resolution of the phosphorylated species (Kinoshita *et al.* 2006). A number of higher apparent molecular weight bands (at least 6) was observed in the Phos-tag™ gel only in SlBti9_1b but not in its kinase inactive mutant, each probably representing different phosphorylated species of SlBti9_1b arising from multiple phosphorylation sites in the protein (Figure 3.19A).

In order to confirm that this mobility shift was caused by auto-phosphorylation, SlBti9_1b samples were treated with λ-phosphatase (New England BioLabs, Inc.). Treatment with λ-phosphatase eliminated the PAGE mobility shift (Figure 3.19B), confirming that SlBti9_1b is subject to auto-phosphorylation when over-expressed *in planta*; phosphorylation that had been shown to be required for SlBti9_1b to induce cell death (Figure 3.16A).

Discussion

Although several PAMPs have been identified to date (e.g., cold-shock protein, lipopolysaccharide), conclusive data demonstrating binding of a PRR to those PAMPs is lacking. A few well-known examples include FLS2 and flagellin (Chinchilla *et al.* 2006), EFR and EF-Tu (Zipfel *et al.* 2006) and CERK1 and

Figure 3.19. SlBti9_1b mobility shift in Polyacrylamide gels is due to auto-phosphorylation. (**A**) Immunoblot with anti-HA (α-HA) antibodies from samples separated in a Mn^{2+}-Phos-tag™ AAL-107 (25 μM) 8 % polyacrylamide gel (Wako Chemicals USA) shows an enhanced mobility shift of several phosphorylated forms of SlBti9_1b. (**B**) Immunoblot with α-HA antibodies of SlBti9_1b and its kinase inactive mutant shows that the mobility shift in SlBti9_1b is abolished after λ-phosphatase treatment. Samples were extracted with either phosphatase inhibitors (PP_{inh}) or not (No PP_{inh}) and incubated for 20 minutes at 30 °C with (λ-PPase) or without (Control) 600 U of λ-phosphatase (New England BioLabs, Inc.). A reaction with λ-phosphatase and phosphatase inhibitors was also performed as a control (PP_{inh} + λ).

A Ponceau S stain shows the total amount of protein loaded. Three times more total protein was loaded for the SlBti9_1b and pER8 empty vector samples than for SlBti9_1b K355N. Over-expression was carried out in *Nicotiana benthamiana* leaves and samples were collected 16 - 17 hours after 1 μM β-estradiol treatment.

A

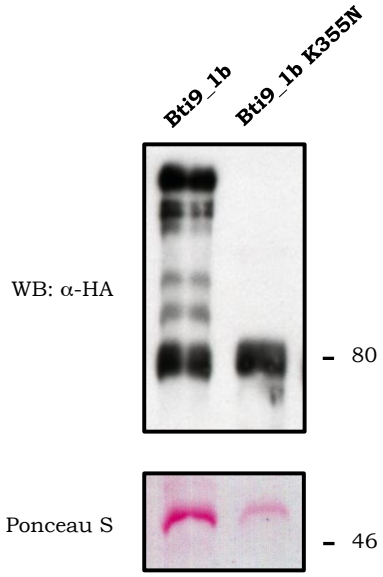
Bti9_1b
Bti9_1b K355N
WB: α-HA
80
Ponceau S
46

B

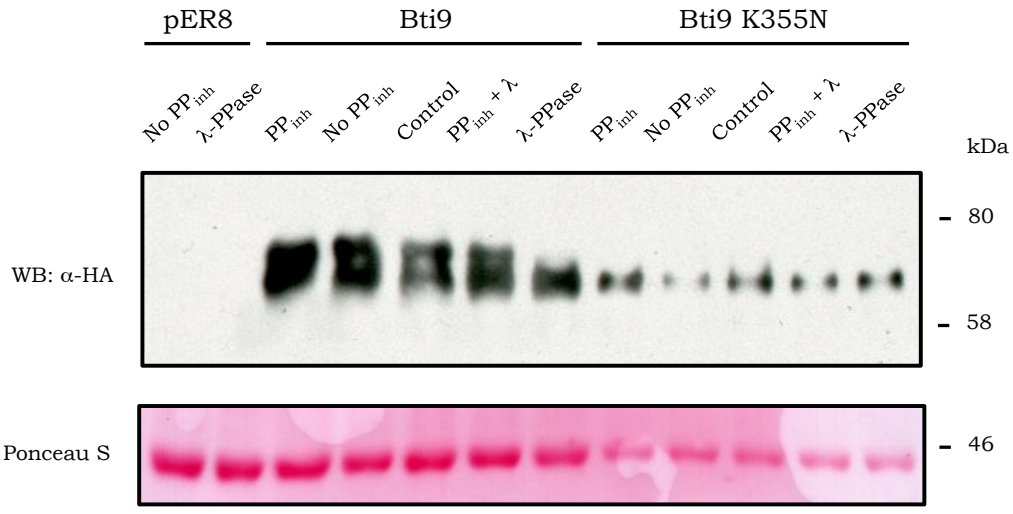
pER8
Bti9
Bti9 K355N
No PP inh
λ-PPase
PP inh
No PP inh
Control
PP inh + λ
λ-PPase
PP inh
No PP inh
Control
PP inh + λ
λ-PPase
kDa
WB: α-HA
80
58
Ponceau S
46

chitin (although for CERK1, experiments were done *in vitro*, Liu *et al.* 2012). SlBti9 and SlLyk13 share many features of PRRs, including an extracellular ligand (carbohydrate)-binding domain for PAMP perception and an intracellular kinase region to transduce the signal once the PAMP is recognized. The protein with the highest amino acid identity in *A. thaliana* to both LysM-RLKs is AtCERK1, which is part of the chitin PRR receptor complex (Shimizu *et al.* 2010). It has also been shown that *A. thaliana cerk1-2* mutant plants are more susceptible to bacterial infection than wild-type plants (Gimenez-Ibanez *et al.* 2009a); this increased susceptibility has been associated with a lack of transcriptional responses after PGN treatment (Willmann *et al.* 2011). However, none of the PGN responses that had been previously demonstrated in *Arabidopsis* (Gust *et al.* 2007; Erbs *et al.* 2008) were found to be impaired in the mutant. Furthermore, Willmann *et al.* (2011) did not address a previous report by Gimenez-Ibanez *et al.* (2009b) in which *Pst* DC3000 PGN-induced ROS production was not compromised in *A. thaliana cerk1-2* mutant plants, irrespective of the absence of a chitin-mediated response. The perception of PGN itself seems to be mediated by a receptor complex that includes AtLym1 and AtLym3 (Willmann *et al.* 2011); the proposed role of AtCERK1 as part of that receptor complex is to mediate signal transduction by phosphorylation of downstream signaling components. However, in *A. thaliana*, mobility shift-dependent phosphorylation and dimerization of AtCERK1 was shown to occur only with chitin and not with PGN treatment (Petutschnig *et al.* 2011; Liu *et al.*

2012). Taken together, it is evident that the involvement of AtCERK1 in immunity against bacteria has yet to be clearly elucidated.

In tomato (cv. Rio Grande), PGN seems to be at most a modest inducer of defense responses with no correlation between transcriptional activation and other immunity-related responses; including MAPK activation, ROS production and protection from bacterial infection. The lack of an observable phenotype by PGN *in planta* suggests that PGN is not responsible for activating PTI and stopping the colonization of non-adapted pathogens in tomato. Activation of immune responses in tomato by a bacterial suspension lacking flagellin (Figure 3.2B) suggests that there are other components besides flagellin that are being detected by the tomato immune system. However, as PGN failed to activate MAPK cascades in tomato, this immunity response was not dependent on PGN but on an unknown elicitor (e.g., cold-shock protein or lipopolysaccharide).

If it is assumed that SlBti9 and/or SlLyk13 are PRRs involved in PAMP recognition, over-expression of either of these proteins would normally not be expected to cause cell death as it does when effectors are expressed with their corresponding resistance proteins. Even though by definition PRR activation is usually not considered to be able to elicit an HR (Jones and Dangl 2006), there are several examples of PAMPs that activate cell death, including flagellin in *N. benthamiana*, tomato and *A. thaliana* (Taguchi *et al.* 2003; Naito *et al.* 2008), INF1 in tobacco (Kamoun *et al.* 1998), Eix (ethylene-inducing xylanase) in tomato (Ron and Avni 2004), and Ax21 in rice (Lee *et al.* 2009). Furthermore, the PAMP concentration required to activate PTI is equivalent to the

concentration needed to elicit cell death. For example, the concentration of flagellin required to induce cell death is similar to the concentration used for disease protection experiments in *A. thaliana* (2 μM and 1 μM, respectively; Zipfel *et al.* 2004; Naito *et al.* 2007). Also, a lower INF1 concentration to that used for ROS production triggered cell death in *N. benthamiana* (Chaparro-García *et al.* 2011). Additionally, Ax21 delivered by *Xanthomonas oryzae* pv. *oryzae* both increased resistance to rice cultivars carrying the *Xa21* resistance gene and triggered cell death (He *et al.* 2000; Lee *et al.* 2009). Interestingly, SlBti9_1b-mediated cell death was not due to toxicity since silencing of several immunity genes abolished the response, supporting the hypothesis that cell death may be involved in PAMP recognition. Taken together, these data suggest that perhaps programmed cell death (PCD) is not necessarily absent from PTI responses and that a re-evaluation of what constitutes PTI is in order (Thomma *et al.* 2011).

Receptor phosphorylation has been shown to be important for many immune signaling cascades. In FLS2, a mutation in the kinase domain that abolished catalytic activity had impaired flagellin binding and responses (*fls2-17* allele; Gómez-Gómez *et al.* 2001). Also, an AtCERK1 kinase-inactive mutant could not restore chitin-induced MAPK activation and ROS production to null mutant *A. thaliana cerk1-2* plants, implicating kinase activity in AtCERK1 function (Petutschnig *et al.* 2011). The same phenomenon was observed for a BAK1 kinase inactive mutant; in this case the mutant was unable to restore flg22 responsiveness to *A. thaliana bak1-4* plants (Schulze *et al.* 2010). This

requirement for kinase activity extends even further than only for immunity-related phenomena as nodulation symbiosis receptors also require kinase activity (*L. japonicus* LjNFR1, Madsen *et al.* 2011). SlBti9_1b is an active kinase (Zeng *et al.* 2012) that is auto-phosphorylated *in planta*. As with most RD kinases, this phosphorylation probably occurs in the activation domain of SlBti9_1b. As judged by the mobility shift observed in PAGE, SlBti9_1a and SlLyk13 are also probably auto-phosphorylated. Importantly, the kinase inactive variants of all these three proteins did not elicit cell death when over-expressed, and therefore, most likely kinase activity is required for their function in immunity.

The Bti9 clade, probably either or both spliceforms of SlBti9 and/or SlLyk13, is not only involved in immunity against bacteria but also in chitin-mediated responses (and therefore, possibly also involved in immunity against fungal pathogens). SlLyk13 and both *SlBti9* spliceforms have 5 conserved amino acids out of the 11 important for binding to chitopentaose (SlBti9_1b has another amino acid with a conservative change) and therefore, these proteins could be involved in chitin binding and may function as the PRR for chitin (Liu *et al.* 2012).

It was unexpected to discover that silencing of the Bti9 clade compromised flagellin perception, as indicated by the diminished ROS response to flg22 treatment and the inability of flg22 pre-treatment to provide full protection to subsequent infections in hpBti9 plants. However, the Bti9 clade is also probably involved in other non-flagellin mediated responses as hpBti9 plants

showed increased susceptibility to a *Pst* strain that lacked flagellin (*Pst* DC3000 Δ*avrPto* Δ*avrPto* Δ*hopQ1-1* Δ*fliC*, Figure 3.11), including perhaps, responses mediated by cold-shock protein. Wan *et al.* (2008) had noticed that *AtCERK1* knockout plants were affected in the expression of more than 300 genes in plants that had only been treated with water. Perhaps, such a disturbance in transcriptional control is also present in hpBti9 plants and explains the loss of flg22 protection. However, it is also possible that in the response to bacteria, SlBti9 and/or SlLyk13 are part of receptor complexes but are not PRR themselves, as is the case for BAK1 (Roux *et al.* 2011).

The expanded family of LysM-RLKs in tomato (14 Lyks have been identified so far) is comparable in size to that of nodule and mycorrhizal-forming *Medicago truncatula* (Arrighi *et al.* 2006). Putative Nod factor receptors are also LysM-RLKs. The best-characterized Nod factor receptors to date are *Lotus japonicus* LjNFR1 and LjNFR5, and *Medicago truncatula* MtNFP (Radutoiu *et al.* 2003; Arrighi *et al.* 2006). Even though tomato is unable to form rhizobial associations with bacteria, it can be colonized by mycorrhizae (Delp *et al.* 2003). The expanded LysM-RLK family in tomato as compared to that of *Arabidopsis* (which cannot form such symbiotic interactions) might provide such receptor, as has been observed for *Parasponia andersonii* where a LysM-RLK, PaNFP, is involved in both mycorrhizal and rhizobial associations (Op den Camp *et al.* 2011).

In conclusion, in tomato LysM receptor-like kinases are involved in immunity against bacteria and possibly against fungi. It is not clear whether SlBti9

and/or SlLyk13 are PRRs that bind to a carbohydrate-elicitor or if they are part of a PRR complex and not directly involved in binding of a PAMP (Figure 3.20). SlBti9 and SlLyk13 require auto-phosphorylation for their activity, potentially to transduce the signal after PAMP detection. PGN does not seem to be the PAMP detected by SlBti9/SlLyk13, as the immunity responses induced by PGN in tomato are minor at most.

Acknowledgments

I would like to thank Dr. Lirong Zeng for providing SlBti9_1b constructs for protein overexpression, the pQ11::*SlBti9* construct and hpBti9 transgenic tomato lines; Dr. Mari-Anne Newman for her kind gift of *Xcc* PGN and muropeptides; Dr. Zhangjun Fei for providing the LysM-RLK sequences from the tomato genome; Dr. Hernán Rosli for sharing his unpublished RNA-seq data and Diane Dunham for technical support. A. Velásquez's research was supported by National Science Foundation grant IOB-0841807.

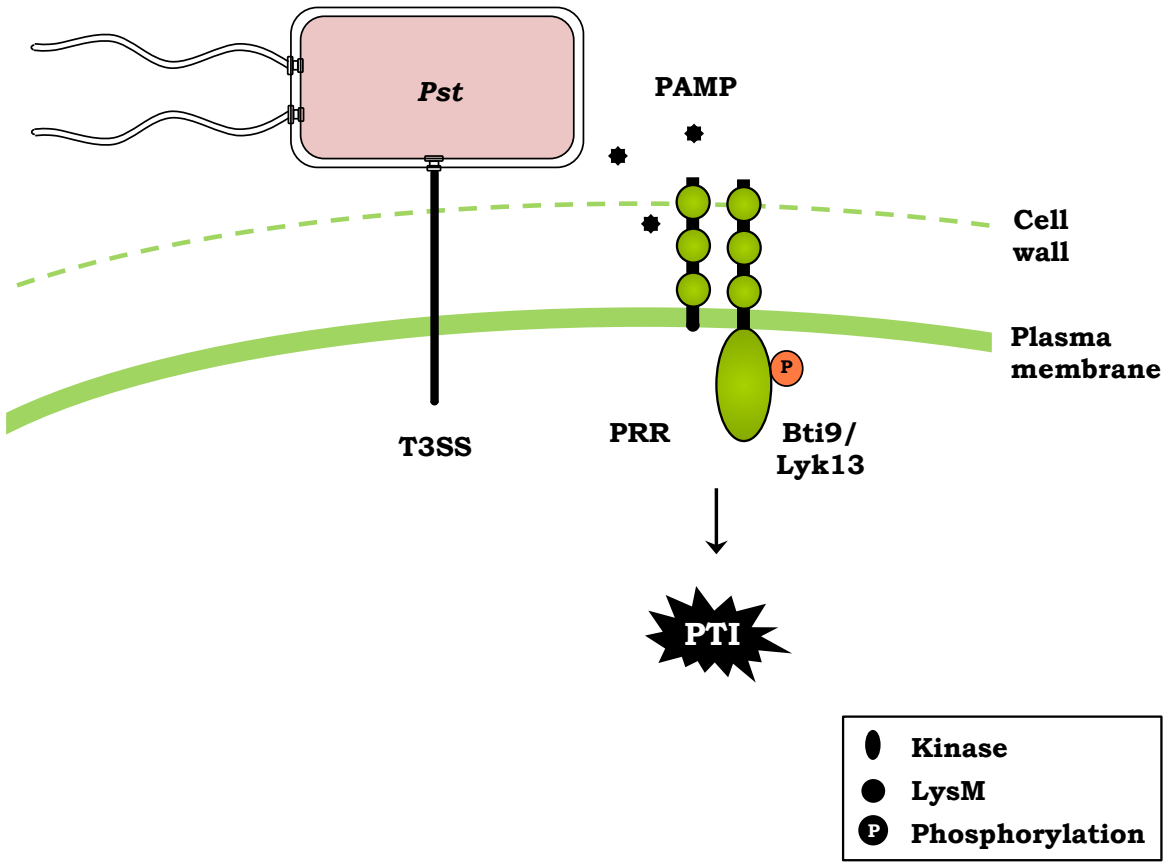

Figure 3.20. Model for SlBti9/SlLyk13 involvement in immunity against bacteria. After *Pseudomonas syringae* pv. *tomato* (*Pst*) comes into contact with plant cells, a yet uncharacterized PAMP is perceived by LysM receptor-like kinases, SlBti9 and/or SlLyk13. Either SlBti9/SlLyk13 act as PRRs by direct binding of a PAMP or they are part of a PRR complex and involved in subsequent signal transduction events, possibly by transducing the signal by phosphorylation.

REFERENCES

Arrighi J.F., Barre A., Amor B.B., Bersoult A., Soriano L.C., Mirabella R., de Carvalho-Niebel F., Journet E.P., Ghérardi M., Huguet T., Geurts R., Dénarié J., Rougé P., and Gough C. 2006. The *Medicago truncatula* lysine motif-receptor-like kinase gene family includes NFP and new nodule-expressed genes. Plant Phys 142: 265–279.

Buell C. R., Joardar V., Lindeberg M., Selengut J., Paulsen I. T., Gwinn M. L., Dodson R. J., Deboy R. T., Durkin A. S., Kolonay J. F., Madupu R., Daugherty S., Brinkac L., Beanan M. J., Haft D. H., Nelson W. C., Davidsen T., Zafar N., Zhou L., Liu J., Yuan Q., Khouri H., Fedorova N., Tran B., Russell D., Berry K., Utterback T., Van Aken S. E., Feldblyum T. V., D'Ascenzo M., Deng W. L., Ramos A. R., Alfano J. R., Cartinhour S., Chatterjee A. K., Delaney T. P., Lazarowitz S. G., Martin G. B., Schneider D. J., Tang X., Bender C. L., White O., Fraser C. M., and Collmer A. 2003. The complete genome sequence of the *Arabidopsis* and tomato pathogen *Pseudomonas syringae* pv. *tomato* DC3000. Proc Natl Acad Sci USA 100: 10181–10186.

Buist G., Steen A., Kok J., and Kuipers O.P. 2008. LysM, a widely distributed protein motif for binding to (peptido)glycans. Mol Microbiol 68: 838–847.

Cai R., Lewis J., Yan S., Liu H., Clarke C.R., Campanile F., Almeida N.F., Studholme D.J., Lindeberg M., Schneider D., Zaccardelli M., Setubal J.C., Morales-Lizcano N.P., Bernal A., Coaker G., Baker C., Bender C.L., Leman S., and Vinatzer B.A. 2011. The Plant Pathogen *Pseudomonas syringae* pv. *tomato* Is Genetically Monomorphic and under Strong Selection to Evade Tomato Immunity. PLoS Pathog 7:e1002130.

Chakravarthy S., Velásquez A.C., Ekengren S.K., Collmer A., and Martin G.B. 2010. Identification of *Nicotiana benthamiana* genes involved in pathogen-associated molecular pattern-triggered immunity. Mol Plant Microbe Interact 23: 715–726.

Chaparro-García A., Wilkinson R.C., Gimene-Ibanez S., Findlay K., Coffey M.D., Zipfel C., Rathjen J., Kamoun S., and Schornack S. 2011. The Receptor-like kinase SERK3/BAK1 is required for basal resisntace against the late blight pathogen *Phytophthora infestans* in *Nicotiana benthamiana*. PLoS One 6:e16608.

Chinchilla D., Bauer Z., Regenass M., Boller T., and Felix G. 2006. The *Arabidopsis* receptor kinase FLS2 binds flg22 and determines the specificity of flagellin perception. Plant Cell 18: 465–476.

Chinchilla D., Zipfel C., Robatzek S., Kemmerling B., Nürnberger T., Jones J.D.G., Felix G., and Boller T. 2007. A flagellin-induced complex of the receptor FLS2 and BAK1 initiates plant defence. Nature 448: 497–500.

del Pozo O., Pedley K.F., and Martin G.B. 2004. MAPKKKalpha is a positive regulator of cell death associated with both plant immunity and disease. EMBO J 23: 3072–3082.

Delp G., Timonen S., Rosewarne G.M., Barker S.J., and Smith S. 2003. Differential expression of *Glomus intraradices* genes in external mycelium and mycorrhizal roots of tomato and barley. Mycol Res 107: 1083–1093.

Ekengren S.K., Liu Y., Schiff M., Dinesh-Kumar S.P., and Martin G.B. 2003. Two MAPK cascades, NPR1, and TGA transcription factors play a role in Pto-mediated disease resistance in tomato. Plant J 36: 905–917.

Erbs G., Silipo A., Aslam S., De Castro C., Liparoti V., Flagiello A., Pucci P., Lanzetta R., Parrilli M., Molinaro A., Newmann M-A., and Cooper R.M. 2008. Peptidoglycan and muropeptides from pathogens *Agrobacterium* and *Xanthomonas* elicit plant innate immunity: structure and activity. Chem Biol 15: 438–448.

Felix G., and Boller T. 2003. Molecular sensing of bacteria in plants. The highly conserved RNA-binding motif RNP-1 of bacterial cold shock proteins is recognized as an elicitor signal in tobacco. J Biol Chem 278: 6201–6208.

Felix G., Duran J.D., Volko S., and Boller T. 1999. Plants have a sensitive perception system for the most conserved domain of bacterial flagellin. Plant J 18: 265–276.

Gimenez-Ibanez S., Hann D.R., Ntoukakis V., Petutschnig E., Lipka V., and Rathjen J.P. 2009a. AvrPtoB targets the LysM receptor kinase CERK1 to promote bacterial virulence on plants. Curr Biol 19: 423–429.

Gimenez-Ibanez S., Ntoukakis V., and Rathjen J.P. 2009b. The LysM receptor kinase CERK1 mediates bacterial perception in *Arabidopsis*. Plant Signal Behav 4: 539–541.

Gómez-Gómez L., Bauer Z., and Boller T. 2001. Both the extracellular leucine-rich repeat domain and the kinase activity of FLS2 are required for flagellin binding and signaling in *Arabidopsis*. Plant Cell 13: 1155–1163.

Gómez-Gómez L., and Boller T. 2000. FLS2: an LRR receptor-like kinase involved in the perception of the bacterial elicitor flagellin in *Arabidopsis*. Mol Cell 5: 1003–1011.

Gust A.A., Biswas R., Lenz H.D., Rauhut T., Ranf S., Kemmerling B., Götz F., Glawischnig E., Lee J., Felix G., and Nürnberger T. 2007. Bacteria-derived peptidoglycans constitute pathogen-associated molecular patterns triggering innate immunity in *Arabidopsis*. J Biol Chem 282: 32338–32348.

Hann D.R., and Rathjen J.P. 2007. Early events in the pathogenicity of *Pseudomonas syringae* on *Nicotiana benthamiana*. Plant J 49: 607–618.

He Z., Wang Z-Y., Li J., Zhu Q., Lamb C., Ronald P., and Chory J. 2000. Perception of brassinosteroid by the extracellular domain of the receptor kinase BRI1. Science 288: 2360–2363.

Heese A., Hann D.R., Gimenez-Ibanez S., Jones A.M.E., He K., Li J., Schroeder J.I., Peck S.C., and Rathjen J.P. 2007. The receptor-like kinase SERK3/BAK1 is a central regulator of innate immunity in plants. Proc Natl Acad Sci USA 104: 12217–12222.

Jones J.D.G., and Dangl J.L. 2006. The plant immune system. Nature 444: 323–329.

Kaku H., Nishizawa Y., Ishii-Minami N., Akimoto-Tomiyama C., Dohmae N., Takio K., Minami E., and Shibuya N. 2006. Plant cells recognize chitin fragments for defense signaling through a plasma membrane receptor. Proc Natl Acad Sci USA 103: 11086–11091.

Kamoun S., Hamada W., and Huitema E. 2003. Agrosuppression: A bioassay for the hypersensitive response suited to high-throughput screening. Mol Plant Microbe Interact 16: 7–13.

Kamoun S., van West P., Vleeshouwers V.G.A.A., de Groot K.E., and Govers F. 1998. Resistance of *Nicotiana benthamiana* to *Phytophthora infestans* is mediated by the recognition of the elicitor protein INF1. Plant Cell 10: 1413–1426.

Kasschau K. 2001. Long-distance movement and replication maintenance functions correlate with silencing suppression activity of potyviral HC-Pro. Virology 285: 71–81.

Kawai-Yamada M., Jin L., Yoshinaga K., Hirata A., and Uchimiya H. 2001. Mammalian Bax-induced plant cell death can be down-regulated by overexpression of *Arabidopsis Bax Inhibitor-1* (*AtBI-1*). Proc Natl Acad Sci USA 98: 12295–12300.

Kinoshita E., Kinoshita-Kikuta E., Takiyama K., and Koike T. 2006. Phosphate-binding tag, a new tool to visualize phosphorylated proteins. Mol Cell Proteomics 5: 749–757.

Kirkman T.W. 1996. Statistics to use. http://www.physics.csbsju.edu/stats/

Kornev A.P., Haste N.M., Taylor S.S., and Ten Eyck L.F. 2006. Surface comparison of active and inactive protein kinases identifies a conserved activation mechanism. Proc Natl Acad Sci USA 103: 17783–17788.

Kunze G., Zipfel C., Robatzek S., Niehaus K., Boller T., and Felix G. 2004. The N terminus of bacterial elongation factor Tu elicits innate immunity in *Arabidopsis* plants. Plant Cell 16: 3496–3507.

Kvitko B.H., Park D.H., Velásquez A.C., Wei C-F., Russell A.B., Martin G.B., Schneider D.J., and Collmer A. 2009. Deletions in the repertoire of *Pseudomonas syringae* pv. *tomato* DC3000 type III secretion effector genes reveal functional overlap among effectors. PLoS Pathog 5: e1000388.

Lee S-W., Han S-W., Sririyanum M., Park C-J., Seo Y-S., and Ronald P.C. 2009. A type I–secreted, sulfated peptide triggers XA21-mediated innate immunity. Science 326: 850–853.

Lin N-C., and Martin G.B. 2005. An *avrPto/avrPtoB* Mutant of *Pseudomonas syringae* pv. *tomato* DC3000 does not elicit Pto-mediated resistance and is less virulent on tomato. Mol Plant Microbe Interact 18: 43–51.

Liu T., Liu Z., Song C., Hu Y., Han Z., She J., Fan F., Wang J., Jin C., Chang J., Zhou J-M., Chai J. 2012. Chitin-induced dimerization activates a plant immune receptor. Science 336: 1160–1164.

Liu Y., Schiff M., and Dinesh-Kumar S.P. 2002a. Virus-induced gene silencing in tomato. Plant J 31: 777–786.

Liu Y., Schiff M., Marathe R., and Dinesh-Kumar S.P. 2002b. Tobacco *Rar1*, *EDS1* and *NPR1/NIM1* like genes are required for *N*-mediated resistance to tobacco mosaic virus. Plant J 30: 415–429.

Madsen E.B., Antolín-Llovera M., Grossmann C., Ye J., Vieweg S., Broghammer A., Krusell L., Radutoiu S., Jensen O.N., Stougaard J., and Parniske M. 2011. Autophosphorylation is essential for the *in vivo* function of the *Lotus japonicus* Nod factor receptor 1 and receptor-mediated signalling in cooperation with Nod factor receptor 5. Plant J 65: 404–417.

Miya A., Albert P., Shinya T., Desaki Y., Ichimura K., Shirasu K., Narusaka Y., Kawakami N., Kaku H., and Shibuya N. 2007. CERK1, a LysM receptor kinase, is essential for chitin elicitor signaling in *Arabidopsis*. Proc Natl Acad Sci USA 104: 19613–19618.

Naito K., Ishiga Y., Toyoda K., Shiraishi T., and Ichinose Y. 2007. N-terminal domain including conserved flg22 is required for flagellin-induced hypersensitive cell death in *Arabidopsis thaliana*. J Gen Plant Pathol 73: 281–285.

Naito K., Taguchi F., Suzuki T., Inagaki Y., Toyoda K., Shiraishi T., and Ichinose Y. 2008. Amino acid sequence of bacterial microbe-associated molecular pattern flg22 is required for virulence. Mol Plant Microbe Interact 21: 1165–1174.

Navarro L., Zipfel C., Rowland O., Keller I., Robatzek S., Boller T., and Jones J.D.G. 2004. The transcriptional innate immune response to flg22. Interplay and overlap with Avr gene-dependent defense responses and bacterial pathogenesis. Plant Phys 135: 1113–1128.

Newman M-A., von Roepenack-Lahaye E., Parr A., Daniels M.J., and Dow J.M. 2002. Prior exposure to lipopolysaccharide potentiates expression of plant defenses in response to bacteria. Plant J 29: 487–495.

Nguyen H.P., Chakravarthy S., Velásquez A.C., McLane H.L., Zeng L., Nakayashiki H., Park D-H., Collmer A., and Martin G.B. 2010. Methods to study PAMP-triggered immunity using tomato and *Nicotiana benthamiana*. Mol Plant Microbe Interact 23: 991–999.

Op den Camp R., Streng A., De Mita S., Cao Q., Polone E., Liu W., Ammiraju J.S.S., Kudrna D., Wing R., Untergasser A., Bisseling T., and Geurts R. 2011. LysM-type mycorrhizal receptor recruited for rhizobium symbiosis in nonlegume *Parasponia*. Science 331: 909–912.

Peart J.R., Lu R., Sadanandom A., Malcuit I., Moffett P., Brice D.C., Schauser L., Jaggard D.A.W., Xiao S., Coleman M.J., Dow M., Jones J.D.G., Shirasu K., and Baulcombe D.C. 2002. Ubiquitin ligase-associated protein SGT1 is required for host and nonhost disease resistance in plants. Proc Natl Acad Sci USA 99: 10865–10869.

Petutschnig E.K., Jones A.M.E., Serazetdinova L., Lipka U., and Lipka V. 2010. The lysin motif receptor-like kinase (LysM-RLK) CERK1 is a major chitin-binding protein in *Arabidopsis thaliana* and subject to chitin-induced phosphorylation. J Biol Chem 285: 28902–28911.

Radutoiu S., Madsen L.H., Madsen E.B., Felle H.H., Umehara Y., Grønlund M., Sato S., Nakamura Y., Tabata S., Sandal N., and Stougaard J. 2003. Plant recognition of symbiotic bacteria requires two LysM receptor-like kinases. Nature 425: 585–592.

Robatzek S., Bittel P., Chinchilla D., Köchner P., Felix G., Shiu S-H., and Boller T. 2007. Molecular identification and characterization of the tomato flagellin receptor LeFLS2, an orthologue of *Arabidopsis* FLS2 exhibiting characteristically different perception specificities. Plant Mol Biol 64: 539–547.

Ron M., and Avni A. 2004. The receptor for the fungal elicitor ethylene-inducing xylanase is a member of a resistance-like gene family in tomato. Plant Cell 16: 1604–1615.

Roux M., Schwessinger B., Albrecht C., Chinchilla D., Jones A., Holton N., Malinovsky F.G., Tör M., de Vries S., and Zipfel C. 2011. The *Arabidopsis* leucine-rich repeat receptor-like kinases BAK1/SERK3 and BKK1/SERK4 are required for innate immunity to hemibiotrophic and biotrophic pathogens. Plant Cell 23: 2440–2455.

Schulze B., Mentzel T., Jehle A.K., Mueller K., Beeler S., Boller T., Felix G., and Chinchilla D. 2010. Rapid heteromerization and phosphorylation of ligand-activated plant transmembrane receptors and their associated kinase BAK1. J Biol Chem 285: 9444–9451.

Shimizu T., Nakano T., Takamizawa D., Desaki Y., Ishii-Minami N., Nishizawa Y., Minami E., Okada K., Yamane H., Kaku H., and Shibuya N. 2010. Two LysM receptor molecules, CEBiP and OsCERK1, cooperatively regulate chitin elicitor signaling in rice. Plant J 64: 204–214.

Taguchi F., Shimizu R., Nakajima R., Toyoda K., Shiraishi T., and Ichinose Y. 2003. Differential effects of flagellins from *Pseudomonas syringae* pv. *tabaci*, *tomato* and *glycinea* on plant defense response. Plant Physiol Biochem 41: 165–174.

Takai R., Isogai A., Takayama S., and Che F-S. 2008. Analysis of flagellin perception mediated by flg22 receptor OsFLS2 in rice. Mol Plant Microbe Interact 21: 1635–1642.

Thieme F., Koebnik R., Bekel T., Berger C., Boch J., Büttner D., Caldana C., Gaigalat L., Goesmann A., Kay S., Kirchner O., Lanz C., Linke B., McHardy A.C., Meyer F., Mittenhuber G., Nies D.H., Niesbach-Klösgen U., Patschkowski T., Rückert C., Rupp O., Schneiker S., Schuster S.C., Vorhölter F-J., Weber E., Pühler A., Bonas U., Bartels D., and Kaiser O. 2005. Insights into genome plasticity and pathogenicity of the plant pathogenic bacterium *Xanthomonas campestris* pv. *vesicatoria* revealed by the complete genome sequence. J Bacteriol 187: 7254–7266.

Thomma B.P.H.J., Nurnberger T., and Joosten M.H.A.J. 2011. Of PAMPs and effectors: The blurred PTI-ETI dichotomy. Plant Cell 23: 4–15.

Velásquez A.C., Chakravarthy S., and Martin G.B. 2009. Virus-induced gene silencing (VIGS) in *Nicotiana benthamiana* and tomato. J Vis Exp. doi: 10.3791/1292.

Voinnet O. 2008. Use, tolerance and avoidance of amplified RNA silencing by plants. Trends Plant Sci 13: 317–328.

Wan J., Zhang X.C., Neece D., Ramonell K.M., Clough S., Kim S.Y., Stacey M.G., and Stacey G. 2008. A LysM receptor-like kinase plays a critical role in chitin signaling and fungal resistance in *Arabidopsis*. Plant Cell 20: 471–481.

Willmann R., Lajunen H.M., Erbs G., Newman M-A., Kolb D., Tsuda K., Katagiri F., Fliegmann J., Bono J-J., Cullimore J.V., Jehle A.K., Götz F., Kulik A., Molinaro A., Lipka V., Gust A.A., and Nürnberger T. 2011. *Arabidopsis* lysin-motif proteins LYM1 LYM3 CERK1 mediate bacterial peptidoglycan sensing and immunity to bacterial infection. Proc Natl Acad Sci USA 108: 19824–19829.

Xiao F., He P., Abramovitch R.B., Dawson J.E., Nicholson L.K., Sheen J., and Martin G.B. 2007. The N-terminal region of *Pseudomonas* type III effector AvrPtoB elicits Pto-dependent immunity and has two distinct virulence determinants. Plant J 52: 595–614.

Zeng L., Velásquez A.C., Munkvold K.R., Zhang J., and Martin G.B. 2012. A tomato LysM receptor-like kinase promotes immunity and its kinase activity is inhibited by AvrPtoB. Plant J 69: 92–103.

Zhang X.C., Wu X., Findley S., Wan J., Libault M., Nguyen H.T., Cannon S.B., and Stacey G. 2007. Molecular evolution of lysin motif-type receptor-like kinases in plants. Plant Phys 144: 623–636.

Zipfel C., Kunze G., Chinchilla D., Caniard A., Jones J.D.G., Boller T., and Felix G. 2006. Perception of the bacterial PAMP EF-Tu by the receptor EFR restricts *Agrobacterium*-mediated transformation. Cell 125: 749–760.

Zipfel C., Robatzek S., Navarro L., Oakeley E.J., Jones J.D.G., Felix G., and Boller T. 2004. Bacterial disease resistance in *Arabidopsis* through flagellin perception. Nature 428: 764–767.

Zuo J., Niu Q-W., and Chua N-H. 2000. An estrogen receptor-based transactivator XVE mediates highly inducible gene expression in transgenic plants. Plant J 24: 265–273.

CHAPTER IV

CONCLUSIONS

There is a need to investigate the diversity of Pathogen-associated molecular pattern (PAMP)-triggered immunity (PTI) responses and to develop robust assays for their detection in non-model plant species. Although callose deposition has been used to study PTI responses in *Arabidopsis thaliana,* the callose response in *Nicotiana benthamiana* is relatively weak (Nguyen *et al.* 2010). Additionally, ethylene production and Ca^{2+} burst after PAMP perception are two other processes that have been examined almost exclusively in *A. thaliana*, with a few exceptions (Felix and Boller – 2003 – in tomato leaves and Segonzac *et al.* – 2011 – in transgenic *N. benthamiana* plants expressing aequorin). Fourteen genes involved in PTI in *N. benthamiana* were identified in this dissertation. Their identification relied on virus-induced gene silencing of the target gene coupled to a cell-death-based assay, the latter exploiting the inhibitory effect on effector delivery of PTI-induced tissue. Using specific PAMPs as PTI inducers allowed the assignment of some of those genes to flagellin-mediated responses.

qRT-PCR primers for transcriptionally upregulated genes following PTI activation in tomato were also developed in this study, and these may be used to investigate the involvement of a particular gene in PTI. However, more assays are required to study PTI responses in order to develop a better understanding of the mechanisms that plants use to stop pathogen

colonization. For instance, programmed cell death is usually not believed to be associated with PAMP perception but even for the best studied PAMP/Pattern recognition receptor pair, flagellin and FLS2, it has been shown that recognition is able to trigger cell death in *A. thaliana* and *N. benthamiana* (Hann and Rathjen 2007; Naito *et al.* 2007). Both PTI and ETI may produce weak or robust responses since natural phenomena do not follow the strict separation that our definitions ascribe to them, and therefore, a rethinking of plant immunity as a continuum rather than as individual isolated processes is required, with PAMPs being able to trigger a hypersensitive response (HR) and effector recognition being able to stop pathogen colonization without a concomitant HR (as has been shown for cyclic nucleotide-gated ion channel mutants; Clough *et al.* 2000; Jurkowski *et al.* 2004).

As described in this dissertation, two tomato LysM receptor-like kinases (RLKs), SlBti9 and SlLyk13, were implicated in immunity against bacteria. However, the mechanism by which they are involved in PTI is still unclear. LysM domains are typically involved in binding of carbohydrates containing N-acetylglucosamine (Buist *et al.* 2003), such as peptidoglycan (PGN) and chitin. However, since PGN did not offer any protection from bacterial infections, failed to activate MAPK cascades and did not induce reactive oxygen species production in tomato, it does not seem that PGN perception plays an important role in tomato immunity (or that LysM-RLKs are involved in this process), as has been previously reported for *A. thaliana* (Willmann *et al.* 2011).

LysM-RLKs have been shown to be involved in plant symbiotic associations with rhizobacteria (Radutoiu *et al.* 2003), in which lipochitooligosaccharides (Nod factors, which have an N-acetylglucosamine backbone) are believed to be directly recognized by LysM-RLKs. Therefore, it is possible that LysM-RLKs SlBti9 and SlLyk13 recognize a carbohydrate similar in structure to that of Nod factors. Of the main Nod factor synthesizing enzymes, only NodC homologs are found in *Pseudomonas syringae* pv. *tomato* (*Pst*) DC3000 (although with low amino acid identity, <26%). Both proteins, PSPTO_1027 (wssB) and PSPTO_1524, are predicted to be glycosyltransferases and perhaps may be involved in the synthesis of the PAMP recognized by SlBti9 and SlLyk13. If SlBti9 and SlLyk13 are indeed involved in the perception of a Nod-like molecule, wild-type and hpBti9 plants should be equally susceptible to *Pst* strains that have either or both (if there is functional redundancy) of these genes deleted.

Tomato does not form rhizobial associations but can be colonized by mycorrhizae. Both symbiotic associations share a common signaling pathway and recently, RNAi of a single LysM-RLK was shown to affect both nodulation and mycorrhiza formation (Op den Camp *et al.* 2011). The reduction of transcript accumulation of four LysM-RLKs in hpBti9 plants could affect mycorrhizal associations in tomato, as these proteins are closely related in amino acid sequence to a LysM-RLK involved in nodulation, LjNFR1, and all the LysM-RLKs in the Bti9 clade are expressed in tomato roots (A. Velásquez and G. Martin, unpublished). The non-RD kinase LysM-RLK SlLyk10 could also

be involved in mycorrhizal colonization since it has the highest amino acid identity of all tomato proteins to three LysM-RLKs (LjNFR5, MtNFP and PaNFP) presumed to be Nod factor receptors. The two different mutualistic relationships between plants and either rhizobacteria or Glomeromycota probably arose from parasitic relationships that most likely activated immunity, and as such, it would not be surprising if LysM-RLKs would be involved in both processes.

In order to discern which LysM-RLK of the Bti9 clade is involved in immunity against bacteria, transgenic hairpin lines in which only one specific gene is downregulated (e.g., targeted specifically against *SlBti9_1b*) could be developed. The sequence that codes for the extracellular LysM domains of each LysM-RLKs is divergent enough among these genes for this to be achieved. Another possibility would be to take advantage of artificial microRNA technology to make highly specific silencing constructs that would simultaneously avoid off-target silencing (Schwab *et al.* 2006). If MAPK activation using bacterial extracts is compromised in protoplasts from *A. thaliana cerk1-2* plants, a less time consuming approach to address the involvement of each LysM-RLK of the Bti9 clade in immunity may be to test if over-expression of each LysM-RLK restores MAPK activation. Bacterial extracts lacking flagellin or lacking the carbohydrate molecule synthesized by the *Pst* NodC homologs could be used in these experiments. Those LysM-RLKs that restore MAPK activity to *A. thaliana cerk1-2* protoplasts could then be subsequently targeted by silencing to

determine whether they also show the enhanced bacterial susceptibility observed in the hpBti9 lines.

In *A. thaliana*, LysM receptor-like proteins (RLPs; lacking an intracellular kinase domain) *lym1* and *lym3* knockout mutant plants are more susceptible to *Pst* infection (Willmann *et al.* 2011). Lym1 and Lym3 are believed to be part of bacterial PRR recognition complexes. There are 3 LysM RLPs in tomato (*Solyc01g112080*, *Solyc03g119550* and *Solyc11g012870*), although it does not seem that any of them are transcriptionally upregulated after PAMP treatments in tomato (H. Rosli and G. Martin, unpublished), suggesting that they are not involved in PTI. Plants with downregulated expression of these genes may be tested to evaluate the involvement of LysM RLPs in immunity.

The lack of full flg22-mediated responses in hpBti9 plants is unlikely to be due to any direct involvement of SlBti9 and SlLyk13 in flagellin recognition. Instead, it could be that these proteins are part of PRR complexes (as has been shown for OsCERK1 and LysM RLP OsCEBiP in rice; Shimizu *et al.* 2010) but not PRRs themselves and instead contribute to signal transduction. Protection from bacterial infections using PAMPs other than flg22 (e.g., lipopolysaccharide) could help determine if there is a general defect in immunity in hpBti9 plants and if the Bti9 clade is involved in multiple PAMP perception pathways. Gene expression of more than 300 genes was affected in untreated *A. thaliana cerk1-2* plants when compared to wild-type plants (Wan *et al.* 2008). The transcriptional response of uninoculated hpBti9 plants could also be investigated by taking advantage of high-throughput sequencing

methods like RNA-seq to determine if there is altered gene expression due to the presence of the hpBti9 transgene. Furthermore, the observed reduction of flagellin-mediated responses in hpBti9 plants could be explained if there is a reduced accumulation of the *SlFLS2* transcript in these plants.

Interestingly, both transcriptional gene upregulation and PAMP protection after chitin treatment were compromised in hpBti9 plants. However, it remains to be investigated whether these plants lack full responses to chitin and if this has any effect in immunity against fungal pathogens. To confirm the role of the Bti9 LysM-RLK clade in immunity against fungi, infection with tomato fungal pathogens (e.g., *Cladosporium fulvum*) could be performed in the hpBti9 plants. Also, since there is no MAPK activation after chitin treatment in *A. thaliana cerk1-2* plants (Miya *et al.* 2007), complementation of the phenotype in *cerk1-2* protoplasts with tomato LysM-RLKs could help understand further their role in chitin signaling.

REFERENCES

Buist G., Steen A., Kok J., and Kuipers O.P. 2008. LysM, a widely distributed protein motif for binding to (peptido)glycans. Mol Microbiol 68: 838–847.

Clough S.J., Fengler K.A., Yu I-C., Lippok B., Smith R.K. Jr., and Bent A.F. 2000. The *Arabidopsis dnd1* "defense, no death" gene encodes a mutated cyclic nucleotide-gated ion channel. Proc Natl Acad Sci USA 97: 9323–9328.

Felix G., and Boller T. 2003. Molecular sensing of bacteria in plants. The highly conserved RNA-binding motif RNP-1 of bacterial cold shock proteins is recognized as an elicitor signal in tobacco. J Biol Chem 278: 6201–6208.

Hann D.R., and Rathjen J.P. 2007. Early events in the pathogenicity of *Pseudomonas syringae* on *Nicotiana benthamiana*. Plant J 49: 607–618.

Jurhowski G.I., Smith R.K. Jr., Yu I-C., Ham J.H., Sharma S.B., Klessig D.F., Fengler K.A., and Bent A.F. 2004. *Arabidopssi DND2*, a second cyclic nucleotide-gated ion channel gene for which mutation causes the "defense, no death" phenotype. Mol Plant Microbe Interact 17: 511–520.

Miya A., Albert P., Shinya T., Desaki Y., Ichimura K., Shirasu K., Narusaka Y., Kawakami N., Kaku H., and Shibuya N. 2007. CERK1, a LysM receptor kinase, is essential for chitin elicitor signaling in *Arabidopsis*. Proc Natl Acad Sci USA 104: 19613–19618.

Naito K., Ishiga Y., Toyoda K., Shiraishi T., and Ichinose Y. 2007. N-terminal domain including conserved flg22 is required for flagellin-induced hypersensitive cell death in *Arabidopsis thaliana*. J Gen Plant Pathol 73: 281–285.

Nguyen H.P., Chakravarthy S., Velásquez A.C., McLane H.L., Zeng L., Nakayashiki H., Park D-H., Collmer A., and Martin G.B. 2010. Methods to study PAMP-triggered immunity using tomato and *Nicotiana benthamiana*. Mol Plant Microbe Interact 23: 991–999.

Op den Camp R., Streng A., De Mita S., Cao Q., Polone E., Liu W., Ammiraju J.S.S., Kudrna D., Wing R., Untergasser A., Bisseling T., and Geurts R. 2011. LysM-type mycorrhizal receptor recruited for rhizobium symbiosis in nonlegume *Parasponia*. Science 331: 909–912.

Radutoiu S., Madsen L.H., Madsen E.B., Felle H.H., Umehara Y., Grønlund M., Sato S., Nakamura Y., Tabata S., Sandal N., and Stougaard J. 2003. Plant recognition of symbiotic bacteria requires two LysM receptor-like kinases. Nature 425: 585–592.

Schwab R., Ossowski S., Riester M., Warthmann N., and Weigel D. 2006. Highly specific gene silencing by artificial microRNAs in *Arabidopsis*. Plant Cell 18: 1121–1133.

Segonzac C., Feike D., Gimenez-Ibanez S., Hann D. R., Zipfel C., and Rathjen J. P. 2011. Hierarchy and roles of pathogen-associated molecular pattern-induced responses in *Nicotiana benthamiana*. Plant Physiol 156:687-699.

Shimizu T., Nakano T., Takamizawa D., Desaki Y., Ishii-Minami N., Nishizawa Y., Minami E., Okada K., Yamane H., Kaku H., and Shibuya N. 2010. Two LysM receptor molecules, CEBiP and OsCERK1, cooperatively regulate chitin elicitor signaling in rice. Plant J 64: 204–214.

Wan J., Zhang X.C., Neece D., Ramonell K.M., Clough S., Kim S.Y., Stacey M.G., and Stacey G. 2008. A LysM receptor-like kinase plays a critical role in chitin signaling and fungal resistance in *Arabidopsis*. Plant Cell 20: 471–481.

Willmann R., Lajunen H.M., Erbs G., Newman M-A., Kolb D., Tsuda K., Katagiri F., Fliegmann J., Bono J-J., Cullimore J.V., Jehle A.K., Götz F., Kulik A., Molinaro A., Lipka V., Gust A.A., and Nürnberger T. 2011. *Arabidopsis* lysin-motif proteins LYM1 LYM3 CERK1 mediate bacterial peptidoglycan sensing and immunity to bacterial infection. Proc Natl Acad Sci USA 108: 19824–19829.